

Regulation of *Emx2* expression by antisense transcripts in the murine developing CNS

Thesis submitted for the degree of “Doctor Philosophiae”

Academic Year 2008/2009

Candidate:

Giulia Spigoni

Supervisor:

Prof. Antonio Mallamaci

To my Family

Regulation of *Emx2* expression by antisense transcripts in the murine developing CNS

Candidate:
Giulia Spigoni

Supervisor:
Prof. Antonio Mallamaci

Table of contents:

1 Introduction	7
1.1 Cerebral cortex formation	7
1.1.1 Development of mammalian telencephalic vesicles	7
1.1.2 Development of the mammalian cerebral cortex	9
1.1.3 Cortical field specification	16
1.1.4 Models of regionalization of the cortical primordium	20
1.1.5 Signaling centers involved in cortical arealization	21
1.1.6 Transcription factors genes regulating areas identity	25
1.1.7 Role of Emx2 in mouse cerebral cortex development	27
1.2 Natural Antisense Transcripts (NATs) in the genome	33
1.2.1 Antisense transcription: structural and functional aspects	33
1.2.2 Antisense function	38
1.2.3 Antisense transcription in development	42
1.2.4 Emx2OS in mouse cerebral cortex development	44
1.3 Aim of the work	46
2 Results	47
2.1 Expression pattern of Emx2OS-ncRNA	47
2.2 Emx2OS antagonizes Emx2 expression in a Dicer-dependent way	52
2.3 Emx2OS transcripts promote both Emx2-mRNA and Emx2OS-ncRNA expression	60
2.4 Absence of Emx2 sense transcription and/or its products impairs Emx2OS-ncRNA expression	64
3 Discussion	66
4 Materials and methods	69
4.1 Animal handling	69
4.2 Reagents and standard procedures	69
4.3 Preparation of histological samples	69
4.4 Preparation of single-stranded RNA probes	70
4.5 Preparation of Dig-labelled probe	70
4.6 In situ hybridization protocol	70
4.7 Probes used for the in situ hybridization	71
4.8 Cell cultures	72

4.9 Quantitative RT-PCR	72
4.10 Plasmids construction	74
4.11 3 rd generation Lentiviral vectors: production titration and usage	75
4.12 Statistical analysis	77
5 Tables	78
6 References	80
7 Acknowledgements	96

Abstract

In this thesis I studied the expression pattern of *Emx2OS*, the antisense partner of the homeobox gene *Emx2*, in the developing mouse nervous system. *Emx2OS* was detectable in telencephalon, mammillary recess, mesencephalon, nasal pits and otic vesicle, all of them also expressing *Emx2*. Within dorsal telencephalon, *Emx2OS* peaked in post-mitotic neurons, specifically at the time when they completed radial migration and turned *Emx2* off. Such pattern suggested that *Emx2OS* may be implicated in regulation of *Emx2*, according to complex and even antithetic ways. By artificially modulating *Emx2OS* in primary cortico-cerebral precursors, via lentiviral RNAi and somatic transgenesis, we found that such transcript contributes to down-regulation of its sense partner, possibly by a Dicer-dependent post-transcriptional mechanism. On the other side, by ectopically activating *Emx2OS* in primary rhombo-spinal precursors, we elicited a robust activation of *Emx2*. Further inspection of *Emx2* null cortices conversely showed a collapse of *Emx2OS* expression. Taken together, these results suggest that a mutual positive loop involving *Emx2* and *Emx2OS* is necessary to adequate expression of either transcript in the early neural tube.

1 Introduction

1.1 Cerebral cortex formation

1.1.1 Development of mammalian telencephalic vesicles

The neural plate is formed from the neuro-ectodermal layer of the gastrulating embryo and gives rise to the entire central nervous system (CNS). Neural folds arise in the neural plate, appose and fuse to form the neural tube (Fig., 1A e 1B).

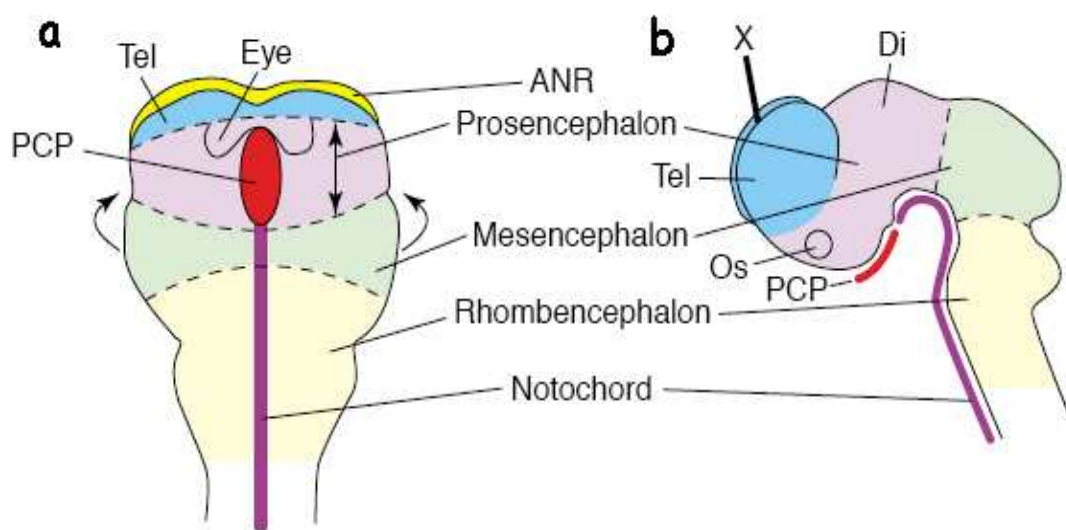


Figure 1 | Neural plate and neural tube stages in mouse. a) The anterior neural plate at around E8.5. The neural plate folds in the direction of the arrows to form the neural tube. b) The brain viewed from the side after neural tube closure (at around E10.5). The brain vesicles are the prosencephalon (comprised of the telencephalon (tel) and diencephalon (di)), mesencephalon and rhombencephalon. The prechordal plate (pcp) underlies the rostral part of the neural tube (at the level of the diencephalon) whereas the notochord underlies the caudal neural tube. (Adapted from Zaki et al., 2003).

The mammalian brain arises from three vesicles forming at the anterior end of the neural tube: the prosencephalon (or forebrain), the mesencephalon (or midbrain) and the rhombencephalon (or hindbrain). The vesicles are generated at very early stages of the development; for example, in the mouse embryo the prosencephalon develops at around embryonic day 9 and in human embryos around week 6. Later, the prosencephalic vesicle gives rise to two laterally enlarged bulges, termed telencephalon and a medial secondary vesicle, the diencephalon.

The telencephalon is subsequently subdivided into the ventral and the dorsal telencephalon. The dorsal telencephalon gives rise to a thin sheet, the pallium, where from the cerebral cortex develops. The ventral telencephalon, or subpallium, develops two hill-like extensions, the Lateral and Medial Ganglionic Eminences (LGE/MGE), which are the forerunners of basal ganglia (Rubenstein et al., 1998). The basal ganglia, placed in the bottom of the telencephalic vesicles, consist of three major groups of neurons: the striatum, the globus pallidus and the amygdala. The dorsal part of the striatum, involved in motor control, includes the caudate nucleus and the putamen (Fig. 2). Afferents coming from three main sources, the cerebral cortex, the medial part of the thalamus, the substantia nigra (pars compacta), reach the striatum. The striatum projects to the globus pallidus. Efferents leaving the globus pallidus reach the thalamus, the substantia nigra (pars reticularis) and the subthalamic nucleus. The amygdala is bidirectionally connected with the hippocampus, the thalamus and the hypothalamus.

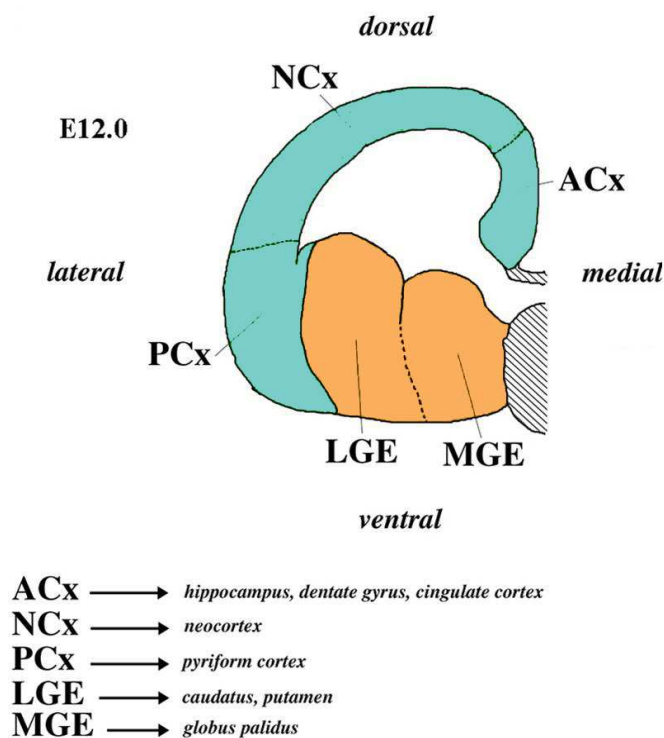


Figure 2 | Schematic view of a section through the developing telencephalic vesicle at E12.0. Acx, archicortex; Ncx, neocortex; Pcx, paleocortex; LGE, lateral ganglionic eminence; MGE, medial ganglionic eminence. (A.Mallamaci, unpublished).

1.1.2 Development of the mammalian cerebral cortex

The development of the forebrain and in particular of the cerebral cortex is one of the most intriguing fields of developmental neurobiology. It is the result of a concerted action of several processes, such as proliferation, differentiation and migration of neuroblasts, from germinative areas to different regions of the brain.

The mammalian cerebral cortex has undergone an immense enlargement during evolution and two main different cortical regions can be distinguished: a phylogenetically older region, the allocortex, and a younger region, the neocortex. The allocortex can be further subdivided into paleocortex (including olfactory piriform cortex and entorhinal cortex) and archicortex (including subiculum, hippocampus and dentate gyrus), (Fig., 2). These regions are distinguished on the basis of their lamination: neurons in the allocortex are organized in three horizontal layers, whereas those of the neocortex form six layers. Cortical layers located between the neocortex and the allocortex display three to six layers, reflecting their transitional nature. The six layered neocortex, which is the largest part of the mammalian brain, is divided into distinct areas according to their functions and cytological organization (Brodmann, 1909). Each cortical layer contains two distinct neuronal types: projection (pyramidal or granule) and interneurons (non pyramidal) (Ramon y Cajal, 1911). The former are glutamatergic and excitatory whereas the latter are GABAergic and inhibitory. Cortical projection neurons originate from progenitors located in the cortical ventricular zone. In contrast, most, if not all, cortical interneurons originate from progenitors located outside the cortex and primarily in the ventral telencephalon, at least in rodents (Marin and Rubenstein, 2001; Gorski et al., 2002). Following their birth in the ventral telencephalon, interneurons use multiple and complex routes of tangential migration to reach their final position in the developing cortex (Marin and Rubenstein, 2001).

The mouse neural tube, derived from the neural plate, is first distinguishable at embryonic-day 9.0 (E9.0). In the forebrain, cerebral cortex is visible from E9.5-10.0, when it consists of a unique layer of proliferating neuroblasts, the germinative neuroepithelium or ventricular zone (VZ). Neurogenesis starts here at E11.0 ventrolaterally and at E12.0 dorsomedially, peaks around E12.5-13.5, and continues at lower levels until post-natal-day 17 (P17). Neuronal differentiation and migration also continue after birth (Bayer and Altman, 1991). Around E11-12 a first layer, the preplate (PP), differentiates above the VZ. This layer contains the first postmitotic neurons that will later populate the two layers originated from its splitting, the marginal zone (MZ) with Cajal

Retzius cells (layer I) and the subplate (SP) (Fig., 3) (Bagirathy Nadarajah and John G. Parnavelas, 2002).

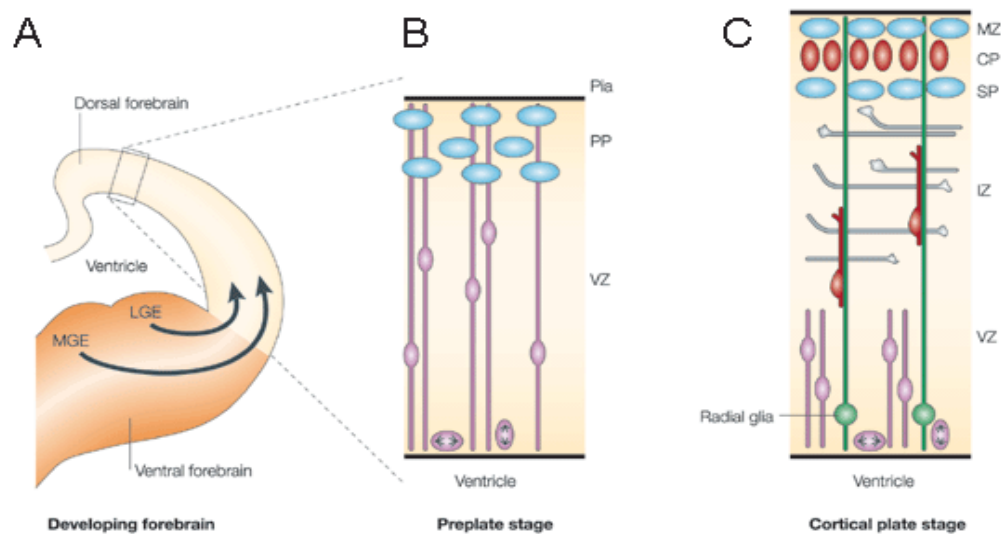


Figure 3 | (A) Schematic diagram of a section through the developing rodent forebrain. (B), (C) Illustrations of the different stages of neocortical development. The dorsal forebrain gives rise to the cerebral cortex. The lateral ganglionic eminence (LGE) and medial ganglionic eminence (MGE) of the ventral forebrain generate the neurons of the basal ganglia and the cortical interneurons; the latter follow tangential migratory routes to the cortex (a; arrows). In the dorsal forebrain (a; boxed area), neuronal migration begins when the first cohort of postmitotic neurons moves out of the ventricular zone (VZ) to form the preplate (PP) (b). Subsequent cohorts of neurons (pyramidal cells) migrate, aided by radial glia, through the intermediate zone (IZ) to split the PP into the outer marginal zone (MZ) and inner subplate (SP) (c). CP, cortical plate. (Adapted from Bagirathy Nadarajah and John G. Parnavelas, 2002).

Cajal Retzius cells provide diffusible signals crucial for the migrations of cortical plate neurons (Frotscher, 1997) (Fig., 4). They secrete the Reelin glycoprotein, essential for neuronal glia-mediated migration (De Rouvoit et al., 2001).

Moreover, Reelin induces neurons to migrate past their predecessor (D'arcangelo and Curran, 1998), but it has also been thought to provide a stop signal to migrating cells, which detach from the radial glia. In fact, Reelin has been shown to inhibit neuronal migration via its interaction with $\alpha3\text{-}\beta1$ integrin, a downstream component of its signaling pathway (Dulabon et al., 2000). This migration-inhibiting activity of Reelin should be relevant at the end of radial migration, when the neuronal leading process contacts the marginal zone and pyramidal neurons detach from the radial glial scaffold (Nadarajan et al., 2001).

The SP is a layer of early-generated neurons, the majority of which disappear in adult life and are thought to participate in early *functional* circuitry: these cells receive synaptic inputs from

thalamic afferents fibers and make axonal projections to the cortical plate (CP) (Allendoerfer and Shatz, 1994).

Between SP and ventricular zone (VZ), a “transitional field” (TF) develops. It will give rise to the subventricular zone (SVZ) and the intermediate zone (IZ), which is a transition layer for differentiating neurons before they migrate (from E 15.5 onwards) to the CP, the future cortical gray matter. Moreover, the sub-ventricular zone is a source of pyramidal neurons and glial cells (Tarabikyn et al., 2001).

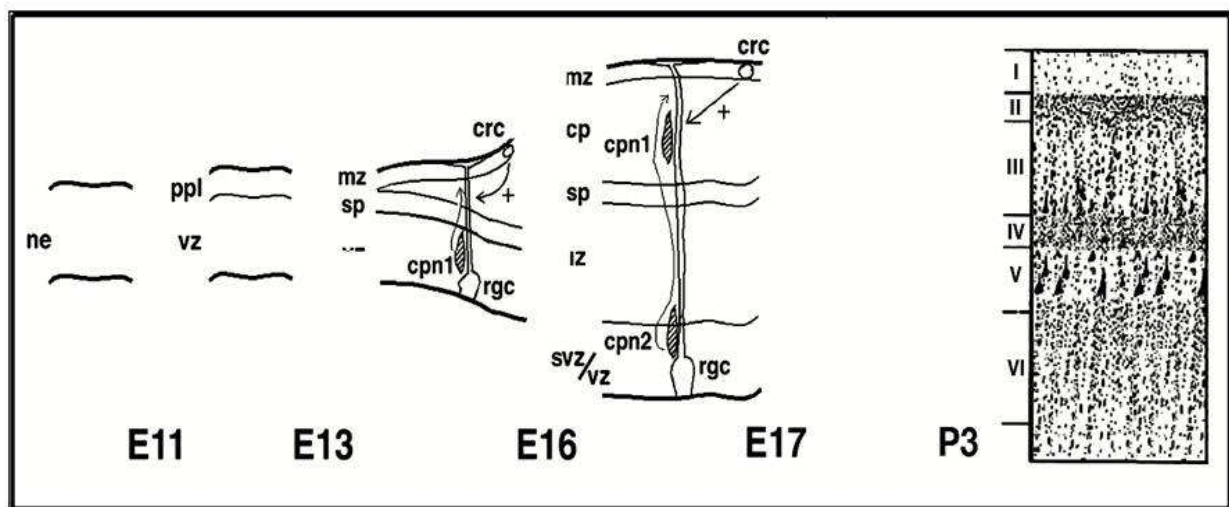


Figure 4 | Schematic representation of the cortical wall during cerebral cortex development. Ventricular zone is at the bottom and marginal zone is at the top. Ne, neuroepithelium; ppl, preplate; vz, ventricular zone; mz, marginal zone; sp, subplate; crc, Cajal –Retzius cell; cpn, cortical late neuron; rgc, radial glia cell; cp, cortical plate; iz, intermediate zone; svz, sub-ventricular zone (Adapted from Frotscher, 1997).

During the development of the embryo, the VZ becomes thinner, whereas the thickness of the TF and CP progressively increases. At the end of cortical development, the CP consists of six layers originated according to the “inside-out” developing rule (Bayer and Altman, 1991): neurons located deep in the cortex are generated first and neurons that are generated later bypass them by active migration, settling above in more-external locations (radial migration).

Cellular mechanisms of radial migration of pyramidal neurons from proliferative layers to the forming cortical plate have been the subject of intense experimental investigations and two moving patterns have been recently demonstrated to take place. During early stages of the cerebral cortex development, when the cerebral wall is relatively thin, neurons move by “somal translocation”. Later, during cortical plate formation, they proceed by “glia-guided locomotion”.

The cells that undergo somal translocation typically have a long, radially oriented basal process that terminates at the pial surface, and a short, transient, trailing process. The migratory

behavior is characterized by continuous advancement that results in a faster rate of migration. By contrast cells that adopt glia-guided locomotion have a shorter radial process that is not attached to the pial surface. These cells show a characteristically slow saltatory pattern of locomotion. They perform short burst of forward movements that are interspersed with stationary phases. For this reason they display slow average speed. Interestingly, neurons showing this saltatory pattern of movement switch to somal translocation in the terminal phase of their migration, once their leading process reach the marginal zone (Nadarajan et al., 2001).

Two apolipoprotein E (apoE) receptors, the very low density lipoprotein (VLDL) receptor and apoE receptor 2 (apoER2), have been shown to participate in a neuronal signaling pathway that governs the layering of the developing cortex (Trommsdorff et al., 1999), and they are associated with Reelin. ApoE is a component of lipoproteins that mediates the transport and receptor-mediated uptake of these particles by target tissues (Mahley et al., 1995). ApoE is produced by several tissues in the body including glial cells in the brain, predominantly astrocytes. In the human population, ApoE occurs in three major isoforms, among which, ApoE3, results to be the most common. It has been reported by Schmechel in 1993 (Schmechel et al., 1993), that the apoE4 isoform is genetically associated with late onset Alzheimer disease.

The lack of Reelin (D'Arcangelo et al., 1995), its receptors (VLDLR) and apoER2 (Trommsdorff et al., 1999), or the cytoplasmic adaptor protein Dab1 (Ware et al., 1997), all results in the same phenotype, which is characterized by cerebellar dysplasia and abnormal layering of the neocortex.

After the fetal phase of brain development, Reelin-expressing Cajal-Retzius neurons in the subpial layer are largely replaced by Reelin-expressing GABA-ergic interneurons that are dispersed throughout the neocortex and in the hippocampus. The Reelin receptors apoER2 and VLDLR and the adaptor protein Dab1, all essential to Reelin signaling, remain expressed in the adult brain, but their function is not clear. An association of Reelin with synapses has been reported (Rodriguez et al., 2000), raising the possibility of a potential role in neurotransmission that might involve signaling through apoE receptors. Mice lacking the Reelin/apoE receptors VLDLR and apoER2 have pronounced defects in memory formation and long term potentiation LTP and Reelin greatly enhances LTP in hippocampal slice cultures (Edwin et al., 2002). An hypothetical model of the actions of Reelin in LTP induction is shown in figure 5.

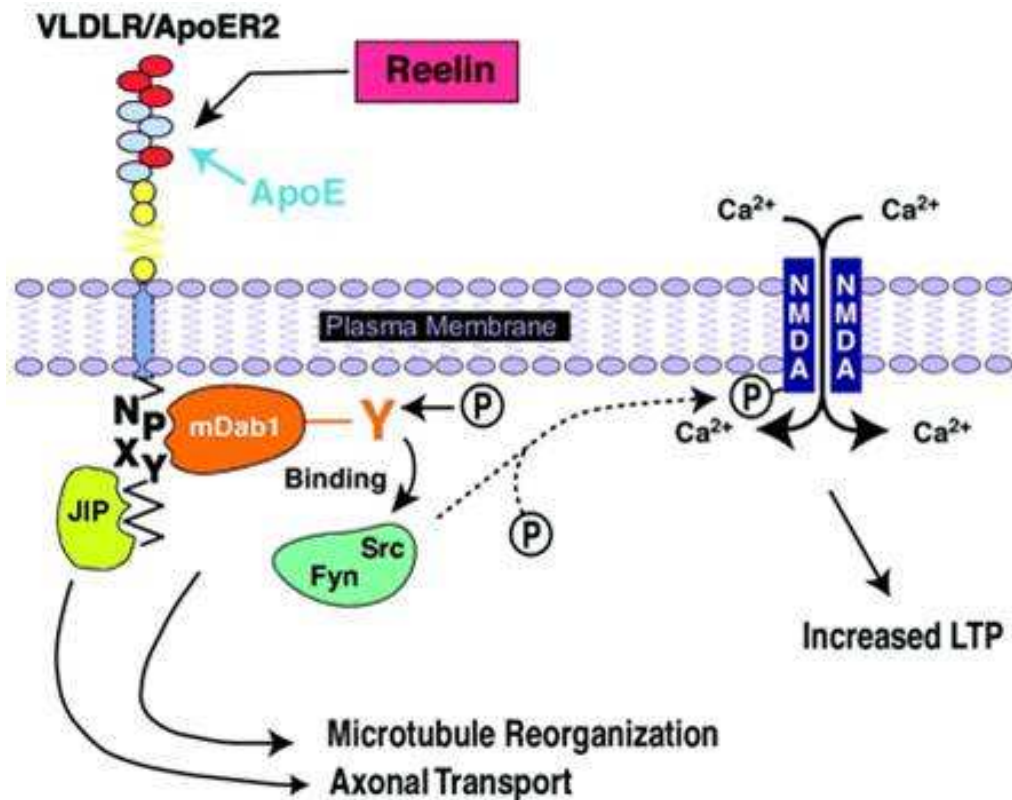


Figure 5 | Hypothetical model of the actions of Reelin in LTP induction. Reelin binding to apoER2 and the VLDL receptor stimulates intraneuronal tyrosine kinase activity and induces Dab tyrosine phosphorylation. Non-receptor tyrosine kinases of the Src family are thus activated and may stimulate NMDA receptor activity, thereby increasing Ca²⁺ influx and LTP. ApoE can compete for Reelin binding to the extracellular domains of apoER2 and the VLDL receptor and thereby suppress tyrosine phosphorylation of Dab1. ApoER2 binds members of the JIP family of scaffolding proteins on its cytoplasmic tail and thus indirectly interacts with the microtubule-associated molecular motor kinesin. Blue ovals designate alternatively spliced ligand binding repeats in apoER2 (Adapted from Edwin et al., 2002).

Cortical GABAergic interneurons, generated in sub-pallial telencephalon (both in the lateral and medial ganglionic eminences), leave the proliferative epithelium and then initiate their long tangential migratory routes, moving parallel to the surface of the telencephalon. They cross the cortico-striatal boundary and enter the cortical wall, reaching their appropriate laminar-areal locations (Anderson et al., 1997; Tan et al., 1998; Tamamaki et al., 1997).

Three general and partially overlapping phases of tangential migration of GABAergic neurons can be distinguished.

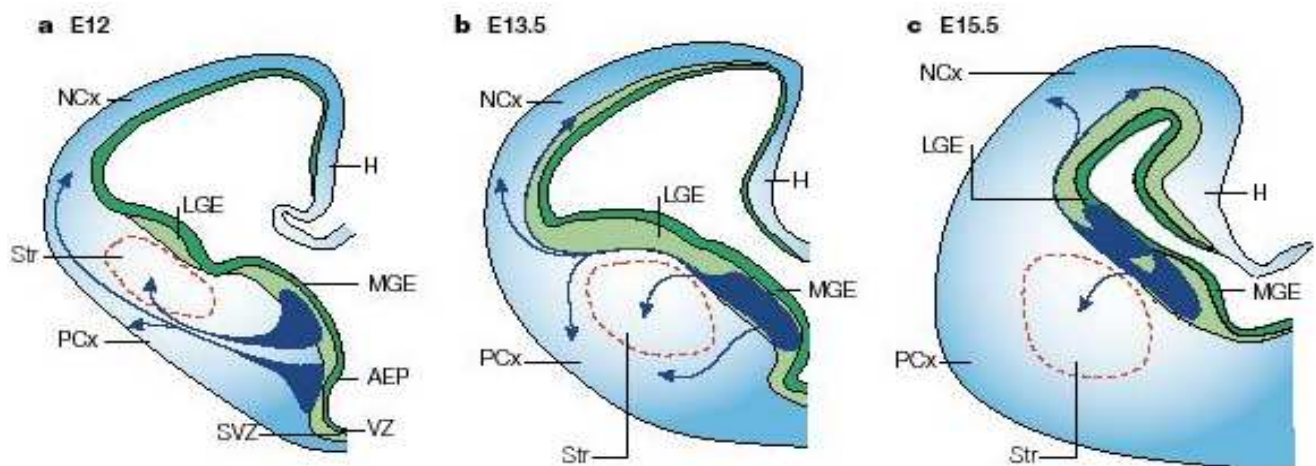


Figure 6 | At least three spatially and temporally distinct routes can be distinguished, as depicted here in schemas of transverse sections through the embryonic telencephalon. a | Early during development (embryonic day (E) 12), interneurons that migrate to the cortex arise primarily from the medial ganglionic eminence (MGE) and the anterior entopeduncular area (AEP), and follow a superficial route. b | At the peak of migration (E13.5), interneurons migrating to the cortex arise primarily from the MGE and follow a deep route to the developing striatum (Str). Some interneurons also migrate superficially. c | At later stages (E15.5), cells migrating to the cortex might also arise from the lateral ganglionic eminence (LGE) and follow a deep route. GP, globus pallidus; H, hippocampus; LIZ, lower intermediate zone; MZ, marginal zone; NCx, neocortex; PCx, piriform cortex; VZ, ventricular zone. (Adapted from Marin et al., 2001).

First, an early migration from medial ganglionic eminence and anterior entopeduncular area takes place at around E11.5. In this case, cells move superficially to the developing striatum and invade the cortical marginal zone and subplate. Second, around mid-embryonic stages (E12.5-14.5), the medial ganglionic eminence seems to be the principal source of cells that migrate tangentially into the cortex. (Fig., 6) (Marin and Rubenstein, 2001). These neurons migrate either deep or superficially to the developing striatum, and they populate both the sub-ventricular zone/lower-intermediate zone and the subplate, from where they extend into the cortical plate (Anderson et al., 2001). Third, at late stages of the development (E15.5-16.5), cells that migrate tangentially into the cortex seem to derive from both the lateral and the medial ganglionic eminence (Marin and Rubenstein, 2001). Interestingly, some migrating cells are directed toward the proliferative regions of the cortex at this stage (Anderson et al., 2001). Presently unknown is the biological significance of this phenomenon.

Remarkably, a subset of LGE-derived interneurons plays a key role in allowing correct pathfinding of thalamocortical axons (TCAs). Such axons arise in the dorsal thalamus, and follow a stereotyped pathway into the developing neocortex. Repelled by Slit 1 and Slit 2 expressed in the hypothalamus, TCAs extend rostrally into the telencephalon and turn sharply before extending dorsolaterally to enter the MGE. They then extend through the developing striatum and into the

neocortex. In order to reach the cortex, such axons require the formation of a permissive *corridor* through non-permissive MGE territory, and that this corridor is generated by cells which undergo a tangential migration from the LGE (Lopez-Bendito et al., 2006) (Fig., 7).

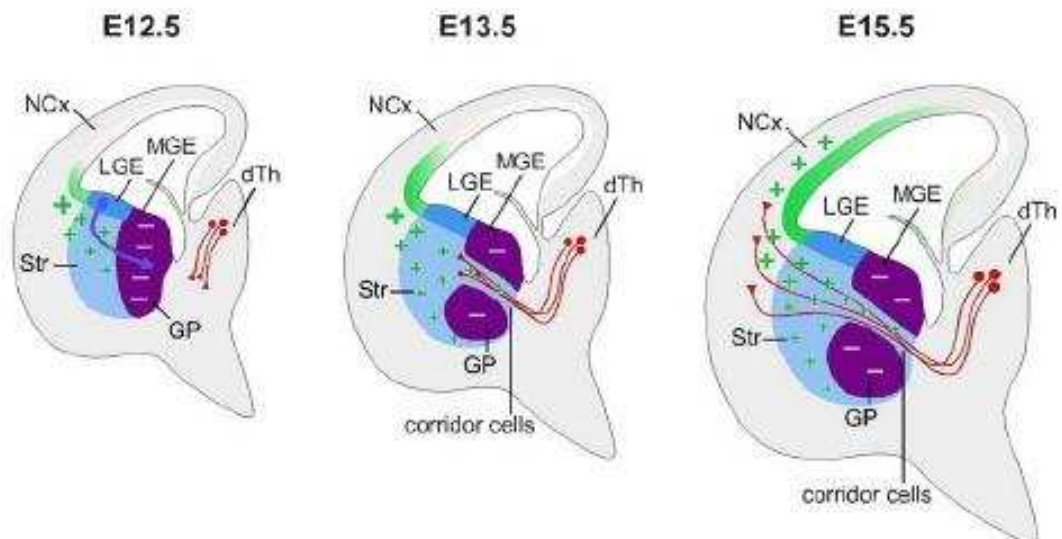


Figure 7 | Schematic diagram showing how tangential neuronal migration forms a permissive corridor through which thalamocortical axons (TCAs) extend. TCAs (red) originate in the dorsal thalamus and extend rostroventrally into the developing telencephalon. At embryonic day (E) 12.5 in the mouse, an unidentified chemorepellant (purple) prevents TCAs from entering the medial ganglionic eminence (MGE). Islet1+ interneurons migrate from the lateral ganglionic eminence (LGE) into the MGE. By E13.5, the LGE-derived neurons have generated a permissive corridor, which TCAs use to extend through the MGE. Corridor cells express NRG1 (green crosses), which contributes to the navigation of TCAs. The developing neocortex also expresses NRG1, which may be required for the final stage of TCA pathfinding (Adapted from Lopez-Bendito et al., 2006).

1.1.3 Cortical field specification

The specification of the cortical field is a fundamental process of neural development. The development of neural tube follows a rostro-caudal and dorso-ventral pattern of specification. It starts with secreted factors. These are diffusible molecules normally expressed around specific borders of the neural field and along defined gradients, which, acting as morphogens, regulate the expression of transcription factors, restricting them to different rostro-caudal and dorso-ventral domains.

Rostro-caudal specification starts with Wnt signals coming from the caudal-most neural plate. In response to them, two different domains are defined along the antero-posterior axis by the expression of two homeobox genes: Otx2 and Gbx2. The Otx-expressing region, rostrally located, will give rise to the forebrain and midbrain, whereas the Gbx2-expressing region, at caudal position, will develop into hindbrain and spinal cord. The boundary between them corresponds anatomically to the isthmus, a narrowing of the neural tube at the border between mesencephalon and metencephalon. Canonical Wnt signaling represses directly Otx2 expression, whereas induces Gbx2 (Fig. 8, top row). Wnts also control the expression of other two genes, Irx3 and Six3, confining Six3 to the telencephalon/rostral diencephalon field and promoting posterior expression of Irx3, caudally to the anlage of the zona limitans intrathalamica (ZLI), placed between the thalamic and prethalamic primordia (Braun et al., 2003) (Fig. 8, bottom row).

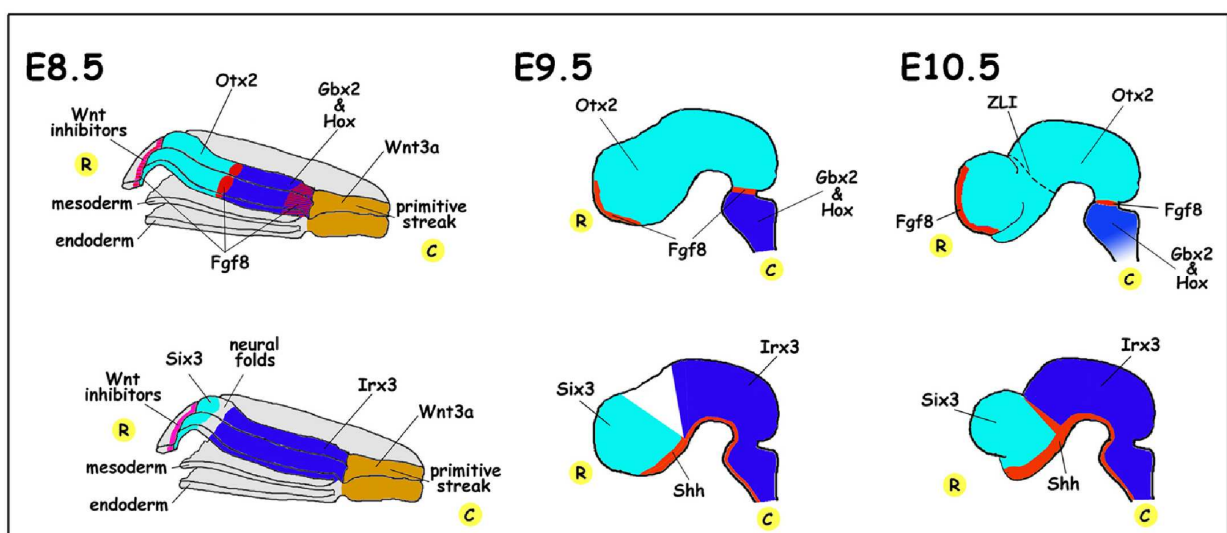


Fig 8 | Adapted from A. Mallamaci, unpublished lessons.

Slightly later, two other diffusible molecules, fibroblasts growth factor 8 (Fgf8) and Sonic Hedgehog (Shh), dictate the further rostro-caudal patterning of the neural field. Fgf8 is

synthesized by the anterior neural boundary and around the isthmus. It promotes the expression of *Foxg1* in the telencephalon and of *En2* in the tectum of mesencephalon (Fig. 9 above). *Shh*, initially confined to the notochord, is rapidly induced within a discrete triangular wedge of cells that is located at the ventral midline of the neural tube. Moreover, it is activated in the thin region deriving from the collapse of the primary subfield interposed between prethalamic and thalamic anlagen and corresponding to the ZLI. Such expression seems to be crucial to the subsequent subdivision of the anterior brain, promoting the activation of the transcription factors *Dlx2* and *Gbx2* in the ventral and dorsal thalamus, respectively (reviewed in Kiecker and Lumsden, 2005).

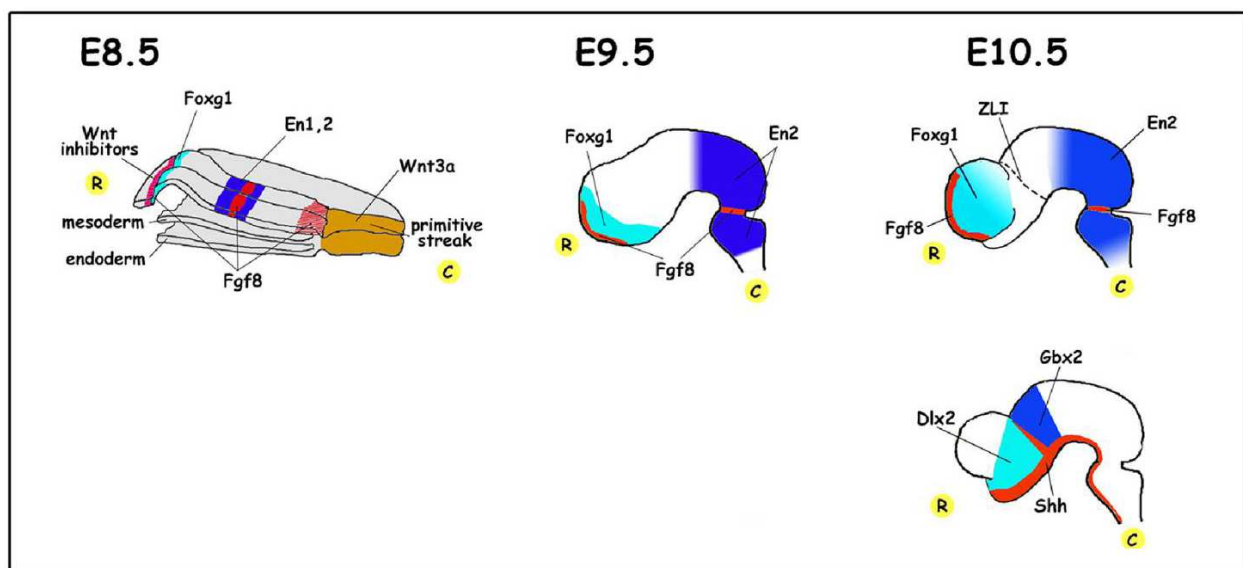


Fig 9 | Adapted from A. Mallamaci, unpublished lessons.

The dorso-ventral determination, starts from the expression of *Shh* around the Hensen's node, at the anterior end of the primitive streak and near the caudal edge of the forming neural plate. Such early *Shh* expression commits the whole anterior neural plate to express *Nkx2.1*, a transcription factor specifying ventral identity (Fig. 10a). Then, Wnts factors, secreted at the border between the neural folds and the ectodermal field, activate dorsal, i.e. cortical, genes such as *Pax6* and, at the same time, antagonize *Shh* effects, so inhibiting *Nkx2.1* expression in the dorsal neural field (Fig. 10b). After the closure of the neural tube, retinoic acid (RA) synthesized by the adjacent lateral ectoderm has a pivotal role in the activation of striatum-specific genes (*Meis2*, *Gsh2*), between the domains of *Pax6* and *Nkx2.1*, which results in turn inhibited (Fig. 10c). Finally, *Fgfs*, secreted around the anterior neural midline, cooperate with Wnts to activate *Emx1* in presumptive cortex and protect *Nkx2.1* from RA-dependent inhibition in the globus pallidus anlage (Fig. 10d) (Gunhaga et al., 2003; Marklund et al., 2004).

D/V determination: secreted factors

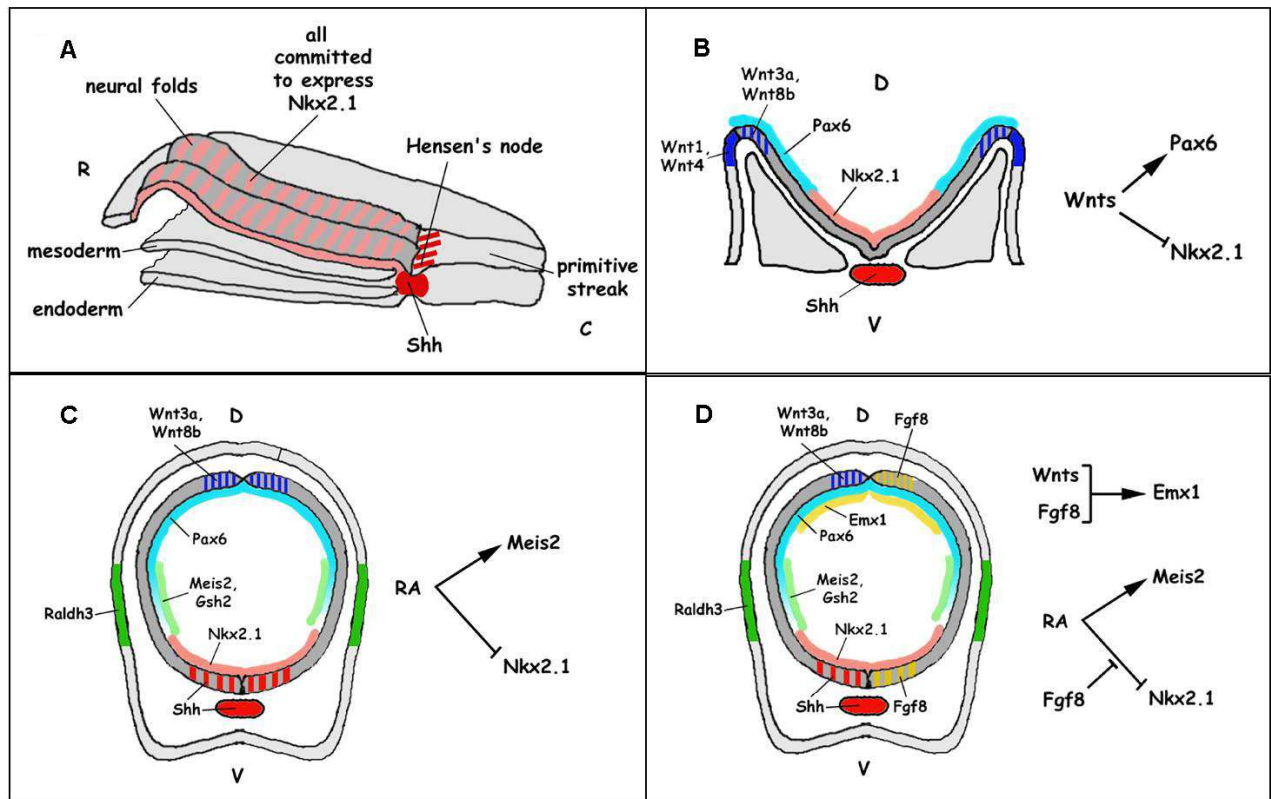


Fig 10 | Adapted from A. Mallamaci, unpublished lessons.

So, around E9.5/E10, several transcription factors conferring distinct positional identities to specific anatomical regions aligned along the dorso-ventral axis are differentially expressed along such axis, as shown in Fig. 11.

The importance of the correct function of these genes has been demonstrated by knocking-out them. In particular:

- In the absence of *Nkx2.1* the pallidal program collapses and the striatal field enlarges (reviewed in Rallu et al., 2003).
- In the absence of *Gsh2*, the striatal program collapses and pallidal and cortical anlagen are enlarged (reviewed in Rallu et al., 2003).
- In the absence of both *Emx2* and *Pax6*, cortical development collapses and a rudimentary structure with features intermediate between striatum and cortical hem develops (Muzio et al., 2002).

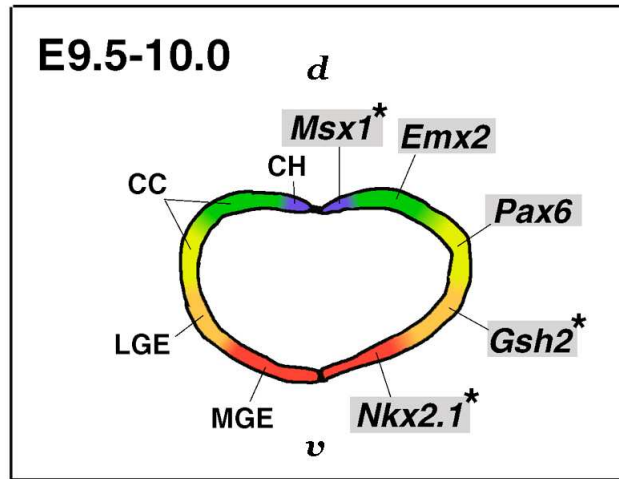


Fig 11 | Adapted from A. Mallamaci, unpublished lessons.

1.1.4 Models of regionalization of the cortical primordium

From embryonic day 7.5 (E7.5) onward the presumptive dorsal telencephalic field is progressively specified, thanks to a complex cascade of events involving secreted ligands released by the surrounding structures as well as transcription factors genes expressed by the field itself (Grove et al., 1998; Acampora et al., 1999; Muzio et al., 2002b; Kimura et al., 2005). The result of this specification, the cortical primordium of the E11 mouse embryo, looks like a thin neuroepithelial sheet and does not display any major region-specific morphological peculiarity.

Subsequently it undertakes a complex and articulated process of regional diversification and areal differentiation commonly termed “cortical arealization”, which leads to the development of the mature cerebral cortex.

Two main models have been proposed for the cellular and molecular mechanisms controlling cortical arealization: the protomap model (Rakic, 1998) and the protocortex model, suggested by Van der Loos & Woolsey (1973) and subsequently developed by O’Leary (1989).

According to the former, cortical arealization would occur on the basis of molecular cues intrinsic to the cortical proliferative layer. These cues would be transferred by periventricular neural progenitors, lying in distinctive cortical regions, to their neuronal progenies, migrating along fibers of radial glia and sharing with them the same rostrocaudal and mediolateral locations. According to the latter, the cortical primordium would not have any areal bias at all.

Arealization would take place on the basis of informations conveyed to the developing cortex by thalamocortical and other subcortical afferents (*tabula rasa model*). This information would be used to “write” distinctive areal programs onto the cortical primordium. Both models are supported by very robust bodies of experimental data, which resulted in a very hot scientific debate. Two main lines of evidence support the protomap model. First, explants taken from different regions of the cortical anlage at E10.5-E12.5 (before the arrival of thalamocortical projections), grown *in vitro* or heterotopically transplanted, appear specifically committed to express molecular markers peculiar to their region of origin (Arimatsu et al., 1992; Ferri & Levitt, 1993; Tole & Grove, 2001; Vyas et al., 2003). Second, the cortex of *Mash1* or *Gbx2* knock-out mice, constitutively lacking any thalamocortical projections, displays a normal molecular regionalization profile (Nagakawa et al., 1999; Miyashita-Lin et al., 1999). Two main lines of evidence also support the *tabula rasa* hypothesis. First, embryonic visual cortex transplanted to the parietal cortex (and thus possibly exposed to information coming from the thalamic

ventrobasal complex), acquires barrel features peculiar to the somatosensory cortex (Schlaggar & O'Leary, 1991). Second, chirurgical misrouting of visual information to adult somatosensory or auditory cortices makes these cortices to acquire architectonic and high-order functional properties peculiar to the visual cortex (Schneider, 1973; Frost & Schneider, 1979; Sur et al., 1998).

Presently, contrasts between supporters of tabula rasa and protomap models have been overcome and it is commonly accepted that two main phases can be distinguished in the process of cortical arealization. During the earlier, prior to the arrival of thalamocortical projections, molecular regionalization of the cortical primordium would occur on the basis of information intrinsic to this primordium, as in protomap model. During the latter, after the arrival of these projections (from E13.5 onward), cortical arealization would be refined based on information transported by thalamocortical fibres, as in protocortex model.

At the moment, two main classes of molecules are supposed to be crucial for early regionalization of the cortical primordium; secreted ligands, released around the borders of the cortical field, and transcription factors, gradually expressed within primary proliferative layers of this field. Secreted ligands would diffuse through the cortical morphogenetic field where they would be degraded according to specific kinetics, so generating variously orientated concentration gradients. Secreted ligands would regulate the expression of cortical transcription factor genes, in dose dependent manners, so accounting for the further generation of concentration gradients of these factors. Graded and transient expression of these factors would finally encode for positional values peculiar to distinctive regions of the cortical field.

1.1.5 Signaling centers involved in cortical arealization

Ligands are released around three structures lying at the borders of the cortical field and relevant for its arealization (Fig., 13) (Storm et al., 2006):

- The cortical hem, which forms between the cortical and the choroidal fields, at the caudomedial edge of the cortical neuroepithelial sheet;
- The commissural plate, at the rostromedial pole of telencephalon;
- The cortical antihem, a recently discovered signalling structure, which forms on the lateral side of the cortical field, at the pallial-subpallial boundary.

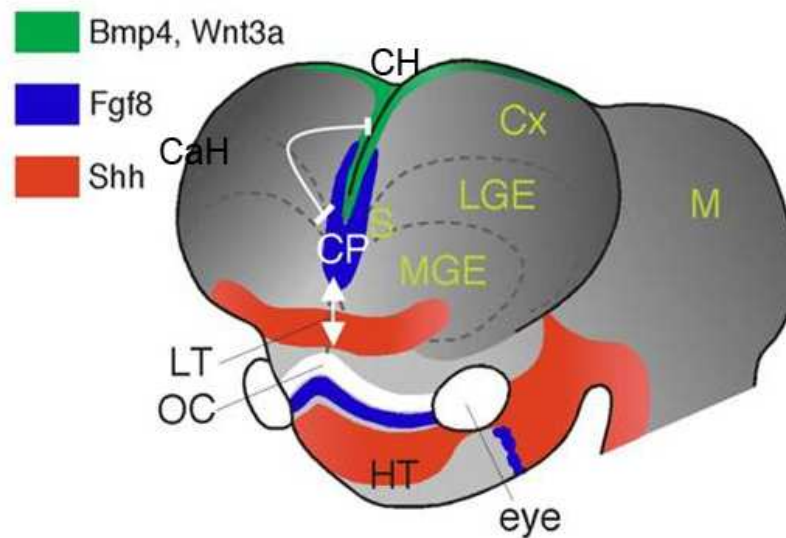


Figure 13 | Dose-dependent functions of *Fgf8* in regulating telencephalic patterning centers. Schema of a frontolateral view of the telencephalon showing the patterning centers as marked by expression of the genes indicated, the cross regulation between the *Fgf8* and *Bmp4/Wnt3a*-expressing centers, and the positive interactions between the *Fgf8* and *Shh*-expressing domains. CP, commissural plate; Cx, cortex; CH, cortical hem; CaH: cortical α -hem; HT, hypothalamus; LGE, lateral ganglionic eminence; LT, lamina terminalis; M, mesencephalon; MGE, medial ganglionic eminence; OC, optic chiasm; S, septum. (Adapted from Storm et al., 2006).

From E10, the cortical hem is a source of Wnts and Bmps, expressed in nested domains which also span the adjacent dorsomedial cortical field (Furuta et al 1997; Lee et al., 2000). Wnt signalling may normally promote the expansion of the archicortical progenitor pool (Fukuchi-Shimogori & Grove, 2001), further contributing to areal hippocampal determination (Machon et al., 2007). As for Bmps, little is known about the role of these ligands in telencephalic patterning, because the resulting phenotype was confounded by early defects in neural tube closure (Solloway & Robertson, 1999).

Bone morphogenetic proteins (Bmps) are phylogenetically conserved signaling molecules that belong to the transforming growth factor (TGF)- β superfamily and are involved in the cascades of body patterning and morphogenesis. Bmp receptors consist of heterodimers of inducible and constitutively active kinases of type I and II receptors, respectively. Both contain serine/threonine kinase domains and form heteromeric high-affinity complexes for BMPs to transducer external signals to an intracellular phosphorylation cascade.

Several Bmps are expressed in the mouse dorsal forebrain and facial primordia (Barlow and Francis-West, 1997; Furuta et al., 1997). It has shown that Bmps antagonize telencephalic rostro-medial programs. Ectopic application of Bmp4 to the ventral forebrain leads to holoprosencephaly in chick (Golden et al., 1999) and reduces expression of both *Shh* and *Fgf8*

(Ohkubo et al., 2002). Double knock-out of Chordin (CHRD) and Noggin (NOG), encoding for the secreted factors which specifically bind Bmp proteins and prevent ligation of their receptors (Sasai and De Robertis, 1997), results in severe forebrain truncations. Bmps have been also suggested to actively promote dorso-medial programs, as Bmp signalling and Wnt signalling synergically promote the transcription of a key transcription factor gene promoting cortical caudal-medial programs, *Emx2* (Theil et al., 2002). However, the electroporation of a transgene encoding for a constitutively active Bmp receptor 1a into the telencephalon as well as the conditional inactivation of *Bmpr1a* in this structure, while showing that *Bmpr1a* promotes choroidal vs. cortical specification, do not point to any apparent influence of Bmps on the subsequent regionalization of the cortical field (Panchision et al., 2001; Hebert et al., 2002).

Moreover, the electroporation of a transgene encoding for a constitutively active Bmp receptor 1a into the telencephalon as well as the conditional inactivation of *Bmpr 1a* in this structure showed that *Bmpr 1a* promotes choroidal vs. cortical specification, without exerting any apparent influence on the subsequent regionalization of the cortical field (Panchision et al., 2001; Hebert et al., 2002).

From earlier than E10 to ~ E12.5, the commissural plate and the surrounding regions release Fgfs secreted ligands, which have been predicted to promote rostral vs. caudal areal programs (Bachler & Neubuser, 2001). The electroporation of an *Fgf8* expressing plasmid into rostral telencephalon lead to a caudal shift of the parietal cortex. A rostral shift of the somatosensory cortex was conversely obtained when a plasmid encoding for a truncated form of the Fgf receptor 3, able to chelate Fgfs and to counteract them, was electroporated into the same region (Fukuchi-Shimogori & Grove, 2001). Moreover, telencephalon-restricted inactivation of the Fgf receptor gene *Fgfr 1a* results in olfactory bulb agenesis as well as in patterning defects of the frontal cortex (Hebert et al., 2003). Finally, homozygosity for a hypomorphic *Fgf8* loss-of-function allele elicits a sensible caudalization of the rostrocaudal cortical molecular profile, even in the absence of any apparent anomaly in the distribution of thalamocortical afferents (Garel et al., 2003).

Around E12.5 and afterwards, neural progenitors within the antihem specifically express five secreted signalling molecules: *Fgf7*, the Wnt-secreted inhibitor *Sfrp2* and three Egf-related ligands (Assimacopoulos et al., 2003). Even though their patterning activities on the cortex have not yet been characterized, the Egf family members seem to be involved in the regional specification of cortical areas associated with the limbic system. This is suggested by the up-regulation of the limbic system associated membrane protein LAMP occurring *in vitro*, in

nonlimbic cortical domains, in response to Egf family ligands (Ferry & Levitt, 1995; Levitt et al., 1997).

1.1.6 Transcription factors genes regulating area identity

Several transcription factors genes, including *Emx2*, *Emx1*, *Lhx2*, *Pax6*, *Foxg1* and *Coup-tf1*, are expressed by neural progenitors within periventricular proliferative layers, in graded manners along the tangential axes (Fig., 14) (Mallamaci and Stoykova, 2006).

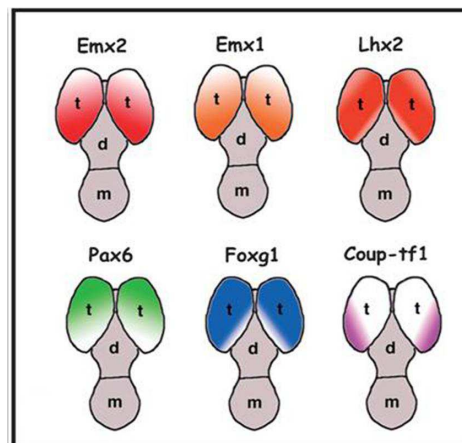


Figure 14 | Graded transcription factor genes in the early cortical primordium. E12.5 brains, dorsal views: t, telencephalon; d, diencephalon; m, mesencephalon. (Adapted from Mallamaci and Stoykova, 2006).

Furthermore the analysis of mice mutant for each of them has confirmed the hypothesis that these genes were crucial for imparting distinctive regional identities to neural progenitors.

The homeobox gene *Emx2*, expressed by the cortical primary proliferative matrix along a caudomedial^{high}-rostrolateral^{low} gradient, shapes the cortical areal profile as a promoter of caudomedial fates (Simeone et al., 1992; Gulisano et al., 1996; Mallamaci et al., 1998; O’Leary et al., 1994; Bishop et al., 2000; Mallamaci et al., 2000). In the absence of *Emx2*, the full repertoire of areal identities is preserved but caudomedial areas are shrunken and rostrolateral ones expanded. It was pointed out that abnormalities in cortical distribution of thalamic afferents taking place in *Emx2*^{-/-} mutants might reflect subpallial misrouting of these afferents rather than problems in their final cortical sorting and targeting (López-Bendito et al., 2002). However, the overall areal profile is finely tuned to the *Emx2* dosage: relative and absolute sizes of occipital areas of *Emx2*^{+/-} mutants are intermediate between null and wild-type mice and an expansion of caudal medial areas can be achieved by introducing one or better two alleles of a nestin-promoter-driven *Emx2*-expressing transgene into a wild-type genome (Hamasaki et al., 2004).

The *Emx2* paralog *Emx1* is expressed in the primary proliferative layer of the cortex along a gradient similar to that of *Emx2*. Its expression, however, is not confined to intermitotic

neuroblasts but extends into postmitotic glutamatergic neurons (Simeone et al., 1992). As such, it was suspected that *Emx1*, like *Emx2*, promoted cortical caudomedial fates and the analysis of double mutants confirmed this hypothesis (Shinozaki et al., 2004; Muzio and Mallamaci, 2003).

Pax6 encodes for an evolutionary conserved transcription factor, including two DNA binding motifs, a paired domain and a paired-like homeodomain. Its expression in the mouse begins at E8.0 and is restricted to the anterior surface ectoderm and the neuroepithelium of the closing neural tube in the regions of the spinal cord, forebrain and hindbrain (Walther & Gruss, 1991; Grindley et al., 1995). Within the telencephalon, *Pax6* is mainly expressed by the dorsal part and contributes to its pallial vs. subpallial specification (Stoykova et al., 1997). In the absence of functional Pax6 protein, as seen in the *Pax6* mutant *Small eye* (Hill et al., 1991), a progressive ventralization of the molecular identity of the pallial progenitors occurs (Stoykova et al., 2000; Kroll & O'Leary, 2005). Within the developing cortex, *Pax6* is expressed in a subpopulation of cortical progenitors, the radial glial cells (Götz et al., 1998). Remarkably, within the cortical periventricular proliferative layer, *Pax6* expression shows a rostralateral^{high}-caudomedial^{low} gradient (Stoykova et al., 1997; Muzio et al., 2002a). This suggests that *Pax6* plays a role complementary to that exerted by *Emx2* in the determination of cortical area sizes and of their distribution along the rostrocaudal axis of the cortex (Bishop et al., 2000).

The winged helix transcription factor gene *Foxg1*, expressed in the early telencephalon along a caudomedial^{low}-rostralateral^{high} gradient and relevant for basal ganglia morphogenesis as well as for cortical neuroblast differentiation, is also crucial for the proper laminar histogenetic progression of cortical progenitors (Xuan et al., 1995; Hanashima et al., 2002; Martynoga et al., 2005). In its absence, neocortical neuroblasts generate mainly preplate elements and only a few, poorly differentiated cortical plate cells, finally giving rise to an aberrant cerebral cortex where a large fraction of neurons express the Cajal-Retzius cell marker Reelin (Hanashima et al., 2004; Muzio and Mallamaci, 2005).

The LIM-box-homeobox gene *Lhx2* is expressed in the whole telencephalic neuroepithelium except the cortical hem, along a caudomedial^{high}-rostralateral^{low} gradient. As for regionalisation control, first, it represses fimbriochoroidal programs, committing neuroblasts within the dorsal telencephalon to cortical fates (Bulchand et al., 2001; Monuki et al., 2001), second, within the cortical field, it promotes hippocampal and neo-cortical vs. paleocortical programs (Vyas et al., 2003). In the absence of *Lhx2*, the choroidal region and the cortical hem are considerably enlarged (Bulchand et al., 2001; Monuki et al., 2001), the residual pallium fails

to activate archicortical markers and the same pallium conversely expresses specific sets of markers normally limited to ventral pallium (Bulchand et al., 2001; Vyas et al., 2003).

The nuclear receptor gene *Coup-tf1* is specifically restricted to the caudolateral cortex. Its inactivation leads to a complex areal phenotype, including an enlargement of hippocampus at expenses of paleocortex, plus a reshaping of neocortex, with a collapse of primary sensory areas and a dramatic expansion of frontal motor areas (Fig., 15), (Armentano et al., 2007).

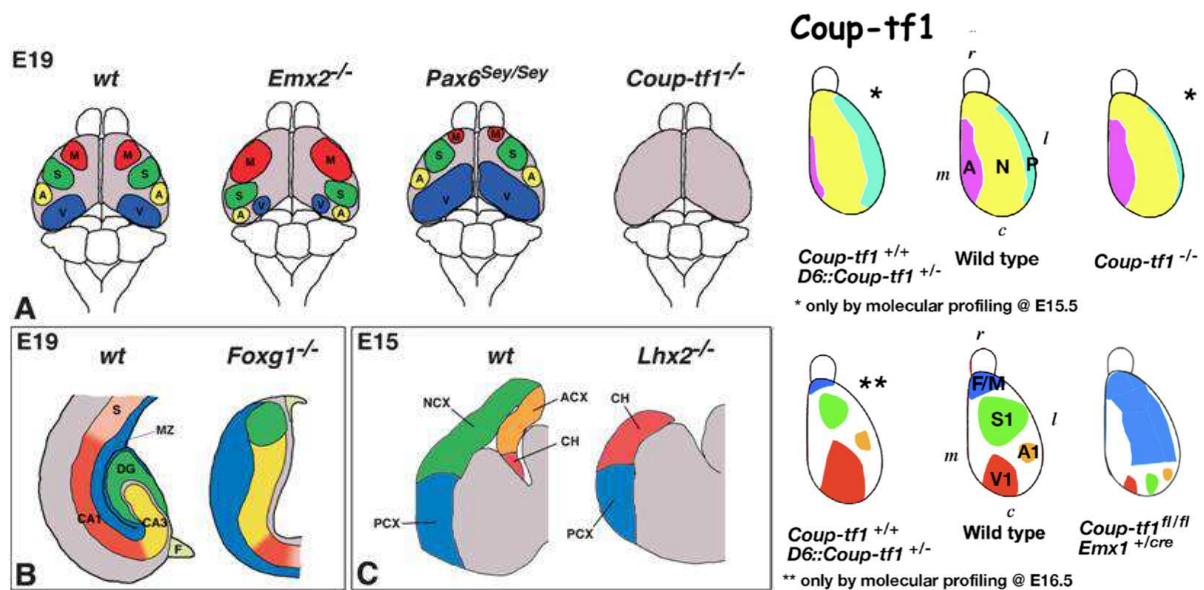


Figure 15 | Areal phenotypes of mice knock-out for the graded transcription factors (A) *Emx2*, *Pax6* and *Coup-tf1*, (B) *Foxg1* and (C) *Lhx2*. (A) E19 brains, dorsal views: M, motor cortex; S, somatosensory cortex; A, auditory cortex; V, visual cortex. (B) E19 brains, mid-frontal sections: S, subiculum; CA1, cornu ammonis 1 field; CA3, cornu ammonis 3 field; DG, dentate gyrus; F, fimbria; MZ, marginal zone. (C) E15 brains, frontal sections: CH, cortical hem; ACX, archicortex; NCX, neocortex; PCX, palaeocortex. (Adapted from (Adapted from Mallamaci and Stoykova, 2006; Muzio and Mallamaci, 2005; Mallamaci, unpublished lessons; Armentano et al., 2007).

1.1.7 Role of *Emx2* in mouse cerebral cortex development

Emx2 is one of the two vertebrate homologues of the *Drosophila melanogaster empty spiracles* homeodomain transcription factor. It was originally found in mouse and man (Simeone et al., 1992a,b) and subsequently isolated in chicken (Mallamaci, unpublished data; Fernandez et al., 1997), frog (Pannese et al., 1998), and fish (Morita et al., 1995; Patarnello et al., 1997). It is expressed in the central nervous system where it plays a critical role in brain and skeletal development, as well as in urogenital tissues during development, with mRNA evident in the earliest stages of differentiation in the primordia that will give rise to the kidneys, gonads, and genital tract.

The onset of expression of *Emx2* in mouse embryonic CNS is around E8.0-E8.5 (Gulisano et al., 1996). In mouse embryo, *Emx2* is expressed predominantly in extended regions of the developing rostral brain, including the presumptive cerebral cortex, olfactory bulbs and olfactory epithelium. It is also expressed in the inner ear and digit primordia, as well as in adult ovary testis (Simeone et al., 1992) (Fig., 16).

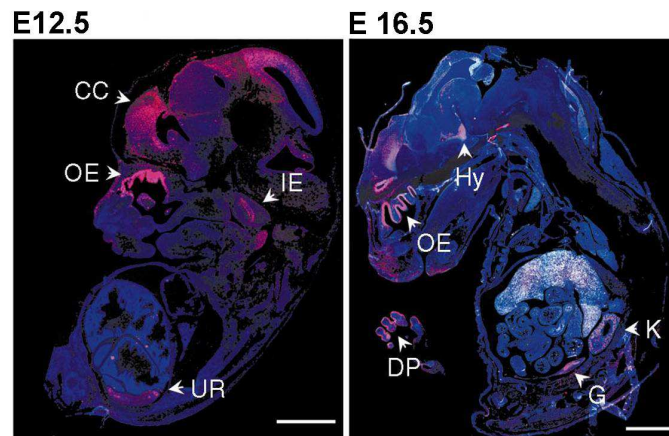


Figure 16 | *Emx2* expression profile. In situ analysis on sagittal sections of embryonic day 12.5 (E12.5) and E16.5 mouse embryos shows that *Emx2* gene is highly expressed in the telencephalon, particularly in cerebral cortex (CC) and olfactory epithelium (OE) from the very beginning of their development. Later on, at E16.5 a strong signal for *Emx2* is detected in the hypothalamus (Hy) (diencephalon), in the IE, in the digits primordia (DP), and in the gonads (G) and K. Scale bars, 1 mm in the E12.5 embryos and 4 mm in the E16.5 embryos. Abbreviations: OB, olfactory bulb; UR, uro-genital ridge. (Adapted from Simeone et al., 1992).

Emx2 is one of the earliest dorsal markers for the developing cerebral cortex. From E8.5, a signal is visible in anterior dorsal neuroectoderm regions of the embryo. By E9.5, the expression domain extends to the olfactory placodes, and is delimited by an anterior boundary, which overlaps that of *Emx1*, and a posterior one, which is located within the roof of the presumptive diencephalon. From E10.0 and during the formation of cerebral cortex, *Emx2*-mRNA is detectable only in the neuroepithelium, whereas it is absent from most post mitotic neurons of the TF and CP, as confirmed by bromo-deoxyuridine (BrdU) pulse-labeling experiments (Gulisano et al., 1996). At E12.5, *Emx2* expression in this layer follows a gradient along the anterior-posterior axis, which becomes more pronounced from E14.5 onwards (Simeone et al., 1992; Gulisano et al., 1996). The signal appears to be stronger in the posterior dorsal telencephalon, where it shows a sharp boundary, and gradually decreases in intensity in anterior and ventrolateral regions. Moreover, the distribution of the *Emx2* protein (EMX2) follows the same anterior-posterior and medial-lateral gradient (Fig., 17) (Mallamaci et al., 1998).

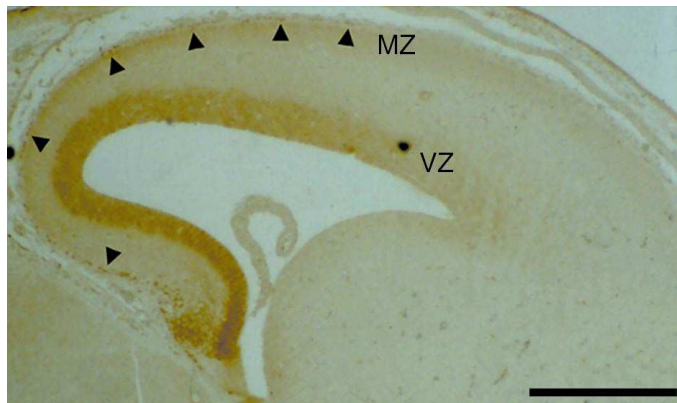


Figure 17 | Immunohistochemical analysis showing a coronal section of an embryonic-day 15.5 mouse cerebral cortex. EMX2 distribution covers the ventricular zone (VZ) and the marginal zone (MZ) where Cajal–Retzius cells lie (arrowheads). EMX2 seems to participate in the cascade mediated by reelin and to regulate neuronal radial migration across the cortical plate. Scale bar, 0.5 mm. (Adapted from Mallamaci et al., 1998).

Interestingly, cortical neurogenesis follows the opposite gradient, with a rostral-lateral maximum and a caudal-medial minimum (Bayer and Altman, 1991). EMX2 might therefore have a role either as an inhibitor of cell proliferation or as a positive regulator of cell differentiation. Graded expression of *Emx2*, both at the mRNA and protein levels, indicates the gene contributes to cortical polarity, cell identity and patterning in an early arealization process that takes place in the VZ (O’Leary et al., 1994). Finally, the localization of EMX2 in the proliferative layer of the forming cerebral cortex suggests a potential role for this protein in the control of neuronal migration of cortical neuroblasts, as well as in the preparation of their subsequent differentiation.

The early graded expression of *Emx2* in the VZ suggests that it could be involved in controlling early, thalamus-independent phases of cortical arealization and the phenotype of *Emx2*^{-/-} mice confirms this hypothesis and indicates a role in lamination. In *Emx2*^{-/-} mice, rostral-lateral areas, where *Emx2* is poorly expressed (Mallamaci et al., 1998), were enlarged and caudally shifted (Bishop et al., 2002; Mallamaci et al., 2000), while caudal-medial areas, where *Emx2* products are normally very abundant (Gulisano et al., 1998, Mallamaci et al., 1998) were strongly reduced (Mallamaci et al., 2000), indicating the involvement of *Emx2* in the caudal-medial area identity determination (Fig.,18).

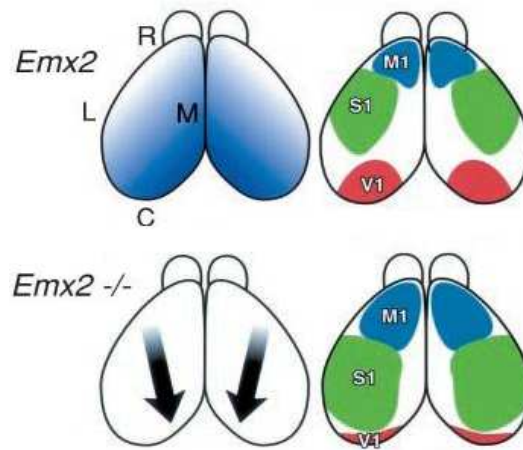


Figure 18 | Hypotheses, predicted results, and interpretations of analyses in this study. Diagrams are of dorsal views of the mouse neocortex. *A*, Graded expression patterns of the transcription factors *Emx2*, across the embryonic neocortex. *Emx2* is expressed in a high caudomedial to low rostralateral gradient. *Arrows* indicate the direction of the predicted shifts in markers of area identity in loss-of-function mutants. *On the right*, Organization of the mouse neocortex into areas predicted by our findings. Motor (*M1*), Somatosensory (*S1*) and Visual (*V1*) areas are shown. *C*, Caudal; *L*, lateral; *M*, medial; *R*, rostral. (Adapted from Mallamaci et al., 2000).

In the absence of *Emx2*, indeed, tangential expansion rates of the pseudostratified ventricular epithelium (PVE) are reduced. The first reason is that cortical progenitors proliferate slower: in *Emx2*^{-/-} mice, there is an elongation in neuroblast cycling time (T_C) due to lengthening of T_S (DNA synthesis phase). Due to T_C elongation, the proliferative pool of the mutant caudal-medial cortex “loses” one cell cycle out of four/five, with respect to its wild type counterpart.

Moreover, cortical progenitors leave cell cycle more frequently. So, because of exaggerated neuronal differentiation, the caudal-medial proliferating pool is deprived of its components at even doubled rates. Those kinetic changes are associated to increased proneural/antineural gene expression ratio, down-regulation of lateral inhibition machinery and depression of canonical Wnt signalling. Remarkably, by pharmacologically reactivating Wnt signaling in *Emx2*^{-/-} mutants, the neurogenic rates are rescued. Wnt and Bmp signalling synergically promote *Emx2* transcription, through a beta-catenin/Smad1,4 binding module located within the *Emx2* telencephalic enhancer (Theil et al., 2002). In turn, *Emx2* up-regulates the final output of the canonical Wnt-signaling machinery, thanks to concerted modulation of ligands (*Wnt3a*, *Wnt8b*, *Wnt5a*, *Wnt2b*), surface receptors (*Fzd9*, *Fzd10*), intracellular beta-catenin agonists (*Lef1*) and intracellular beta-catenin antagonists (*Groucho*) (Muzio et al., 2005).

In this way, near the cortical hem, a positive regulatory loop establishes between *Emx2* and Wnt signaling, crucial for proper sizing of occipital cortex and hippocampus. All these

phenomena are much more pronounced in caudal-medial than in rostral pallium, substantially contributing to selective hypoplasia of occipital cortex and hippocampus in the late gestation *Emx2* null embryos.

Radial migration of cortical plate neurons is specifically affected in *Emx2*^{-/-} mice, similar to that observed in *reeler* mutant mice. In *reeler* mice, early cortical plate neurons do not penetrate the preplate, which is not split in marginal zone and subplate and give rise to the so-called super-plate.

Moreover, late born cortical plate neurons do not overcome earlier ones, so that the classical inside-out rule is not followed. In *reeler* mutants, these migratory defects originate from constitutive functional ablation of the *Reln* gene, whose expression in the cortical marginal zone is necessary and sufficient to properly orchestrate neocortical neuron layering (D'Arcangelo et al., 1995). In the *Emx2*^{-/-} marginal zone, *Reln* mRNA expression is apparently normal at E11.5, it is reduced at E13.5 and completely absent since E15.5. In the same mutants, early phases of cortical plate radial migration are poorly affected whereas late phases are impaired in a *reeler*-like way (Mallamaci et al., 2000). It is reasonable to hypothesize that the same Cajal-Retzius neurons do not require the products of *Emx2* at the very beginning of their life and only subsequently become dependent on them for surviving and/or retaining their proper differentiation state. However, the increase of the absolute total number of *Reln*-expressing cells taking place in wild-type animals between E11.5 and E15 (Alcantara et al., 1998), as well as E10.5-E19 and E12-E19 birthdating-survival data (Mallamaci et al., 2000), suggest that at least two different populations of *Reln*-expressing cells do exist, which can be operationally distinguished on the basis of their dependence on *Emx2* function. We have an early transient population, prevalently generated before E11.0 and not dependent on the *Emx2* function, and a later one, still detectable at approximately birth, prevalently generated after E11.5 and dependent on the *Emx2* function for crucial steps of its development.

Furthermore, the caudomedial telencephalic wall and the cortical hem are one of the main sources of neocortical *Reln*-positive Cajal-Retzius (CR) cells (Takiguchi-Hayashy et al., 2004), being the other two the ventral pallium and the septum (Bielle et al., 2005). Cortical hem-born CR cells tangentially migrate beneath the pia mater, in an overall posterior-anterior direction, and finally distribute throughout the entire neocortex, along a caudomedial-high to rostromedial-low gradient. Embryos lacking *Emx2* display an impaired development of their cortical caudomedial region. Thus, absence of CR cells in these mutants may be a subset of this regional phenotype,

possibly arising from dramatic size-reduction of the caudal-medial proliferating pool that generates them.

Finally, *Emx2*, together with *Pax6*, plays a key role in telencephalic development as promoter of cortical versus non cortical morphogenetic programs. Indeed, if the two homeobox genes, normally expressed at high levels in the developing cortical primordium, are inactivated, (Fig., 19) (Muzio and Mallamaci, 2003) the telencephalic pallial neuroblasts are respecified as subpallial neuroblasts and this is followed by formation of an additional striatum-like structure in place of the cerebral cortex (Muzio et al., 2002).

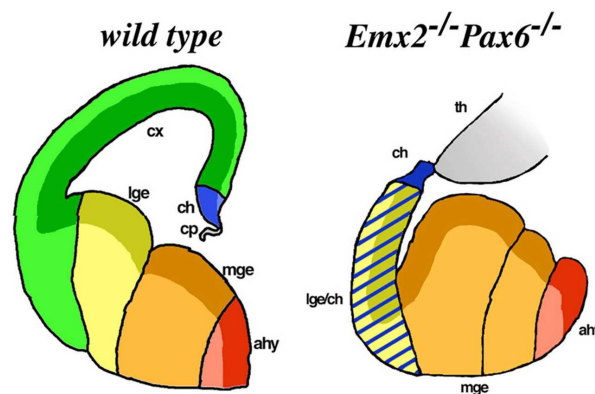


Figure 19 | Area identity shifts in cerebral cortices of perinatal *Emx2*^{-/-} and *Pax6*^{-/-} brains, dorsal views. telencephalic wall: choroid plexus (cp, gray); cortical hem (ch, blue); cortex (cx, green); lateral ganglionic eminence (lge, yellow); medial ganglionic eminence (mge, brown); anterior hypothalamus (ahy, red). VZ is in dark color, extraventricular layers in light color. (Adapted from Muzio and Mallamaci, 2003).

As for the role of *Emx2* in controlling neural precursors proliferation and differentiation kinetics, published data are not fully consistent. Acute inspection of embryonic brains and short term analysis of neural stem cells derived from them indicate that *Emx2* promotes cell cycle progression and inhibits premature neuronal differentiation (Heins et al., 2001; Muzio et al., 2005). Kinetic profiling and molecular analysis of perinatal neural stem cells upon their long term in vitro culture gives opposite results (Gangemi et al., 2001; Galli et al., 2002; Gangemi et al., 2006). Molecular and cellular mechanisms underlying these apparent inconsistencies are presently unknown. It is possible that, depending on the stage, embryonic or post-natal, *Emx2* may undergo different post-translational covalent modifications or also may be bound by different age-specific co-factors. That might modify its recruitability to distinct chromatin loci and/or its transcription trans-modulating properties, so making it alternatively able to promote neural precursors self-renewal or neuronal differentiation.

1.2 Natural Antisense Transcripts (NATs) in the genome

1.2.1 Antisense transcription: structural and functional aspects

Natural antisense transcripts (NATs) are endogenous RNA molecules containing sequences that are complementary to other transcripts. The role of antisense RNAs in regulating gene expression is well established in prokaryotic systems. The first cellular antisense RNA, *micF*, was identified in *E. Coli* in 1984 and was shown to repress translation of its target, *OmpF* mRNA, through base pairing with its 5'-end (Coleman et al., 1984). Since then other antisense RNAs have been described in bacteria and have been shown to repress (and in some cases activate) gene expression through RNA-RNA base pairing (Wagner and Flardh, 2002). Recently, a large number of Natural Antisense Transcripts (NATs) have been described in mice and humans. Antisense transcripts in eukaryotes are remarkably diverse. They can be distinguished by size, coding potential and orientation with respect to complementary target sequences. The term “antisense regulation” generally refers to regulation of expression of an RNA target through direct base pairing with a complementary RNA. NATs can be divided into *cis*-NATs, which are transcribed from opposing DNA strands at the same genomic locus, and *trans*-NATs, which are transcribed from separate loci (for example the micro-RNAs).

cis-NAT pairs display perfect sequence complementarity (as expected from their genomic overlap), whereas *trans*-NAT pairs display imperfect complementarity and can therefore target many sense targets to form complex regulation networks (Li *et al*, 2006). Conventionally, the term sense transcript refers to the protein-coding version in cases where only one partner of the sense/antisense pair (S/AS) is a non coding RNA (ncRNA). When both are either non-coding or coding, the distinction is arbitrary. Generally, the sense gene is presumed to be the more abundant and more widely expressed partner that usually has a better characterized or more direct function (Munroe et al., 2006). Often, the sense strand is considered the one that undergoes splicing or has longer intronic sequences (Chen et al., 2005).

Not surprisingly, an huge amount of contribution in antisense transcription comes from non coding RNAs (ncRNAs) and it is a question of common agreement that the dominant fraction of NATs is made up of ncRNA. Moreover, several studies have shown that a significant amount of NATs are not polyadenylated and have a restricted nuclear localization (Cheng et al., 2005; Katayama et al, 2005; Kiyosama et al., 2005).

The importance of NATs is now apparent, and their widespread prevalence has been reported in many genomes. *cis*-NATs can be categorized according to their relative orientation and degree of overlap: head-to-head or divergent (overlapping 5' ends), tail-to-tail or convergent (overlapping 3' ends), or fully overlapping (one gene included within the region of the other), (Fig., 20) (Lapidot & Pilpel., 2006).

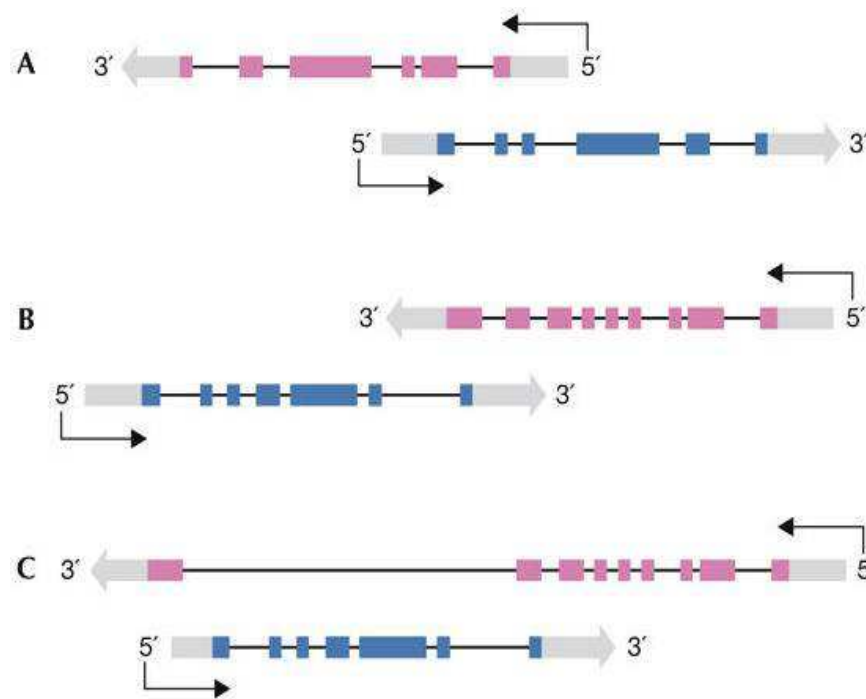


Figure 20 | Relative orientation of *cis*-natural antisense transcript pairs. (A) Head to-head (5' to 5') overlap involving 5'-untranslated regions and coding exons. (B) Tail-to-tail (3' to 3') overlap. (C) Fully overlapping (one gene included entirely within the region of the other). Coloured boxes represent exons, grey boxes represent untranslated regions. (Adapted from Lapidot & Pilpel., 2006).

While earlier works reported convergent S/AS pairs to be more prevalent in the mammalian genome (Lehner et al., 2002; Shendure et al., 2002; Yelin et al., 2003; Chen et al., 2004; Veeramachaneni et al., 2004), more recent studies argue in favour of the divergent orientation (Katayama, et al., 2005; Li et al., 2006; Zhang et al., 2006; Finocchiaro et al., 2007).

Several studies conclude that NATs tend to be expressed in a cell/tissue-specific manner and/or display a tendency to be linked to the expression pattern of their sense counterparts (Bertone et al., 2004; Chen et al., 2004; Richards et al., 2006; Werner et al., 2007). Their expression pattern is also time dependent, a finding that is corroborated by few specific examples of antisense transcripts implicated in embryonic development and cancer progression (Ross et al., 1996). There is increasing evidence that gene order in eukaryotic genomes is not random (Hurst et

al., 2004; Poyatos et al., 2006; Sémon et al., 2006), and genes that have similar and/or coordinated expression are often clustered along the genome. Co-expression can be mediated on the small scale by usage of shared regulatory elements, like common enhancers or bidirectional promoters (Adachi et al., 2002; Trinklein et al., 2004; Carninci et al., 2006; Li et al., 2006; Lin et al., 2007), or, on a larger scale, *via* chromatin-mediated processes (Gierman et al., 2007; Purmann et al., 2007; Kalmykova et al., 2005; Sproul et al., 2005).

Although previous analysis of the mammalian transcriptome suggested that up to 20% of transcripts may contribute to sense –antisense (S/AS) pairs (Kiyosawa et al., 2003; Yelin et al., 2003; Chen et al., 2004), recent studies indicate that antisense transcription is more widespread (RIKEN Genome Exploration Research Group, Genome Science Group and the FANTOM Consortium 2005). Basic studies using mRNA and expressed sequence tag (EST) libraries combined with information like exon-intron splicing structures and poly(A) signals, estimated the extent of the NAT phenomenon in mammals to be in the range between 15 and 25 % of all transcriptional units (Li et al., 2006; Yelin et al., 2003). However, because there is only partial overlap among published data sets, and because a large fraction of non-polyadenylated and unspliced NATs is generally excluded from these studies (for the sake of higher stringency), it is highly likely that numbers of NATs are considerably higher. Many complementary sources of expression data including cap analysis of gene expression (CAGE), serial analysis of gene expression (SAGE), massively parallel sequencing of cDNA pools, and tiling arrays, give rise to an expansion of NATs in the mammalian transcriptome (Kampa et al., 2004; Ge et al., 2006). It has been estimated that at least 40% of all transcriptional units may have concurrent overlapping antisense partners (Engström et al., 2006).

One of the most fundamental criteria used to distinguish long ncRNAs from mRNAs is ORF length. Since short putative ORFs can be expected to occur by chance within long non-coding sequences, minimum ORF cutoffs are usually applied to reduce the likelihood of falsely categorizing ncRNAs as mRNAs. For instance, the FANTOM consortium originally used a cutoff of 300 nt to help identify putative mRNAs (Okazaki et al., 2002). However there are some exceptions. *H19*, *Xist*, *Mirg*, *Gtl2* and *KcnqOT1* all have putative ORFs >100 codons, but have been characterized as functional ncRNAs (Prasanth et al., 2007). Applying a traditional ORF cutoff of 300 nt will therefore misclassify many ncRNAs as mRNAs, and this is especially true for very long ncRNAs (Fig., 21) (Dinger et al., 2008).

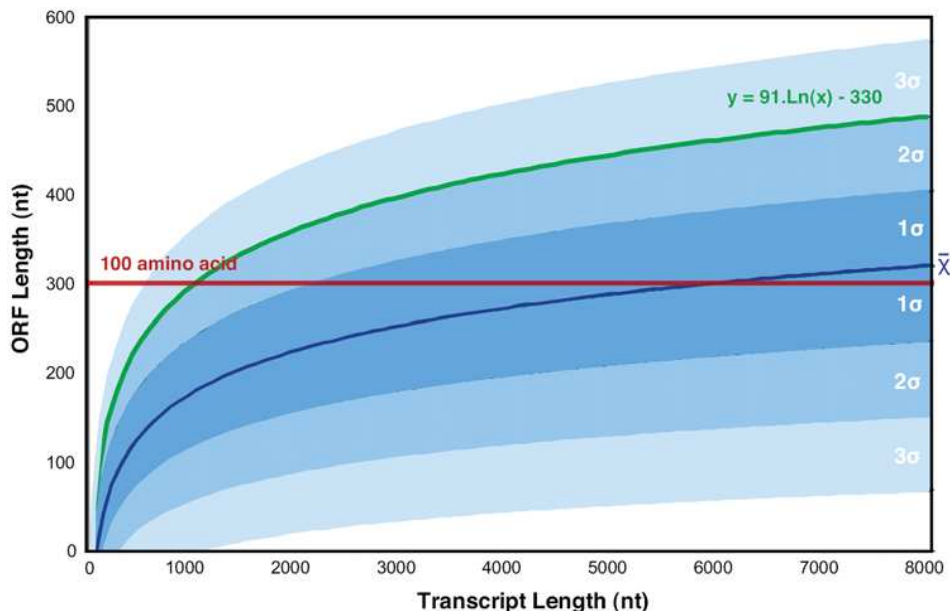


Figure 21 | Incidence of open reading frames (ORFs) in randomly generated transcripts of increasing length. Twenty thousand transcripts of varying length and random nucleotide composition were computationally generated and scanned for ORFs. The maximum ORF and transcript lengths were plotted and fitted to a logarithmic curve. The shaded regions represent incidences of randomly occurring ORFs at 1, 2, or 3 standard deviations from the mean. The red line indicates the 300 nt ORF threshold that is commonly used to distinguish protein-coding genes in transcript classification pipelines. Therefore, this plot illustrates that for transcripts longer than ,1000 bp, such a threshold may define transcripts as protein-coding that would be expected to occur by chance. The function $y = 91.Ln(x) - 330$, which approximates random ORF incidence according to transcript length at two standard deviations above the mean (i.e., 95% confidence interval, indicated in green), could be used to discriminate noncoding from protein-coding transcripts in a transcript-length-dependent manner. (Adapted from Dinger et al., 2008).

For example, murine *Xist* is ~15 Kb in size (Brockdorff et al., 1992) and contains a putative ORF of 298 aa, which led to the erroneous conclusion that it was a protein-coding gene when first discovered (Borsani et al., 1991). To avoid errors, a few methods have been introduced to detect ORF conservation and distinguish ncRNAs from mRNAs on a transcriptome-wide scale. The combination of different complementary strategies, such as computational methods and artifact filtering, can be used to obtain the better effect. For example, the program CRITICA, uses statistical techniques in addition to its comparative approach (Badger et al., 1999) and was the best-performing of ten bioinformatic methods used to discriminate ncRNAs and mRNAs from the FANTOM cDNA collection (Frith et al., 2006).

A number of other programs use sophisticated statistical approaches based on integrating a range of characteristic protein-coding signatures, including splice acceptor/donor sites, polyadenylation signals, ORF length, and sequence homology. For example, to discriminate coding regions, DIANA-EST employs a combination of artificial neural networks and statistical approaches (Hatzigeorgiou et al., 2001). Two recently described tools, CPC and CONC, use

supervised learning algorithms known as support vector machines to distinguish mRNAs from ncRNAs (Liu et al., 2006; Kong et al., 2007). These algorithms take into consideration multiple features such as peptide length, amino acid composition, protein homologs, secondary structure, and protein alignment information. Both showed high levels of accuracy when cross-validated against reference protein and ncRNA datasets, and are likely to represent the vanguard of future discrimination methods.

The relative length of ncRNAs is also an index of their proper function, *cis* or *trans*, respectively: *trans*-acting functions are associated with short ncRNAs, such as short interfering (si) RNAs (21 nt), micro (mi) RNAs (~22 nt), piwi-interacting RNAs (26-31 nt) and short nucleolar (sno) RNAs (60-300 nt). By contrast, *cis*-acting functions have so far only been associated with macro ncRNAs. Interestingly, whereas the number of protein-coding genes is no indication of an organism's morphological complexity, macro ncRNA number increases with complexity, indicating a potential functional role in gene regulation (Amaral and Mattick, 2008).

1.2.2 Antisense function

Conservation of NATs across kingdoms, (Wagner & Flardh, 2002) implies that they might constitute a common mechanism for regulating gene expression. Based on various relationships occurring among AS expression levels and those of their sense partners, it has been predicted that the former ones might differentially promote or antagonize the expression of such partners, depending on the gene and on the context. Such prediction has been substantially confirmed in a variety of functional studies, indicating that: (1) AS transcription is not simple transcriptional noise or epiphenomenon of S transcription (He et al., 2008), but often results a prerequisite for proper regulation of “coding” sense genes; (2) molecular mechanisms by which AS transcripts act are extremely complex and largely diversified (reviewed in Munroe and Zhu.; 2006, and Beiter et al., 2009). In some cases, poor sequence conservation but similar exon/intron organization characterizing antisense transcripts from different species suggests that transcription *per se* and not the AS RNA molecule may be crucial to the function.

That has been demonstrated in the case of the silent human retrovirus HERV-K18, where AS transcription promotes S transcription (Leupin et al., 2005), as well as in a variety of other cases, where AS transcription inhibits S transcription, because of competition between the two transcriptional machineries for shared cofactors, or due to collision between them (Mazo et al., 2007). However, the AS transcript may also *act as such*, playing at distinctive regulatory levels (some examples are shown in Fig., 22).

First, it may regulate the epigenetic state of chromatin: the non coding antisense RNA *Air* promotes cytosine-methylation and repression of the overlapping, paternally imprinted, *Igf2r* gene (Sleutels et al., 2001). Another non coding antisense RNA, *Kcnq1ot1*, recruits H3K9- and H3K27-methyltransferases to the overlapping, maternally methylated, *KvDMR1* gene (Pandey et al., 2008). Recruitment of a H3K27-methyltransferase is also elicited by *HOTAIR*, an antisense ncRNA encoded by the *HoxC* locus: here, however, the recruitment does not take place in *cis*, but in *trans*, at the paralogous *HoxD* locus (Rinn et al., 2007).

Second, the AS ncRNA may facilitate recruitment of transcription factors to enhancers impinging on the partner sense gene, so promoting its transcription. This is the case of the *Evf2* ncRNA. The *Dlx-5/6* ultraconserved region is transcribed to generate the ncRNA *Evf2*. *Evf2* specifically cooperates with *Dlx2* to increase the transcriptional activity of the *Dlx5/6* enhancer in a target and homeodomain-specific manner. A stable complex containing the *Evf2* ncRNA and the

Dlx2 protein forms *in vivo*, suggesting that the *Evf2* ncRNA activates transcriptional activity by directly influencing Dlx2 activity (Feng et al., 2006).

Third, the AS ncRNA may modulate the splicing of its partner sense pre-mRNA, as supposed for the *TRa2* and *Zeb2* loci (Hastings et al., 2000; Beltran et al., 2008).

Forth, AS transcripts may regulate the half-life of their sense partners. Pairing of retrotransposon sense and antisense transcripts paves the way to Dicer -dependent (Dicer is part of the RNaseIII-family protein) cutting of resulting dsRNAs. This is in turn followed by siRNA-instructed silencing of sense transcripts, from the same or paralogous loci (Tam et al., 2008; Okamura et al., 2008; Watanabe et al., 2008). Recent reports, in fact, have established that co-expressed sense transcripts/NATs are processed into short RNAs, the so called “endo-NATs” by analogy with the recently defined “endo-siRNAs.” It is not new that S/AS hybrids could potentially provide the templates for transcript cleavage involving Dicer, (Hausecker and Proudfoot, 2005) which forms the molecular basis for RNA interference (RNAi) (Ambros, 2004). Dicer cleaves the RNA duplex to produce siRNAs, which in turn catalyze cleavage of the corresponding mRNA.

Processing of NATs, implies that they are able to traffic within the nucleus and are deemed to be exported to the cytoplasm. Exonic complementarity, on the other hand, suggests that RNA hybridization represents an essential step in the processing of endo-NATs. The selective pressure favoring exonic complementarity suggests that the processing of endo-NATs involves hybridization with the sense transcript. Consequently, sense and antisense transcripts would have to be co-expressed in a single cell. Indirect evidence supports this scenario; for example, endo-NATs and the corresponding sense transcripts are enriched in the same cDNA libraries, a tendency that is not observed with sense/antisense transcript pairs that lack exonic overlaps. In addition, the same transcription factor binding sites are often found upstream as well as downstream of protein coding genes (Cawley et al., 2004), indicating potential co-regulation of sense and antisense transcripts expression (Werner et al., 2009).

Fifth, antisense RNAs may modulate translation. Bacteria for example, encode large numbers of small-non-coding RNAs (sncRNAs) (Majdalani et al., 2005; Romby et al., 2006; Storz et al., 2004) and translational repression has emerged as the primary mode of their action. It occurs at the level of translation initiation, by sncRNA binding to the 5' untranslated region (UTR) of a target. In order to repress translation initiation, an sncRNA has to successfully compete with the 30S ribosome for target mRNA binding. Following the block of translation, some target mRNAs are irreversibly inactivated by endonucleolytic degradation (Darfeuille et al.,

2007; Masse' et al., 2003; Morita et al., 2006). Moreover, sncRNA can also act repressing trans-encoded mRNAs by sequestering the 5' proximal part of the CDS of the target downstream of the AUG. (Bouvier et al., 2008). Presently, there are no cases of non coding-dependent-translational inhibition in mammals.

Sixth, antisense ncRNAs may be necessary for proper activity of their sense partners. This is the case of the best known functional mammalian macro ncRNAs, namely the *inactive X-specific transcript (Xist)* and *X (inactive)-specific transcript, antisense (Tsix)*. These are overlapping transcripts required for X chromosome inactivation in female mammals. They follow an epigenetic dosage compensation mechanism that equalizes X-linked gene expression between the sexes. *Xist* is expressed from, and localizes to, the inactive X chromosome, targeting repressive chromatin modifications and gene silencing to this chromosome. *Tsix* overlaps with the entire *Xist* gene in an antisense orientation and silences *Xist* on the active X chromosome (reviewed by Wutz and Gribnau, 2007). Pairing between *Xist*, the triggerer of mouse X-chromosome inactivation, and *Tsix*, its antisense partner, is a prerequisite for Dicer-dependent fragmentation of the resulting dsRNA, driving in turn the subsequent epigenetic changes which lead to X-inactivation (Ogawa et al., 2008).

Finally, there is a large number of AS ncRNAs, whose mechanisms of action have been not yet elucidated. Among them, there are the ncRNAs implicated in mammalian gene imprinting. About 90 genes in mouse show imprinted expression and their imprinted status is mostly conserved in humans. These genes include two *Igf2* (insulin-like growth factor 2) and *Dlk* (delta-like 1 homologue), paternally imprinted genes, and four-*Igf2r* (insulin-like growth factor 2 receptor), *Kcnq1* (potassium voltage-gated channel, KQT-like subfamily, member 1), *Gnas* (guanine nucleotide binding protein α stimulating) and PWS-AS (Prader-Willi and Angelman syndromes), maternally imprinted. Imprinted genes mostly occur in clusters that contain 2-12 genes, in most of these clusters at least one gene is a macro ncRNA and the imprinted macro ncRNA is often required for the imprinted expression of the whole cluster (Barlow and Bartolomei, 2007).

Imprinted expression of genes in a cluster is controlled by one *cis*-acting imprint control element (ICE) (Spahn et al., 2003; Lewis et al., 2006). Importantly, it is the ICE and not the imprinted genes themselves that carries parental information in the form of a DNA methylation imprint, which is acquired during male or female gametogenesis and maintained only on one parental allele after fertilization. Six well characterized clusters are known. Significantly, the parental chromosome carrying the unmethylated ICE is the one that expresses the ncRNA,

indicating that the ICE is a positive regulator of ncRNA expression (Spahn et al., 2003). In all six imprinted clusters, expression of the ncRNA correlates with the repression *in cis* of some or all of the imprinted protein-coding genes (O'Neill 2005; Pauler and Barlow, 2006). In this context, imprinted ncRNAs seem to be an ideal model to study this new level of gene regulation because they control expression of small groups of flanking genes. Although many features of the silencing effect generated by imprinted ncRNAs are known, the actual mechanism is not yet clear. In particular, it is not known whether imprinted ncRNAs silence through the transcript itself or through the act of transcription.

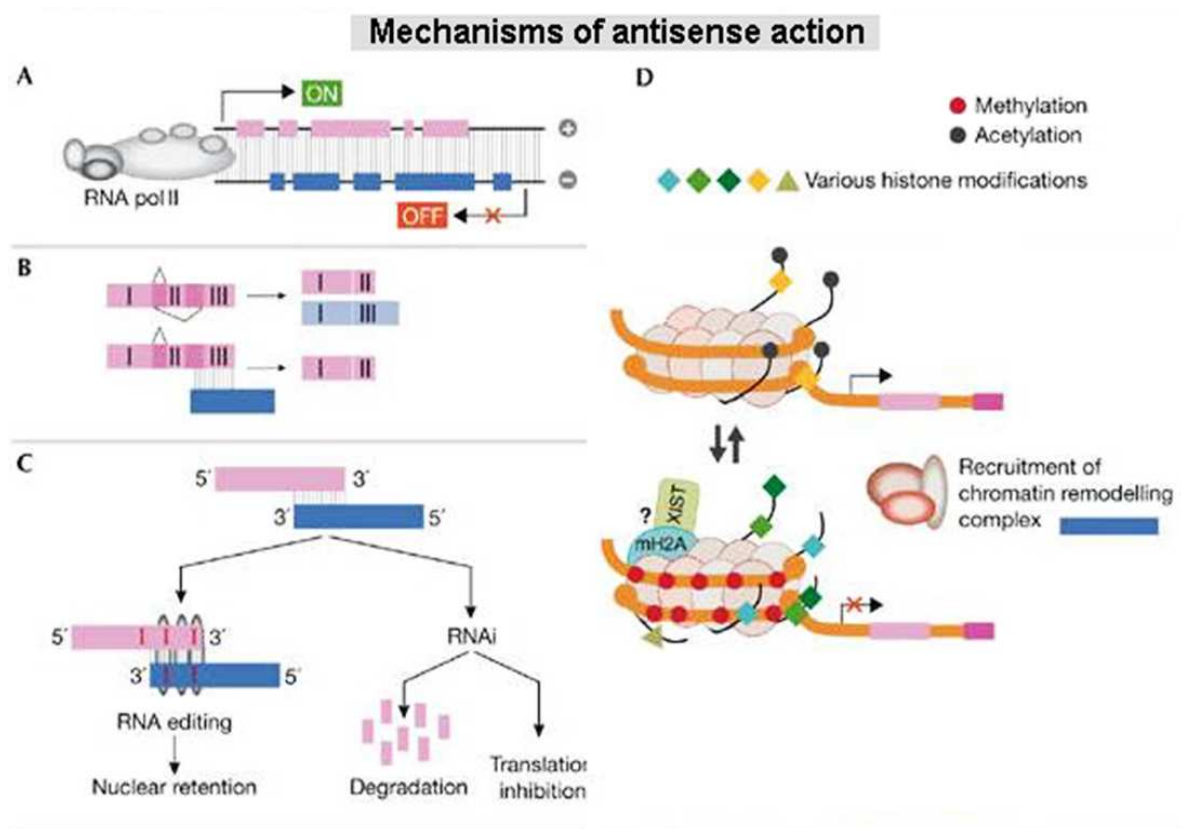


Figure 22 | Mechanisms by which natural antisense transcripts regulate gene expression. (A) Transcriptional interference. Two bulky RNA polymerase II complexes on opposite DNA strands might collide with and stall one another. The interference occurs mostly in the elongation step, resulting in either transcription arrest or transcription in one direction (sense or antisense) only. Such a mechanism might occur in cases in which inverse expression is observed. (B) RNA masking. A specific case is shown in which the antisense masks a splice site on the sense pre-mRNA sequence. (C) Double-stranded RNA-dependent mechanisms such as RNA editing and RNA interference require the simultaneous presence of sense and antisense transcripts for duplex formation, and might therefore account for the observed co-expression of numerous sense–antisense pairs. (D) Chromatin remodelling. Transcription of non-encoding antisense transcripts is involved in monoallelic gene expression. (Adapted from Lapidot and Pilpel, 2006). An additional list of genes undergoing NATs mechanisms' regulation is shown in table 1.

1.2.3 Antisense transcription in development

ncRNA and antisenseRNA are often associated to developmentally relevant genes. Among the first reported cases, there are non-coding transcription associated to *globin* and *immunoglobulin* genes (Ashe et al., 1997; Gribnau et al., 2000; Bolland et al., 2004). Remarkably, it was proposed that intergenic transcription in the *globin* gene cluster may contribute to the opening of large chromatin domains necessary for the proper developmental regulation of the *globin* genes (Gribnau et al., 2000), playing *in cis*. Moreover, intergenic transcripts in the human β -*globin* locus, upregulated in the absence of Dicer, could be indicative of RNAi-related silencing processes, where they would be the source of Dicer-dependent small RNA molecules, to be used for the targeting of silencing complexes (Hausecker and Proudfoot, 2005).

More recently, antisense transcripts have been described to be associated to a variety of transcription factor genes implicated in developmental processes, among which several homeobox-containing genes. A group of newly identified transcripts originating from the opposite strand of different homeobox-containing genes, playing their action *in cis*, was shown to be expressed in the embryonic and postnatal retina (Blackshaw et al., 2004; Alfano et al., 2005). One of these, the non coding *Vax2OS*, corresponds to the antisense of the homeobox-containing gene *Vax2* and its expression level was found to be significantly reduced in *Vax2*-null mice. Moreover, the adenoviral-mediated overexpression of *CrxOS* (predicted to encode a protein of 246 amino acids) in the mouse adult retina, leads to a significant decrease in the expression levels of the corresponding sense gene, the homeobox gene *Crx* (Alfano et al., 2005). The expression was restricted to the retina, also for *Otx2OS*, *RaxOS* and *Pax6OS*. *Six3OS* and *Six6OS* cDNAs instead, were detected in retina/brain and retina/skeletal-muscle, respectively.

Antisense transcripts are also associated to *Six3*, a homologue of the *Drosophila* homeobox gene *Optix*, playing a key role during vertebrate forebrain and visual system development (Olivier et al., 1995; Seimiya and Gehring, 2000; Lagutin et al., 2003; Liu et al., submitted), whose inactivation abolishes in the mouse telencephalon formation (Lagutin et al., 2003). This gene has been associated with eleven antisense transcripts (Alfano et al., 2005), whose expression was found in the optic cup of embryonic day 10.5 (E10.5) mouse embryos and also in the adult chicken and mouse retina (Blackshaw et al., 2004; Alfano et al., 2005). Among these transcripts, only *Six3OS1* contains a putative short open reading frame (ORF) predicted to encode a 200 amino acids long protein. The other ten opposite strand transcripts do not contain any putative ORFs and they are classified as non coding-RNAs. Non coding transcription may be

also fundamental for the opening and maintenance of the active state of HOX clusters. Antisense transcription from the intergenic spacer regions in the human HOXA cluster positively correlates with the activity state of adjacent HOXA genes in embryonic human carcinoma cells. This non-coding transcription is regulated by the retinoic acid morphogen and follows the collinear activation pattern of the cluster. Opening of the cluster at sites of activation of intergenic transcripts is accompanied by changes in histone modifications and a loss of interaction with Polycomb group (Sessa et al., 2007). Finally, AS transcripts are associated to *Msx1* mRNA, a key factor for the development of tooth and craniofacial skeleton. *Msx1* is negatively controlled by its antisense non-coding RNA (*Msx1*-ncRNA) at a post-transcriptional level and *Msx1*-ncRNA is in turn positively controlled by *Msx1*. The tight link between these two genes constitutes a regulatory loop resulting in a fine-tuned expression of *Msx1* which appears to be significant for adult mice homeostasis (Petit et al., 2009).

Intriguingly, antisense transcripts are often associated to genes which underwent accelerated evolution during the transition from ancestors of hominids and other primates to modern humans. Among genomic regions showing accelerated evolution since our divergence from chimpanzee there is *HAR1*, part of the first exon of a 2.8 kb spliced ncRNA termed *HARF1*, that is specifically expressed in Cajal-Retzius neurons in the developing human neocortex, as well as in ovary and testis. *HARF1* is coexpressed with *REELIN*, a protein that is critical for neuroblast migration from paramedian stem cell generative zones and for the specification of the layered structure of the human cortex. Remarkably, there are two alternatively spliced antisense transcripts *HAR1Ra* and *HAR1Rb*, which also contain the *HAR1* region in their first exon and which are expressed in the brain and testis, respectively (Pollard et al., 2006). The temporal and spatial pattern of expression of *HAR1R* suggests that it may have later developmental effects to downregulate *HAR1F* by antisense mediated inhibition. Interestingly, *reelin* exhibits enhanced expression during primate evolution (Molnar et al., 2006) and also undergoes A-to-I RNA editing (Levanon et al., 2004).

1.2.4 *Emx2OS* in mouse cerebral cortex development

Recently a transcript encoded by *Emx2* opposite strand was found both in human and mouse. This gene overlaps with *Emx2* head-to-head. The group that first discovered such a gene, called it *Emx2OS* (Fig., 23) (Noonan et al., 2003).

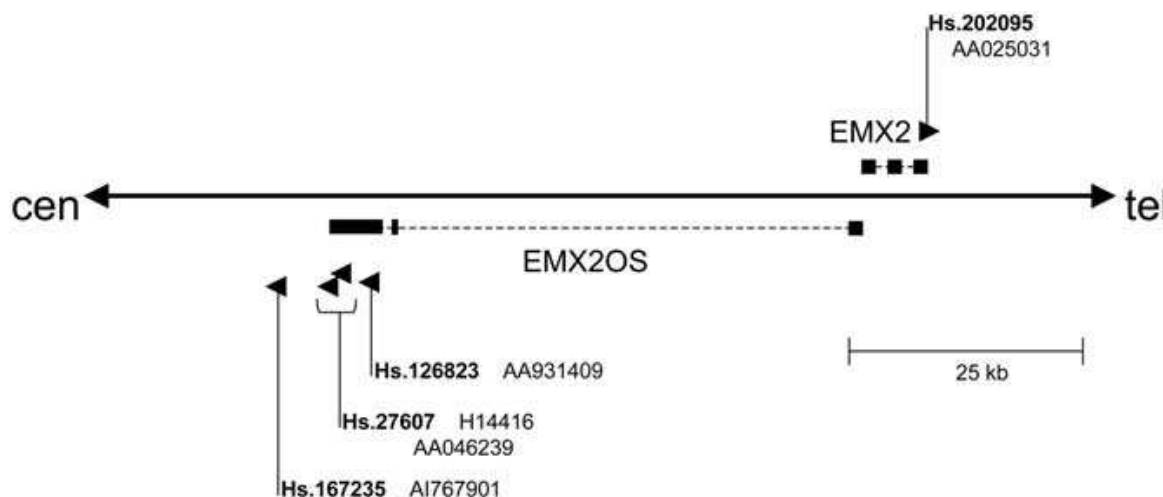


Figure 23 | Genomic location of ESTs expressed in the uterus and located within the 10q26 endometrial cancer deletion region. Above large arrow, black boxes represent exons of *EMX2*. Arrowhead is ESTAA025031 derived from *EMX2*. Below large arrow, black boxes are exons of *EMX2OS* composite cDNA linking three ESTs (AA931409, H14416, AA046239) together. The most 5_ *EMX2OS* exon overlaps with that of *EMX2*, and introns are indicated by a dotted line. EST AI767901 is also expressed in the uterus and represents an alternate 3_ end for *EMX2OS*. Arrowheads indicate the direction of transcription. The accession numbers for the ESTs used in expression analysis are indicated and their representative UniGene clusters are shown in bold. (Adapted from Noonan et al., 2003).

The human *Emx2OS* is expressed in adult uterus, kidney and brain and its length is 8.5 Kb. The murine *Emx2OS* was identified from the adult uterus and kidney and its length is 5035 nucleotides. It is expressed also in mouse brain. It has four exons and three introns and it is polyadenylated. Both of them show splicing variants. The nucleotide sequences of the human and murine *Emx2* opposite-strand sequences show no detectable homology other than those regions that overlap the *Emx2* transcript. Several open reading frames of 450 nucleotides or less are present in the human and murine antisense transcripts. However, none of the predicted peptides are conserved between the two species nor do they share similarity to sequences in GenBank. In human the expression of *Emx2* and *Emx2OS* resulted concordant: they are both highly expressed in normal postmenopausal endometrium, reduced in premenopausal endometrium, reduced in a majority of primary endometrial tumors and absent in four of six endometrial cancer cell lines

investigated. The murine *Emx2* and *Emx2OS* transcripts revealed endometrial cellular expression patterns identical to each other and with the human orthologs. Remarkably, at the beginning of the preparation of this thesis no data were available about *Emx2OS* in situ expression in the developing CNS and nothing was known about any possible implication of it in fine regulation of its sense partner in such structure.

1.3 Aim of the work

In this study, I reconstructed the expression pattern of *Emx2OS*-ncRNA in the developing CNS, by quantitative reverse transcription polymerase chain reaction (qRT-PCR) and in situ hybridisation (ISH). Then, by integrating lentiviral cDNA delivery, drug-induced perturbation of patterning pathways and gain- or loss-of-function (GOF and LOF, respectively) designs, I addressed possible roles of this transcript on regulation of its partner gene, *Emx2*, on primary CNS cultures as well as on cell lines. As suspected, I found that *Emx2* antisense transcripts may both stimulate and refine *Emx2* expression. Moreover, such effects seemed to be exerted at two distinct regulatory levels, transcriptional and post-transcriptional. These results, beyond their contribution to the comprehension of mechanisms regulating cortico-cerebral development, suggest a possible general exploitation of AS-based methods, as a tool for artificial triggering of endogenous gene expression.

2 Results

2.1 Expression pattern of *Emx2OS-ncRNA*

*Expression pattern of *Emx2OS-ncRNA**

To get a first insight into expression and putative functions of *Emx2OS-ncRNA*, I compared its abundance with that of *Emx2-mRNA*, in cortico-cerebral and rhomboencephalic tissues, at four embryonic developmental ages, E10.5, E12.5, E14.5 and E18.5. As expected (Gulisano et al., 1996; Mallamaci et al., 1998), *Emx2-mRNA* was specifically detectable in the cortex, where its levels went progressively down from E10.5 up to E18.5. Interestingly, *Emx2OS-ncRNA* displayed similar spatial specificity and similar temporal progression (Fig. 2).

Then, I studied the *Emx2OS-ncRNA* expression pattern in the developing central nervous system (CNS), by non-radioactive *in situ* hybridisation. At E12.5, within the CNS, the transcript was detectable in the telencephalon (Fig. 3A,B), including both pallium and basal ganglia (Fig. 4A), in the mammillary recess of the hypothalamus (Fig. 3A, arrowhead) and in the midbrain, including tectum and tegmentum (Fig. 3C). No signal was detectable within the rhombo-spinal domain (Fig. 3A,D). *Emx2OS* was also expressed by the nasal pits (Fig. 3E), the otic vesicle (Fig. 3G), the choroid plexus of II and IV ventricle (Fig. 3A,D), as well as by two clusters of head mesenchyme cells, in the snout region (Fig. 3A, asterisk) and in the surroundings of the hypothalamic optic recess (Fig. 3F, arrowheads). This expression pattern was essentially retained at E14.5 (Fig. 3H). At this age, however, *Emx2OS* was expressed within the mesencephalon along a rostral^{low}-to-caudal^{high} gradient and a new expression domain appeared within the superficial cerebellar bud (Fig. 3H,I). Focussing our attention on the developing cerebral cortex, we found *Emx2OS* transcripts within periventricular proliferative layers, from E12.5 to E18.5 (Fig. 4A-F), as well as in the cortical plate (CP), especially in its more superficial part (Fig. 4E,F). Conversely, no signal was detectable within the preplate (PPL) and its derivatives, marginal zone (MZ) and subplate (SP) (Fig. 4D-F). In particular, no *Emx2OS* transcripts could be found within Cajal-Retzius (CR) cells, aligned beneath the *pia mater* and specifically expressing *Reln* mRNA, in both neocortex and hippocampus (Fig. 3G-L, empty and solid arrowheads).

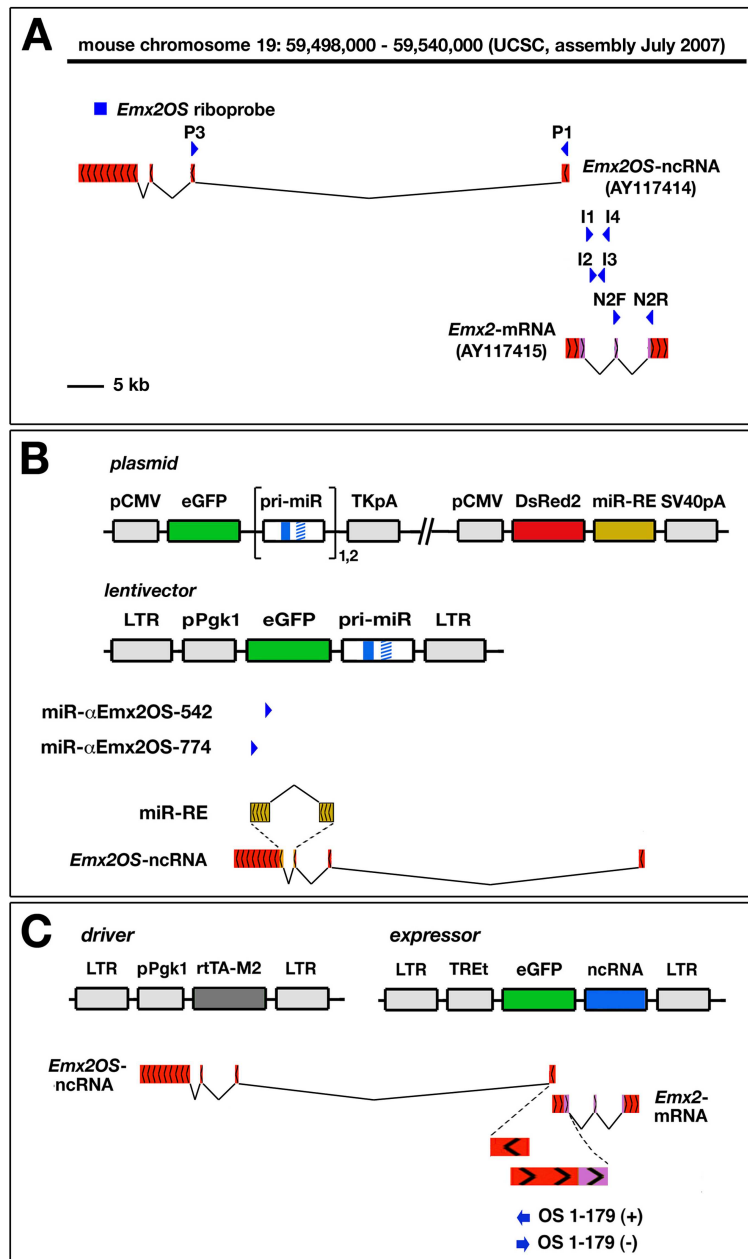


Figure 1. Synopsis of molecular tools used for studying expression and function of *Emx2OS*.

(A) Representation of the murine *Emx2* locus, with the *Emx2*-mRNA and the *Emx2OS*-ncRNA transcription units (red). Genomic localization of the riboprobe used for *in situ* hybridization analysis of *Emx2OS* (blue bar). Genomic localization of the oligonucleotides employed for quantitative RT-PCR evaluation of *Emx2OS*-ncRNA (P1 and P3), *Emx2*-mRNA (N2F and N2R) and *Emx2*-pre-mRNA (I1, I2, I3 and I4) (blue arrowheads).

(B) Structure of the bi-cistronic plasmids employed for assaying activities of artificial miRNAs against *Emx2OS*-ncRNA in HeLa cells and of lentivectors for overexpressing these miRNAs in primary cells. Localization of miR- α Emx2OS-542 and -774 (blue arrowheads) as well as of their responsive element, *miR-RE*, with respect to the antisense transcript. *miR-RE* (dark yellow), showed enlarged over the antisense transcript, extends across the 3rd and the 4th exons of it.

(C) Structure of the “driver” lentivector, guiding constitutive expression of rtTA-M2, and of “expressor” lentivectors, guiding rtTA/doxycyclin-dependent expression of EGFPcds/ncRNA modules. Genomic localization of OS1-179(+) and OS1-179(-)ncRNAs (blue arrows), as compared to *Emx2OS*-ncRNA and *Emx2*-mRNA (for sake of clarity, the sense/antisense overlapping region and its surroundings are represented enlarged; red, non coding sequences; violet, coding sequences).

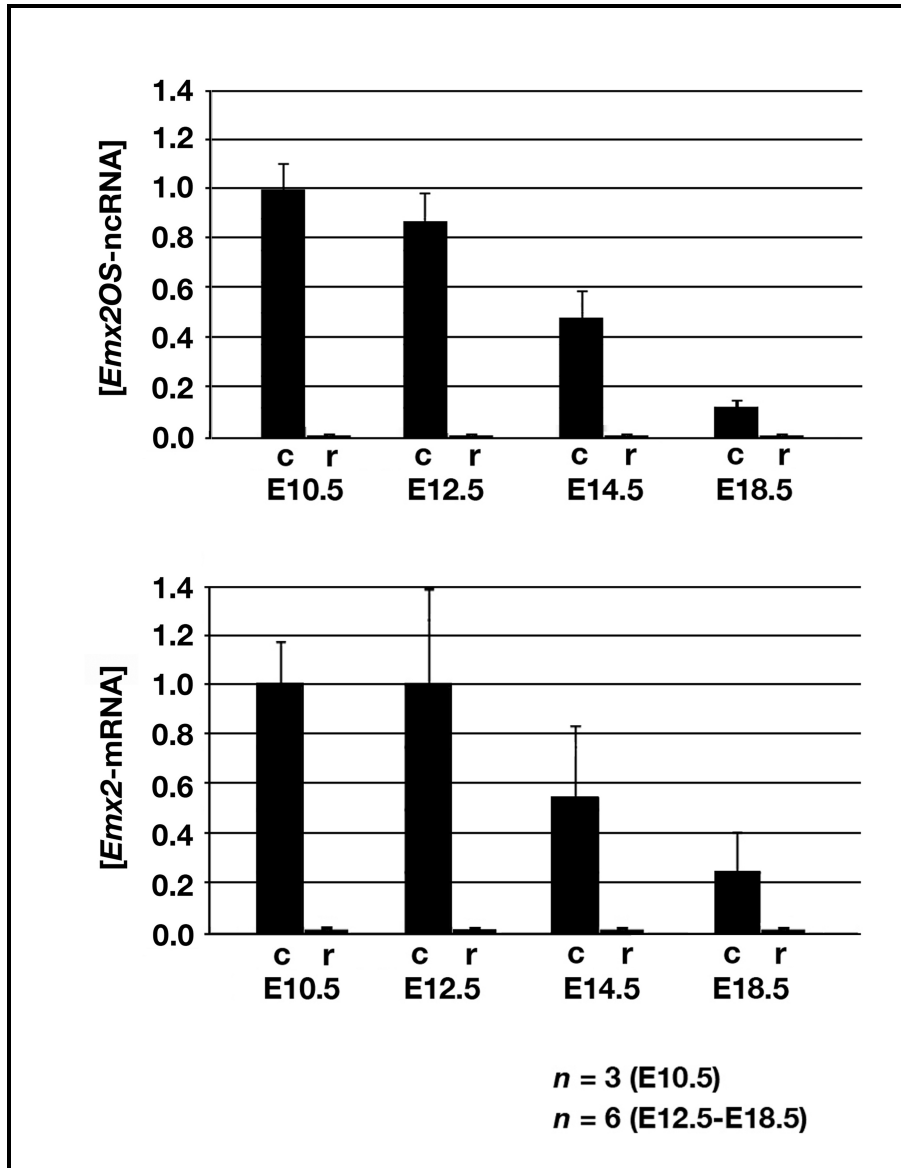


Figure 2. Time course quantitative RT-PCR analysis of *Emx2*-mRNA and *Emx2OS*-ncRNA expression levels in the developing cerebral cortex and rhombencephalon.

Sense and antisense transcripts display concordant spatial distributions (abundant in the cortex, absent in rhombencephalon), from E10.5 to E18.5. Within the cortex, they share a similar temporal trend, being progressively down-regulated from the pre-neuronogenic (E10.5) to post-neuronogenic stages (E18.5). RTs are primed by random hexamers and PCRs by oligos shown in Fig. 1. Data are normalized on E10.5 cortical samples. Abbreviations: c, cortex; r, rhombencephalon.

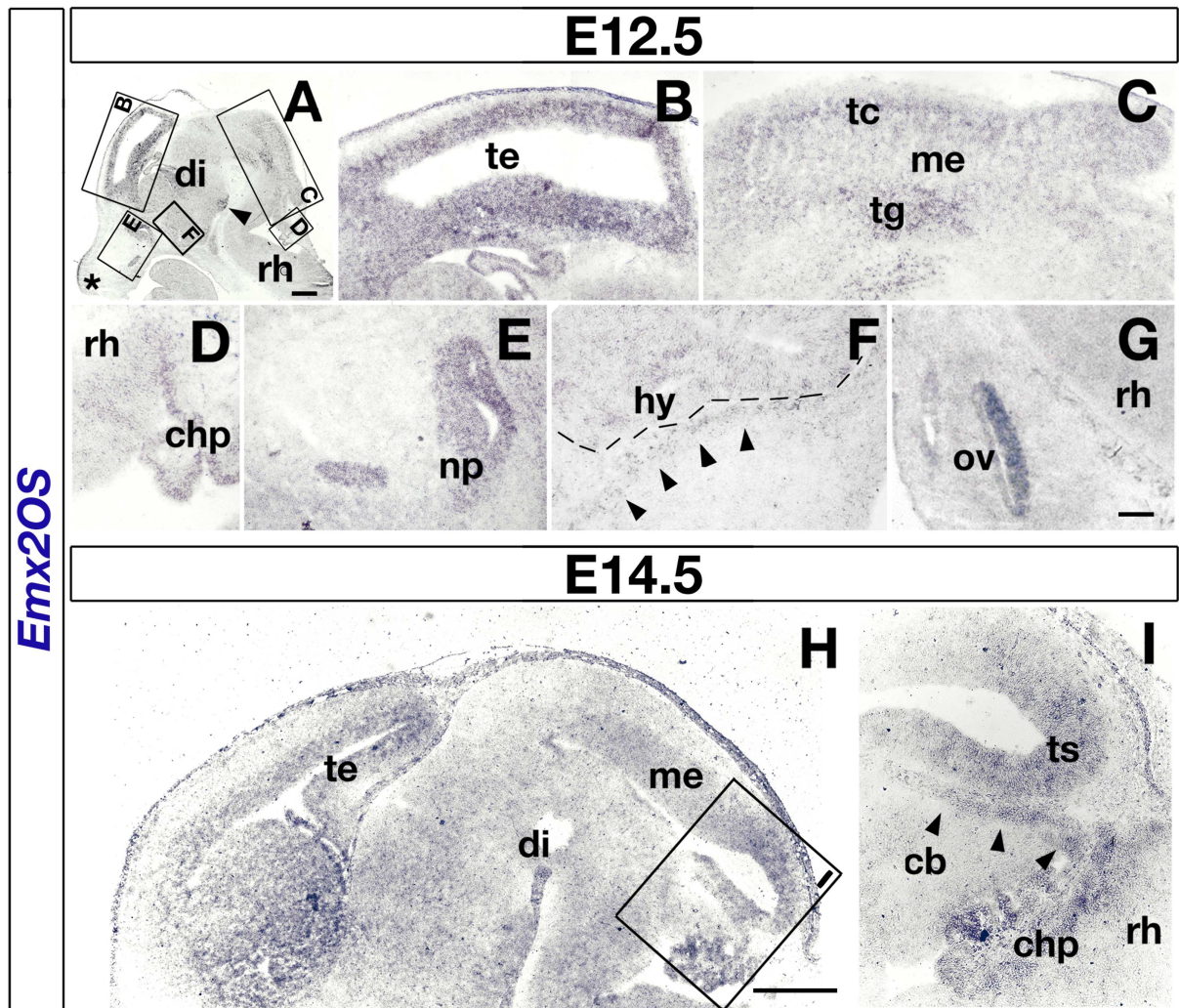


Figure 3. Distribution of *Emx2OS* transcripts on sagittal sections of E12.5 and E14.5 mouse brains.

(A-D) Within the E12.5 developing CNS, *Emx2OS*-ncRNA is detectable in telencephalon (A,B), mesencephalon (me), including both tectum (te) and tegmentum (tg), (panels A,C) and diencephalon, including the mammillary recess (arrowhead in panel A). It is not present in rhombencephalon (rh, panel G), except the choroid plexus of the IV ventricle (chp, panels A,D). Outside the CNS, *Emx2OS* is expressed in primordia of sense organs, nasal pits (np, panel E) and otic vesicle (ov, panel G), as well as in mesenchyme underlying snout epidermis (A, asterisk) and surrounding the hypothalamic (hy) optic recess (F, arrowheads).

(H-I) The E12.5 expression pattern is retained at E14.5. At this age - however - a rostral^{low}-to-caudal^{high} gradient is evident in the mesencephalon, with a maximum in the torus semicircularis (ts, panel H). Moreover, a new expression domain appears within the superficial cerebellar bud (cb, arrowheads in panel I). Scalebars, 200 μ m in A-C,H,I, 50 μ m in D-G.

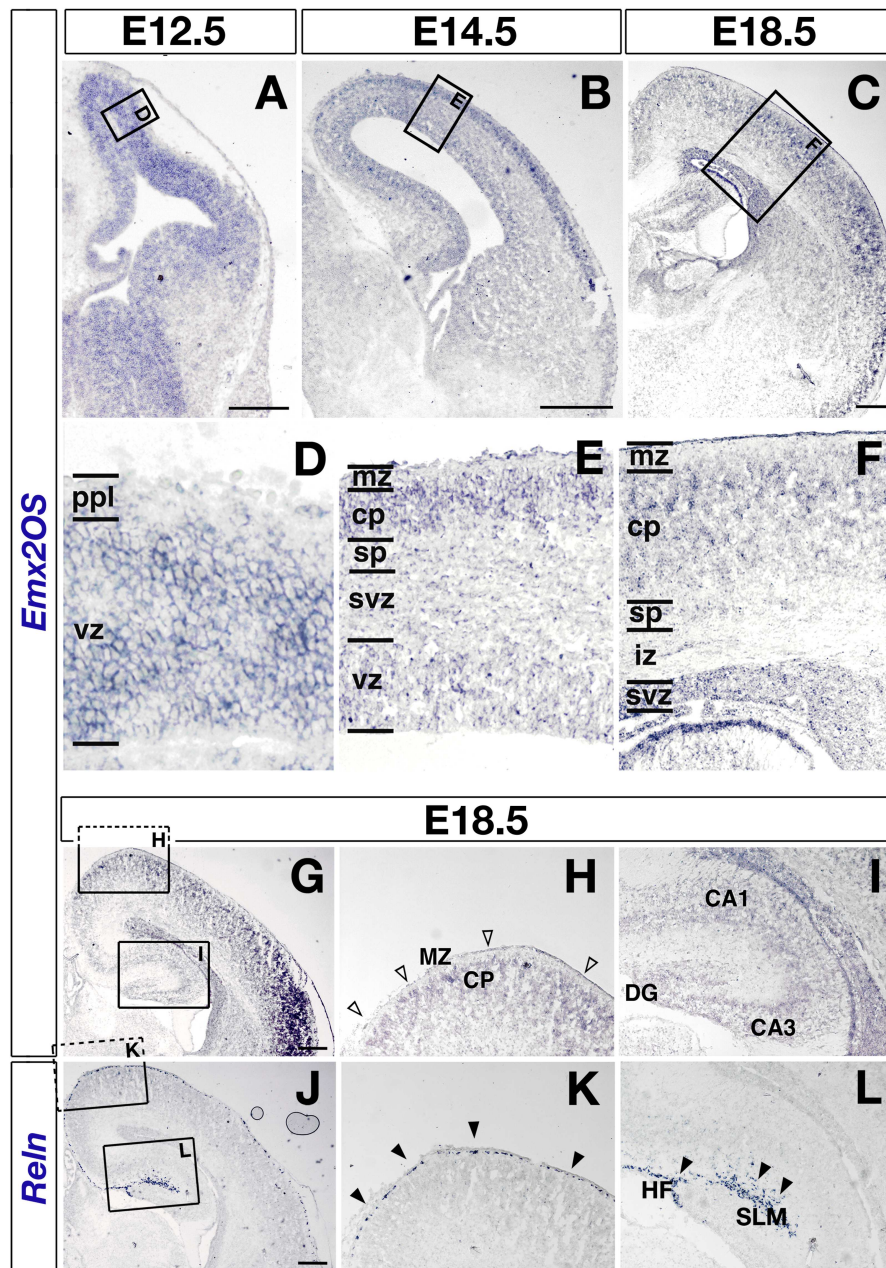


Figure 4. *In situ* hybridization profile of *Emx2OS*-ncRNA in the developing mouse telencephalon.

Distribution of *Emx2OS*-ncRNA (A-I) and *Reln*-mRNA (J-L) on mid-frontal sections of E12.5 (A), E14.5 (B) and E18.5 (C,G,J) mouse telencephalons. (D), (E) and (F) are magnifications of boxed areas in (A), (B) and (C), respectively. (H) and (I) are enlargements of boxed areas of panel (G), respectively; the same applies to panels (K) and (L) with respect to (J); (G) and (J) are adjacent sections from the same brain.

Emx2OS is expressed in periventricular proliferative layers at all ages subject of analysis (A-C). An additional signal is detectable within the cortical plate starting from E14.5 (B) and gets confined to its marginal-most part at E18.5 (C). No *Emx2OS* expression can be detected in the neocortical marginal zone (G,H, empty arrowheads) as well as in the archicortical stratum lacunosum-moleculare (G,I), both rich of *Reln*⁺ Cajal-Retzius cells (J-L, solid arrowheads).

Abbreviations: CA1, cornu Ammonis field 1; CA3, cornu Ammonis field 3; cp, CP, cortical plate; DG, dentate gyrus; HF, hippocampal fissure; iz, intermediate zone; mz, MZ, marginal zone; ppl, preplate; SLM, stratum lacunosum-moleculare; sp, subplate; svz, subventricular zone; vz, ventricular zone; Scalebars, 200 μ m.

2.2 *Emx2OS* antagonizes *Emx2* expression in a Dicer-dependent way

The mutually exclusive distribution of *Emx2*-mRNA and *Emx2OS*-ncRNA among cortico-cerebral neurons (the former expressed by CR neurons, the latter by CP neurons) suggested that reciprocal down-regulation between them could occur and that, in particular, *Emx2OS*-ncRNA could be implicated in repression of *Emx2*mRNA.

I first assayed this hypothesis by a LOF approach, i.e., by knocking-down *Emx2OS*-ncRNA via RNAi and monitoring consequences of that on *Emx2*-mRNA levels.

As for the choice of RNAi reagents, I selected the best two siRNAs suggested by the Invitrogen “BLOCK-iT™ RNAi Designer“ software (miR- α *Emx2OS*-542 and miR- α *Emx2OS*-774) plus the BLOCK-iT™ negative control-miR and compared their activities on HeLa cells. For this purpose, I built up a set of three plasmids, each harboring two distinct transcription units and designed to assay the activity of one specific miR. The former transcription unit, the “sensor”, included the CMV promoter, the DsRed2 coding sequence, the cDNA fragment corresponding to *Emx2OS*-ncRNA nt 795-915 (target in silico of the two miRs above) and the SV40 polyA site.

The latter unit, the “miR expressor”, harbored the CMV promoter, the eGFP coding sequence, a modified 230bp fragment from pri-mmu-miR-155 (where the miR-155 and miR-155* moieties were replaced by those of the artificial miR in order) and the TK polyA site. A fourth plasmid was built up as well, similar to the previous three, but harboring in *cis* sequences encoding for both miR- α *Emx2OS*-542 and miR- α *Emx2OS*-774 (Fig.1B). I transfected HeLa cells with these four plasmids, counted fluorescent cells and calculated for each plasmid the ratio between red cells and total fluorescent cells, as a comprehensive index of pri-miR processing efficiency and mature miR activity. The DsRed2⁺/(total fluorescent cells) ratio varied from 65% (negative control miR), to 39% (miR- α *Emx2OS*-542), 10% (miR- α *Emx2OS*-774) and 2% (miR- α *Emx2OS*-542 & miR- α *Emx2OS*-774), suggesting that the combination in *cis* of the two miRs, -542 and -774, would be the best choice (Fig. 5A). However, I noticed that, using the -542/-774 plasmid, the ratio between eGFP⁺ cells and total cells in the plate was consistently lower (data not shown), possibly because of enhanced Drosha-dependent destabilization of the chimaeric eGFP-cds/Pri-miR molecule. As this could pose serious problems in subsequent production of miR-encoding lentiviruses as well as in tracing cells infected by these virions, I prudently opted for simple miR- α *Emx2OS*-774 for the following knocking-down experiments.

To assess the role of *Emx2OS*-ncRNA in the developing cerebral cortex, I knocked it down in primary neurospheres derived from E12.5 cortical tissue, infecting them with a lentivirus constitutively expressing miR- α *Emx2OS*-774. Infection was performed at m.o.i. (multiplicity of infection) = 20, which resulted in a generalized and robust green fluorescent staining of all neurospheres. RNA, extracted from neural cells 72 hours after infection, was profiled by quantitative RT-PCR (Fig. 1A). I confirmed the capability of miR- α *Emx2OS*-774 to silence *Emx2OS*-ncRNA, whose signal was reduced by more than 2 times ($p < 0.002$; $n = 9$) (Fig. 5B, left). Concomitantly, I observed a modest (+25%), but statistically significant ($p < 0.03$; $n = 9$) increase of *Emx2*-mRNA.

To assess if upregulation of *Emx2* induced by miR- α *Emx2OS*-774 took place at transcriptional or post-transcriptional level, I then measured *Emx2* pre-mRNA levels, following infection of neurospheres with miR- α *Emx2OS*-774 or negative control lentiviruses. For sake of sensitivity and specificity, measurements were done by two-step quantitative RT-PCR, using two sets of nested primers annealing within the first *Emx2* intron (Fig. 1A). Interestingly, no change in *Emx2* pre-mRNA levels was found (Fig. 5B, right), suggesting that *Emx2OS*-dependent regulation of *Emx2* took place at post-transcriptional level.

Remarkably, in previous sets of experiments, neural cultures were performed in DMEM/F12/N2 medium, containing the standard growth factors (GFs) mix which promotes the intermitotic/stem state (Gritti et al., 1996). As during embryonic development *Emx2*-mRNA disappears in post-mitotic neurons, where *Emx2OS*-ncRNA is transiently upregulated, the question arises: is *Emx2OS*-ncRNA able to down-regulate *Emx2*-mRNA *also* in nascent neurons? To assess that, the *Emx2OS*-LOF tests were repeated culturing the infected cells in the presence of 5% serum, stimulating neuronal differentiation, in place of GFs. Moreover, in this new experiment an aliquot of miR-C-infected cells was kept under GFs, as a control. Consistent with expectations, under 5% serum plus miR-C lentivirus, neuronal differentiation was dramatically stimulated, as confirmed by massive activation of neuron-specific β -tubulin (Fig. 5C, top), and *Emx2*-mRNA level decreased, by about 30% ($p < 0.05$; $n = 3$) (Fig. 5C, bottom-right). Remarkably, knock-down of *Emx2OS* induced by miR- α *Emx2OS*-774 rescued such decrease to large extent (Fig. 5C, bottom-right), suggesting that *Emx2OS*-ncRNA substantially contributes to *Emx2* down-regulation at the time when CP neurons are born.

Then, to confirm this model, I verified it by a complementary GOF approach, i.e. by delivering antisense *Emx2* cDNA to embryo-derived neurospheres, via lentiviral vectors, and scoring consequences of that.

Unfortunately, the full-length 5.0kb *Emx2OS* cDNA harbors two canonical polyadenylation signals, which make it hardly suitable for our lentiviral expression system. So, in place of it, I used its 5'-most 179bp fragment, coinciding with the *Emx2-mRNA/Emx2OS-ncRNA* overlapping region minus a low-complexity 74bp polypyrimidine tract. Assuming - in fact - that *Emx2OS-ncRNA* worked by interacting with *Emx2-mRNA* via Watson&Crick base-pairing, this short fragment should recapitulate key regulative properties of the full-length *Emx2OS-ncRNA*. Moreover, in order to assay both consequences of antisense overexpression and their reversibility, I performed *Emx2OS-GOF* manipulations by a dual, TetON-based, lentiviral delivery system, triggered by doxycyclin.

Neurospheres were infected by a “driver virus”, harboring a constitutively expressed rtTA-M2 transactivator gene (at m.o.i.=10), plus an “expressor virus” (at m.o.i.=10 as well), harboring the cDNA sequence subject of investigation. More precisely, the “expressor virus” encoded for a chimaeric transgene, which includes the eGFP coding sequence, as a tracer, plus the cDNA fragment subject of analysis. The transgene was driven by a tTA/rtTA responsive element, tight (TREt) (Fig. 1C). Two “expressor viruses” were built up: the former harbored the cDNA fragment corresponding to nucleotides 1-179 of *Emx2OS-ncRNA* [OS1-179(+)], the latter the reverse-complementary sequence [OS1-179(-)] (Fig. 1C). A third virus, not including any *Emx2* sense or antisense sequences was used as a negative control.

24 hours after cell infection, doxycycline was added and, 48 hours later, cell RNAs were collected and analyzed. Compared to the control, OS1-179(+) reduced the *Emx2-mRNA* level by 24.2% ($p<0.001$) and OS1-179(-) increased it by 34.2% (while not reaching statistical significance). Moreover, *Emx2-mRNA* levels under OS1-179(+) and OS1-179(-) differed by -43.7% ($p<0.01$) (Fig. 6A). Remarkably, these changes of *Emx2-mRNA* levels were mirrored by opposite concomitant changes of *Emx2OS-ncRNA*. In synthesis, OS1-179(+) both down-regulates *Emx2-mRNA* and promotes the expression of the endogenous antisense transcript, which may in turn contribute to such down-regulation.

As for molecular mechanisms mediating *Emx2OS*-dependent *Emx2-mRNA* down-regulation, I hypothesized that the antisense ncRNA might destabilize the sense mRNA, forming a double strand with it and so preparing its degradation by double-strand ribonucleases. Among these enzymes, a reasonable candidate might be Dicer1, involved in dsRNA-mediated destabilization of retrotransposon transcripts (Tam et al., 2008; Okamura et al., 2008; Watanabe et al., 2008) and crucial to generation and survival of cortico-cerebral neurons (De Pietri Tonelli et

al., 2008). To test this hypothesis, I decided to repeat the GOF experiments described above in cells alternatively provided with Dicer1 activity or deprived of it.

The morpholino technology (Summerton et al., 2007) was selected for Dicer1 knock-down. Sequences of anti-Dicer1 morpholino and its reverse negative control were obtained from the Gene-Tools free design service (α -Dicer1 and C, respectively) and the former molecule was validated, by testing its capability to inhibit Dicer1-dependent pri-miR-124a maturation (Winter et al., 2009) [this is assayed by a DsRed2 sensor gene linked to a miR-124a responsive element, co-transfected into these cells with pri-miR-expressor plasmids (for details, see Fig. S1)]. To get the best knock-down, NIH/3T3 cells, among the easiest to transfect by established morpholino reagents, were selected as a substrate.

With these tools, combined Dicer1-knock-down (DicerKD) and OS1-179(+/-)-GOF manipulations were performed, according to the schedule in Fig. 6B. Results were as follows. Lentivirus OS1-179(+) downregulated *Emx2*-mRNA in all tested conditions. Compared with lentivirus-C treated controls, relative levels of *Emx2*-mRNA upon OS1-179(+) infection, changed by a factor of $0.56/1=0.56$ ($p<0.001$) - and $1.42/1.65=0.87$ ($p<0.01$), in wild type and Dicer1-KD NIH/3T3 cells, respectively. As for α -Dicer1, this morpholino gave conversely rise to a robust increase of *Emx2*-mRNA. Compared with morpholino-C-treated controls, relative levels of *Emx2*-mRNA under α -Dicer1 changed by a factor of $1.42/0.56=2.54$ ($p<0.001$), $1.65/1=1.65$ ($p<0.001$), and $1.82/1.31=1.39$ ($p<0.01$), in cells infected by OS1-179(+), control or OS1-179(-) lentiviruses, respectively. The stronger effect elicited by OS1-179(+) in the presence of normal levels of Dicer1 and the more pronounced effect elicited by α -Dicer1 when associated to OS1-179(+) suggested the likely occurrence of a specific functional interaction between Dicer1 and the antisense transcript. Remarkably, two-ways ANOVA re-analysis of *Emx2* expression data confirmed this suspect, with $p<0.025$ (Fig. 6B). Summarizing: (1) *Emx2*-mRNA is normally down-regulated by Dicer1; (2) the antisense RNA fragment overlapping *Emx2*-mRNA destabilizes it; (3) Dicer1 promotes such antisense-dependent mRNA destabilization.

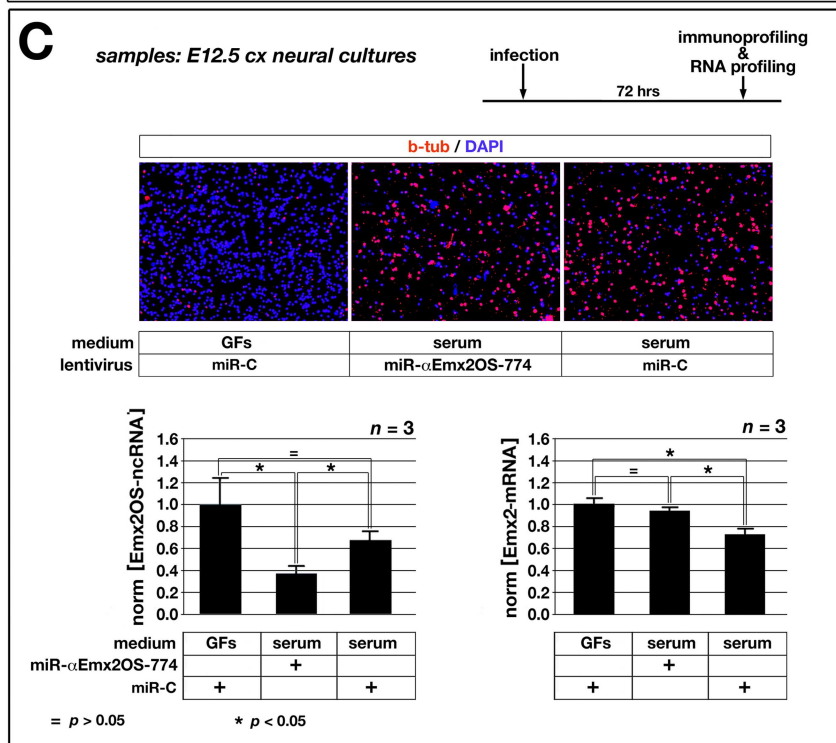
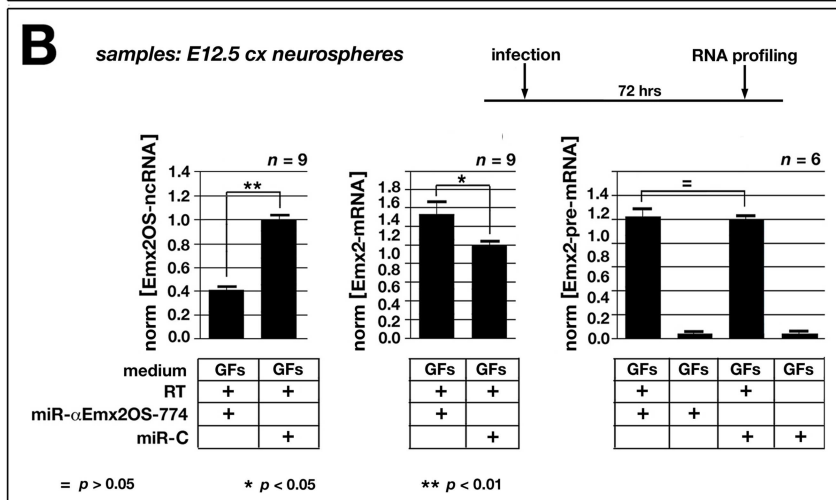
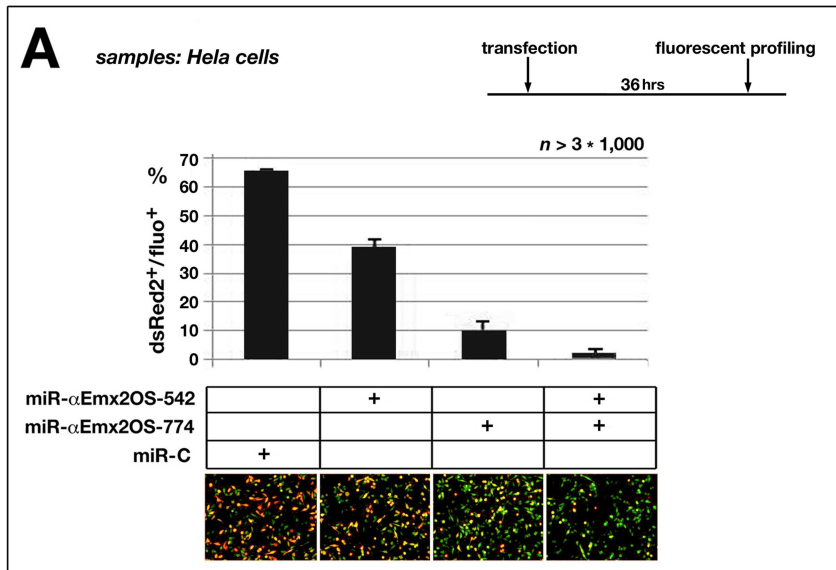


Figure 5. Setting-up *Emx2OS*-ncRNA knock-down by RNAi, in HeLa cells. Up-regulation of *Emx2*-mRNA in cortico-cerebral neurosphere cultures, via *Emx2OS* knock-down. Rescue of *Emx2*-mRNA downregulation in differentiating neurons, via *Emx2OS* knock-down

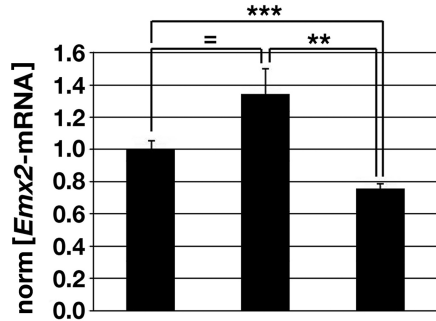
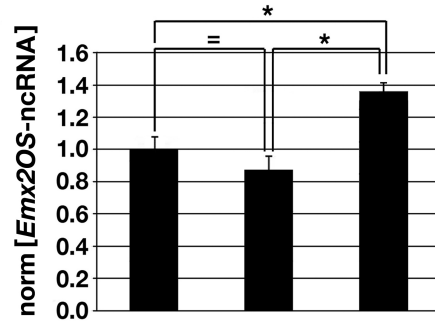
(A) Down-regulation of the miR-RE-sensitized *DsRed2* reporter in HeLa cells, upon overexpression of artificial miRNAs designed against *Emx2OS*.

(B) Down-regulation of *Emx2OS*-ncRNA, up-regulation of mature *Emx2*-mRNA and unchanged levels of immature *Emx2*-pre-mRNA in E12.5-derived cortical primary cells (cx), acutely infected by miR- α Emx2OS-774-expressor lentivirus, kept in Sato medium and harvested 72 hours later. Data are normalized on control-miR-treated samples (miR-C).

(C) Neuronal differentiation of lentivirus-transduced neural precursors kept 72 hours under 5% serum, as assessed by β -tubulin immunoprofiling. Down-regulation of *Emx2*-mRNA in miR-C-infected neural precursors, kept 72 hours under 5% serum in place of growth factors (GFs). Rescue of such down-regulation, elicited via miR- α Emx2OS-774-induced knock-down of *Emx2OS*-ncRNA. qRT-PCR data are normalized on control-miR-treated samples (miR-C), kept under GFs.

A

samples:
E12.5 cx neurospheres

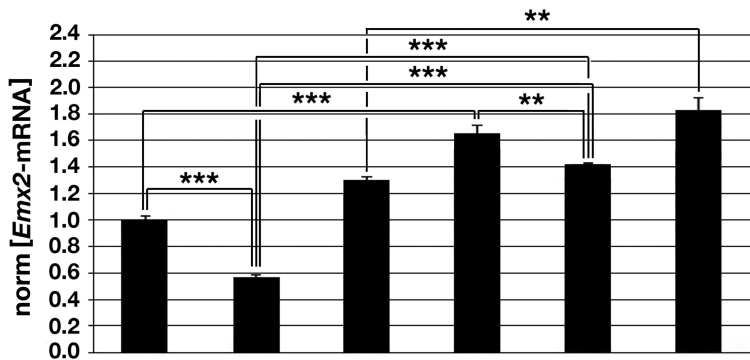
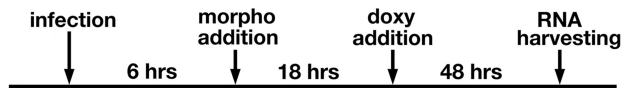
*n* = 6*n* = 6

lentivirus	C	OS1-179(-)	OS1-179(+)
------------	---	------------	------------

lentivirus	C	OS1-179(-)	OS1-179(+)
------------	---	------------	------------

= $p > 0.05$ * $p < 0.05$ ** $p < 0.01$ *** $p < 0.001$ **B**

samples:
NIH/3T3 cells

*n* = 6

morpholino	C	C	C	α-dicer	α-dicer	α-dicer
lentivirus	C	OS1-179(+)	OS1-179(-)	C	OS1-179(+)	OS1-179(-)

two-ways anova	+	+		+	+	
----------------	---	---	--	---	---	--

p(bw viruses) << 0.001
p(bw morpho) << 0.001
p(virus/morpho interaction) < 0.025

= $p > 0.05$ * $p < 0.05$ ** $p < 0.01$ *** $p < 0.001$

Figure 6. Down-regulation of *Emx2* and up-regulation of endogenous *Emx2OS* in cortical neural precursors, upon lentiviral transduction of the artificial antisense transcript OS1-179(+). Assessing the requirement of Dicer1 for *Emx2* antisense-dependent *Emx2* knock-down, in NIH/3T3 cells.

(A) *Emx2*-mRNA and *Emx2OS*-ncRNA expression in primary neural precursor cells, derived from E12.5 cortices (cx) and acutely infected with the “driver” lentivector, plus “expressor” lentivectors [OS1-179(+), OS1-179(-) and control (C)] in different combinations. One day after sample dissociation, cells are administered with doxycyclin and, two more days later, profiled for RNA. Data are normalized on control lentivirus-treated samples. OS1-179(+) induces a moderate (around -25%), but statistically significant down-regulation of *Emx2*-mRNA, as well as a moderate up-regulation (+35%) of the endogenous antisense transcript.

(B) *Emx2*-mRNA expression in NIH/3T3 cells, acutely infected with the “driver” lentivector plus each of the three “expressor” lentivectors [OS1-179(+), OS1-179(-) or C]. Cells are administered 6 hours after infection with an anti-Dicer1 or a control (C) morpholino and 18 more hours later with doxycyclin. Two more days later, they are RNA-profiled by qRT-PCR. Data reported in the histogram are normalized on samples infected by control lentivirus and exposed to control morpholino. Compared with lentivirus-C-treated controls, levels of *Emx2*-mRNA change upon OS1-179(+) infection by a factor of $0.56/1=0.56$ ($p<0.001$) and $1.42/1.65=0.87$ ($p<0.01$), in NIH/3T3 cells treated by control morpholino and α -Dicer1, respectively. Compared with morpholino-C-treated controls, levels of *Emx2*-mRNA change upon α -Dicer1 administration by a factor of $1.42/0.56=2.54$ ($p<0.001$), $1.65/1=1.65$ ($p<0.001$), and $1.82/1.31=1.39$ ($p<0.01$), in cells infected by OS1-179(+), control or OS1-179(-) lentiviruses, respectively. Two-ways ANOVA data analysis points to the occurrence of a functional interaction between Dicer1 and OS1-179(+), with $p<0.025$ (Fig. 6B).

2.3 *Emx2OS* transcripts promote both *Emx2*-mRNA and *Emx2OS*-ncRNA expression

The specific co-expression of *Emx2OS*-ncRNA and *Emx2*-mRNA by neural precursors belonging to defined regions of the developing CNS suggested that antisense transcripts, in addition to trigger destabilization of *Emx2*-mRNA, might be also basically implicated in promoting its transcription. This hypothesis might be easily tested, by over-expressing *Emx2* antisense sequences in neural precursors from segments of the embryonic CNS which normally do not express *Emx2*: among these, for example, the rhombo-spinal tract (Simeone et al., 1992a and b).

So, we infected neural precursor cells obtained from the dissociation of E10.5 rhombo-spinal tracts with the rtTA-M2 driver virus, alternatively associated to OS1-179(+) or control viruses, each at m.o.i. = 10 (Fig. 1C). Moreover, as basal expression levels of *Emx2* in the rhombo-spinal tract are very low, (near the experimental background), to circumvent potential problems arising from that, the experiment was run according to the following design. Some aliquots of the infected cells, were kept under standard neurosphere medium (Galli et al., 2002), whereas some others were further added with a dedicated drug mix. As *Emx2* expression is stimulated by canonical Wnt signalling, via up-regulation of the transcription factor (TF) beta-catenin (Theil et al., 2002), and should be reduced by Shh signalling, via repression of the TF Gli3 (Theil et al., 1999; Rallu et al., 2002), aliquots of the infected rhombo-spinal cells were kept under additional 1mM lithium chloride, potentiating the former (Clément-Lacroix et al., 2005), and 1 μ M cyclopamine, down-regulating the latter (Incardona et al., 1998), so as to increase the baseline of the assay and ameliorate its signal-to-noise ratio. Finally, telencephalic cells, infected by the rtTA-M2-expressor “driver” and control viruses, were grown under the same lithium/cyclopamine mix, as a positive control. All cells were kept in culture for 72 hours and then profiled by qRT-PCR (Fig. 7A).

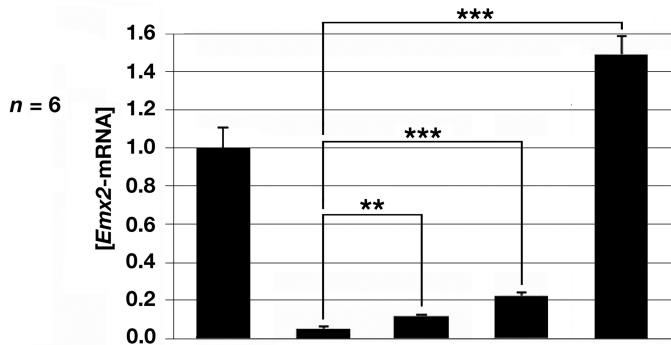
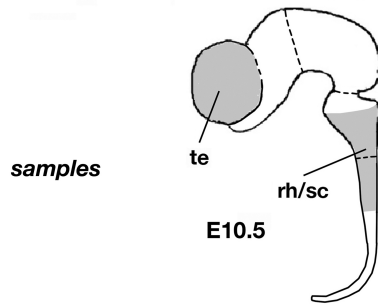
As expected, the *Emx2* expression level in rhombo-spinal cells, infected with control virus and kept in the absence of drugs, resulted far lower than in the positive control. The *Emx2* level slightly rose, upon treatment of rhombo-spinal cells by either the OS1-179(+) virus or the lithium/cyclopamine mix (about 2 and 4 times, with $p < 0.01$ and $p < 0.001$, respectively). Interestingly, simultaneous exposure of rhombo-spinal cells to both OS1-179(+) virus and lithium/cyclopamine elicited a much more dramatic up-regulation effect (almost 30 times, with $p < 0.001$), suggesting a powerful synergy between the bioactive virus and the drug cocktail ($p < 0.001$) (Fig. 7A, upper histograms). In other words, as hypothesized, *Emx2OS* transcripts may

activate *Emx2* expression and the amplitude of this phenomenon is much more prominent, upon appropriate pharmacological modulation of the nuclear TF milieu impinging on *Emx2* regulation (Theil et al., 1999; Rallu et al., 2002; Theil et al., 2002). Noticeably, changes of *Emx2*-mRNA levels elicited by pharmacological and genetic manipulations described above were paralleled by strikingly similar changes of *Emx2OS*-ncRNA (Fig. 7A, lower histograms). This indicated that both reasonably originated from concerted stimulation of sense and antisense transcription at the *Emx2* locus. This also suggested that the upregulation of *Emx2*-mRNA triggered by artificial OS1-179(+) administration might be further sustained by endogenous antisense transcripts from the same locus, induced by OS1-179(+) itself (Fig. 7A).

As the previous experiment was done by keeping the OS1-179(+) transgene chronically on, it was poorly informative about the kinetics and, in particular, the reversibility of the *Emx2* activation triggered by antisense transcripts. To address this issue, we repeated the OS1-179(+) overexpression test, according to a different temporal schedule. Briefly, E10.5 dissociated rhombo-spinal cells, acutely infected by the “driver” plus the OS1-179(+) virus (or its control) and kept chronically under lithium/cyclopamine, were exposed to doxycyclin for different times and finally scored for *Emx2* sense and antisense expression levels, 120 hours after their dissociation (Fig. 7B).

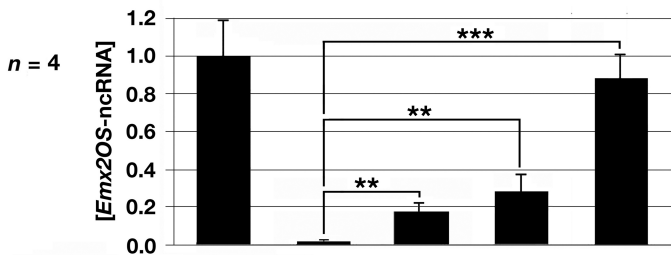
Main results of this test are as follows. Withdrawal of doxycyclin at 72 hours allowed full shutting off of OS1-179(+)-ncRNA at 120 hours, as witnessed by the absence of associated eGFP fluorescence (Fig. 7B, panels to the top). Remarkably, this was accompanied by a collapse of endogenous *Emx2* sense and antisense transcripts to levels peculiar to rhombo-spinal cells infected by the control virus (Fig. 7B, histograms). In other words, even low, but *persisting* levels of antisense transcripts seem to be *sufficient* and strictly *necessary* for proper firing of the *Emx2* transcription unit. This might explain why *Emx2* sense and antisense transcripts have normally to be co-expressed in proliferative layers of the early developing CNS.

A



sample	te	rh/sc	rh/sc	rh/sc	rh/sc
Li ⁺ / cyclopamine	+	-	-	+	+
lentivirus	C	C	OS1-179(+)	C	OS1-179(+)
doxycyclin	hrs 0-72	hrs 0-72	hrs 0-72	hrs 0-72	hrs 0-72

two-ways anova $p[\text{lentivirus}-(\text{Li}^+/\text{cyclopamine}) \text{ interaction}] < 1.0 \times 10^{-3}$

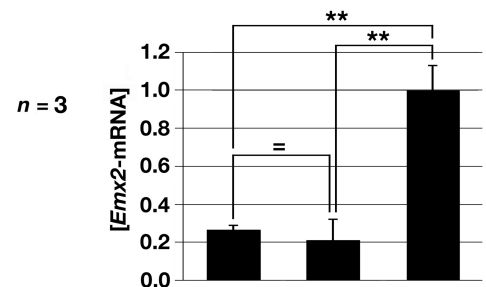
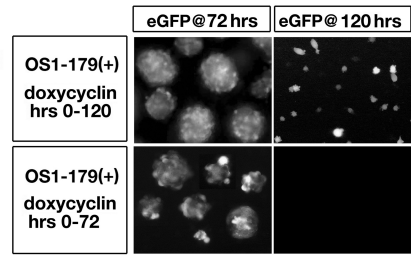


sample	te	rh/sc	rh/sc	rh/sc	rh/sc
Li ⁺ / cyclopamine	+	-	-	+	+
lentivirus	C	C	OS1-179(+)	NC	OS1-179(+)
doxycyclin	hrs 0-72	hrs 0-72	hrs 0-72	hrs 0-72	hrs 0-72

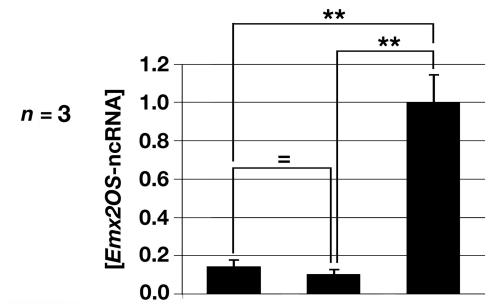
two-ways anova $p[\text{lentivirus}-(\text{Li}^+/\text{cyclopamine}) \text{ interaction}] < 2.2 \times 10^{-2}$

= $p > 0.05$ * $p < 0.05$ ** $p < 0.01$ *** $p < 0.001$

B



sample	rh/sc	rh/sc	rh/sc
Li ⁺ / cyclopamine	+	+	+
lentivirus	C	OS1-179(+)	OS1-179(+)
doxycyclin	hrs 0-120	hrs 0-72	hrs 0-120



sample	rh/sc	rh/sc	rh/sc
Li ⁺ / cyclopamine	+	+	+
lentivirus	C	OS1-179(+)	OS1-179(+)
doxycyclin	hrs 0-120	hrs 0-72	hrs 0-120

= $p > 0.05$ * $p < 0.05$ ** $p < 0.01$ *** $p < 0.001$

Figure 7. Ectopic and reversible activation of *Emx2*-mRNA and *Emx2OS*-ncRNA expression in rhombo-spinal neurospheres, upon lentiviral transduction of *Emx2* antisense transcript.

(A) Ectopic activation of the endogenous *Emx2* locus by OS1-179(+). The two graphs show *Emx2*-mRNA and *Emx2OS*-ncRNA expression levels in primary neural precursors from distinctive portions of the E10.5 CNS, rhombo-spinal tract (rh/sc) and telencephalon (te), acutely infected with “driver” and “expressor” lentivectors (Fig. 1C), kept under doxycyclin and added or not with the Li⁺/cyclopamine mix. Samples are RNA-profiled 72 hours after infection. Data are normalized on telencephalic precursors exposed to Li⁺/cyclopamine, infected by control lentivirus and kept under doxycyclin. Basal *Emx2* expression by rhombo-spinal cells, very low as compared to telencephalic precursors, rises about 2 (p<0.01), 4 (p<0.001) and 30 times (p<0.001), upon treatment of these cells with the OS1-179(+) virus, the drug mix, or both, respectively. Two-ways ANOVA indicates that a specific interaction between OS1-179(+) and the drug mix takes place, with p<0.001. A similar course is shown by *Emx2OS*-ncRNA, whose levels in rhombo-spinal samples - however - fall always below the telencephalic sample.

(B) Reversibility of OS1-179(+)-dependent activation of the endogenous *Emx2* transcription unit. The four panels to the top show time course analysis of eGFP fluorescence in neural precursors, infected by driver and OS1-179(+) lentiviruses and kept under doxycyclin for 72 or 120 hours. The absence of fluorescence in the bottom-right panel means that withdrawal of doxycyclin at 72 hours is sufficient to reset levels of the EGFP/OS1-179(+) chimaeric transcript to zero by 120 hours. The two graphs to the bottom show *Emx2*-mRNA and *Emx2OS*-ncRNA expression levels in primary neural precursors from the E10.5 rhombo-spinal (rh/sc) tract, acutely infected with “driver” and “expressor” lentivectors (Fig. 1C), kept under doxycyclin for 72 or 120 hours and chronically exposed to Li⁺/cyclopamine throughout the experiment. Samples are RNA-profiled 120 hours after infection. Data are normalized on rhombo-spinal cells exposed to Li⁺/cyclopamine, infected by OS1-179(+) lentivirus and kept under doxycyclin throughout the experiment. Removal of doxycyclin at 72 hours abolishes (p<0.01) the 4-fold up-regulation of *Emx2*-mRNA, detectable in Li/cyclopamine-treated rhombo-spinal precursors, upon their further infection by lentivirus OS1-179(+) (p<0.01). Similar consequences are elicited by doxycyclin removal on levels of *Emx2OS*-ncRNA.

2.4 Absence of *Emx2* sense transcription and/or its products impairs *Emx2OS-ncRNA* expression

The association between *Emx2OS* and *Emx2* transcripts might also imply a reciprocal, complementary dependence of *Emx2OS-ncRNA* expression on *Emx2* sense transcription. To address this issue, we compared levels of *Emx2* antisense transcripts in E12.5 cortices from *Emx2*^{+/+}, *Emx2*^{+/-} and *Emx2*^{-/-} mouse embryos (Pellegrini et al., 1996). The *Emx2 null* allele of these mutants - in fact - lacks only a small genomic fragment encoding for the C-term of the homeodomain (250bp), not provided of any known *cis*-regulatory activities, has an intact divergent-promoter region and still harbors the two main enhancers which drive transcription in the developing telencephalon (Pellegrini et al., 1996; Theil et al., 2002). As such, it should in principle be able to normally drive the synthesis of its antisense transcript.

Notwithstanding that, we found that *Emx2OS-ncRNA* was down-regulated by more than 80% in homozygous null mutants and by 50% in heterozygous mutants (Fig. 8), suggesting that - as suspected - *Emx2* sense transcription and/or its products are in turn necessary for proper expression of *Emx2OS-ncRNA*.

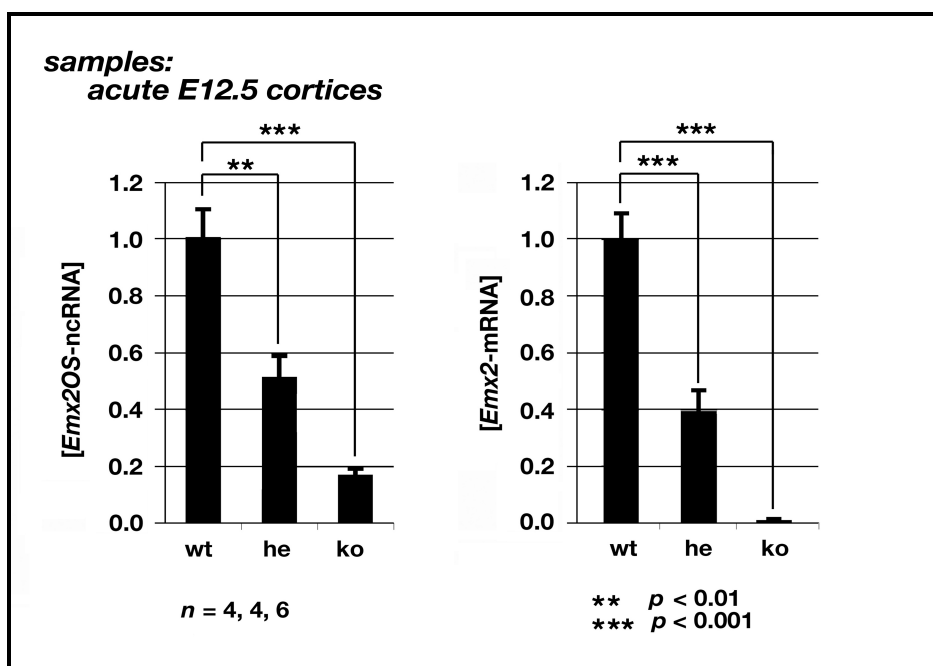


Figure 8. Down-regulation of *Emx2-mRNA* and *Emx2OS-ncRNA* in acutely dissected cortices from E12.5 embryos harboring one (he) or two (ko) *Emx2* null alleles.

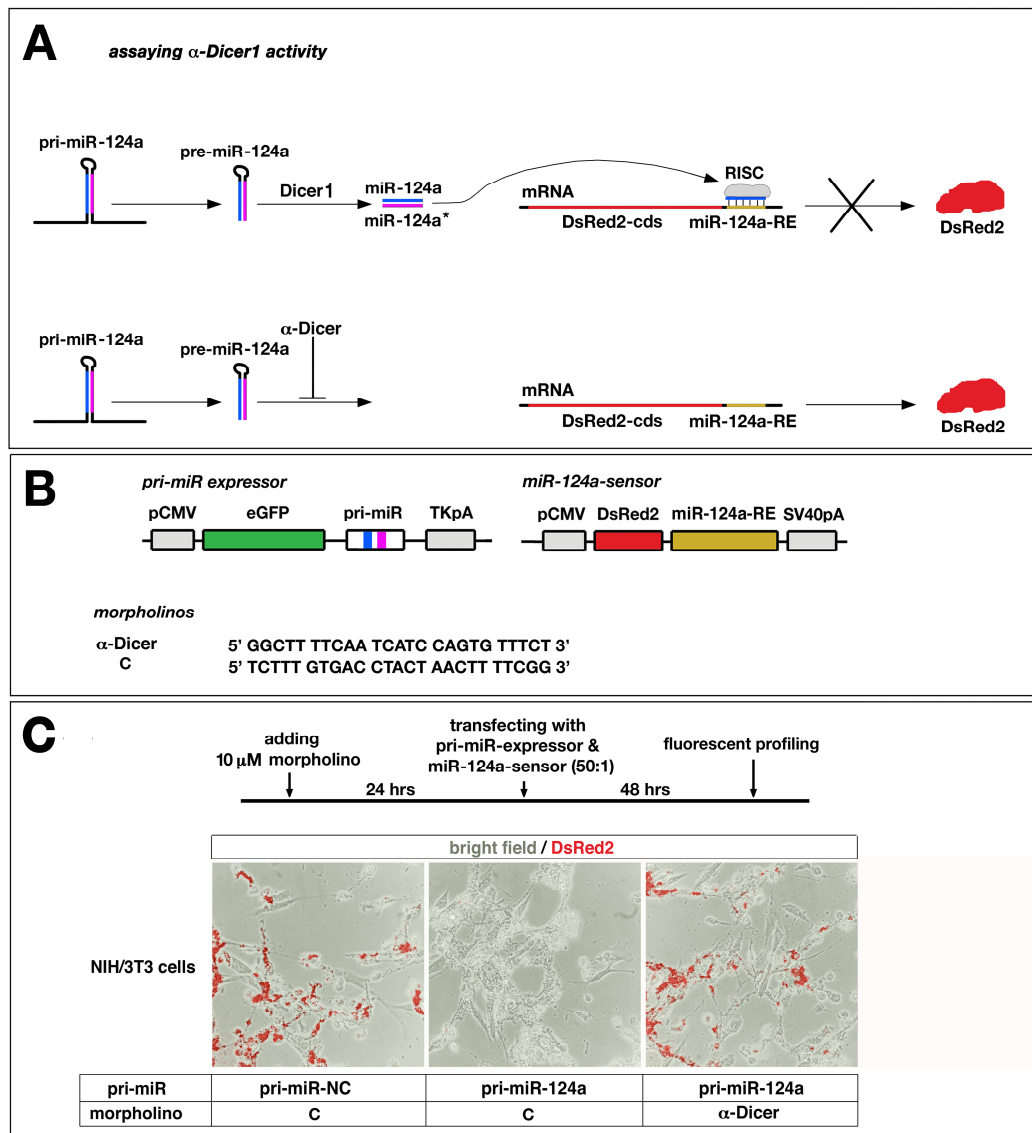


Figure S1. Validation of α -Dicer1 morpholino in NIH/3T3 cells.

(A) Rationale of the assay: α -Dicer1-dependent suppression of pri-miR-124a-dependent DsRed2 inhibition.

(B) Molecular tools for validating α -Dicer1 activity: inserts of pri-miR-expressor and miR-124a-sensor plasmids; sequences of α -Dicer1 and control morpholinos. The miR-124a responsive element (miR-124a-RE) corresponds to the 477-bp 3'UTR fragment of mouse *Lhx2*-mRNA (chr2 (+):38224759-38225235); Pri-miR-124a corresponds to the 285-bp mouse Pri-miR-124(2) genomic fragment (chr3 (+):17695562-17695846); control Pri-miR contains the Pri-miR155 sequence from the BLOCK-iT™ expression vector (Invitrogen).

(C) Rescue of miR124a-dependent DsRed2 inhibition by α -Dicer1 morpholino, in NIH/3T3 cells.

3 Discussion

In this study I reconstructed the expression pattern of *Emx2OS*-ncRNA, the antisense transcript associated to the transcription factor gene *Emx2*, in the developing mouse CNS. Then, I preliminarily investigated its involvement in regulation of *Emx2* expression.

As shown by qRT-PCR (Fig. 2) and *in situ* hybridisation (Fig. 3), *Emx2OS* was specifically expressed by a number of CNS substructures and sense organs also expressing *Emx2*. Among them: telencephalon, mammillary recess, optic tectum, olfactory placode, otic vesicle (Simeone et al., 1992; Mallamaci et al., 1998; our unpublished data). Such colocalization of *Emx2OS* and *Emx2* in periventricular layers of defined neural tube domains might be an epiphenomenon of shared regulatory mechanisms impinging on both. Alternatively, transcription of one or both units might specifically promote the other and, in particular, antisense transcription might contribute to specifically keep *Emx2* on in neural precursors of defined spatial domains.

Remarkably, the two transcripts, both expressed by periventricular neural precursors of the cortical primordium, displayed a mutually exclusive pattern in post-mitotic progenies of such precursors. Newborn neurons belonging to the cortical plate strongly expressed *Emx2OS*-ncRNA, especially at the end of their radial migration (Fig. 4E,F), but not *Emx2*-mRNA (while still harboring residual *Emx2* immunoreactivity) (Simeone et al., 1992a; Mallamaci et al., 1998). Pioneer Cajal-Retzius neurons lying in the marginal zone conversely expressed huge amounts of *Emx2* mRNA and protein (Mallamaci et al., 1998; our unpublished data), but no antisense transcript at all (Fig. 4G,L). Such mutual distribution pointed to a possible negative cross-regulation between *Emx2OS* and *Emx2* expression products and, in particular, to an involvement of the former in fine control of post-mitotic silencing of the latter.

This last hypothesis was tested by artificially modulating *Emx2* antisense levels in neural precursors derived from the cortico-cerebral primordium. An inverse correlation was found between levels of *Emx2OS* and *Emx2* transcripts, confirming that the former might be normally implicated in down-regulation of the latter. However, the amplitude of these phenomena was not dramatic. Halving *Emx2OS*-ncRNA by RNAi up-regulated *Emx2*-mRNA by about 33%. Overexpressing the 5' fragment of the former under the control of a powerful, P_{gk}-promoter/Tre-driven binary system, the latter was reduced by only 25% (with regards to that, it was reasonable to hypothesize that overexpression of the full-length *Emx2OS* molecule might elicit a more powerful effect). This suggested that *Emx2OS* negatively modulates *Emx2*, while being not able to completely shut it off. Moreover, changes of *Emx2*-mRNA levels elicited by *Emx2OS*-RNAi were

not reflected by the course of the corresponding pre-mRNA, that remained stable as found by intronic qRT-PCR, further suggesting that *Emx2OS*-dependent modulation of *Emx2* took place post-transcriptionally. Finally, *Emx2OS*-dependent down-regulation of *Emx2* was promoted by Dicer1, which might act by “dicing” the *Emx2*-mRNA/*Emx2OS*-ncRNA hybrid, similarly to retrotransposon silencing (Okamura et al., 2008; Tam et al., 2008; Watanabe et al., 2008). Consistent with this model, the concomitant up-regulation of *Emx2OS*-ncRNA caused by OS1-179(+) might reflect a reduced degradation rate of the endogenous antisense molecule, following the competition by OS1-179(+) for sense transcript binding.

Subsequently, to cast light on the biological meaning of *Emx2/Emx2OS* transcripts colocalization in defined structures of the early neural tube, the hypothesis that sense and antisense transcription at the *Emx2* locus reciprocally sustain each other was tested.

To assay the capability of *Emx2OS*-ncRNA to promote *Emx2*-mRNA expression, a 5' fragment of the former was overexpressed in rhombo-spinal precursors, normally expressing none of them. As suspected, delivery of this fragment, OS1-179(+)-ncRNA, into such cells elicited strong *Emx2* upregulation. No direct assessment of the level, transcriptional or post-transcriptional at which this phenomenon took place was performed. However two considerations suggest that the former possibility might hold good. First, OS1-179(+) strongly synergizes with a drug cocktail specifically up-regulating beta-catenin, a powerful transcriptional activator able to bind the two telencephalic enhancers of *Emx2* (Theil et al., 2002). Second, up-regulation of *Emx2* is faithfully paralleled by *Emx2OS* up-regulation.

Concerning mechanisms mediating transactivating properties of OS1-179(+) (as well of its target *Emx2OS*-ncRNA), two hypothesis may be taken into account. Both molecules might interact with transcription factors impinging on the *Emx2* locus, ameliorating their binding to the chromatin and/or their processivity (like the *Evf2*-ncRNA at the *Dlx5/6* locus (Feng et al, 2006)). Alternatively, antisense transcripts or their by-products might make the *Emx2* chromatin accessible, by recruiting appropriate modifier enzymes to it. The need of *persistent* OS1-179(+) expression to get *Emx2* activation and the capability of the only drug cocktail to elicit weak but reproducible *Emx2* upregulation induce to rule out this latter hypothesis and to consider the former one more likely. Beyond mechanics of OS1-179(+) action, such activation of *Emx2* by a short antisense transcript is nonetheless remarkable, as possible prototype of a general method for overexpressing *single specific* genes, without any need to introduce additional copies of them into the genome, similarly to RNAa (Li et al., 2006; Chen et al., 2008; Mao et al., 2008; Place et al., 2008).

Finally, to ascertain if *Emx2OS*-ncRNA expression reciprocally depended on *Emx2* transcription (and/or its products), *Emx2OS* levels were scored in mice which harbored one or two *Emx2* null alleles, but no genic lesion obviously incompatible with *Emx2* antisense transcription. Remarkably, in such mice, both *Emx2* and *Emx2OS* transcripts were dramatically down-regulated. Mechanisms of such down-regulation, possibly very complex, were not addressed at all in this study and will be subject of a further dedicated one. Based on such down-regulation as well as on consequences of OS1-179(+) overexpression in rhombo-spinal precursors, I can speculate now that *mutual* promotion of sense and antisense transcription at the *Emx2* locus may be a crucial prerequisite for proper activation and expression of *Emx2*. Maybe that is why *Emx2* sense and antisense transcripts are co-expressed in defined domains of the early neural tube.

4 Materials and methods

4.1 Animal handling

Wild type (w.t) mice (strain CD1, purchased from Harlan-Italy) and *Emx2 null* mutants (Pellegrini et al., 1996) used in this study were maintained at the SISSA-CBM mouse facility.

Embryos were staged by timed breeding and vaginal plug inspection. Animals handling and subsequent procedures were in accordance with European laws [European Communities Council Directive of November 24, 1986 (86/609/EEC)] and with National Institutes of Health guidelines. Embryos (E10.5-E18.5) were harvested from pregnant dames killed by cervical dislocation.

4.2 Reagents and standard procedures

All basic DNA manipulations (extraction, purification, ligation) as well as bacterial cultures and transformation, media and buffer preparations were performed according to standard methods. DNAs were transformed in the E.Coli TOP-10 strains (Invitrogen).

Restriction and modification enzymes were obtained from NEW ENGLAND BioLabs_{Inc} and PROMEGA, and used according to manufactures outlines. DNA fragments were purified from agarose gel by the QIAquick Gel Extraction Kit (Quiagen). Small scale and large scale plasmid preparations were done by purification columns (Quiagen).

4.3 Preparation of histological samples

Dissected embryos were immersion-fixed overnight in 4% paraformaldehyde in 1X phosphate saline buffer (PBS) (except for E 10.5 embryos, immersion fixed for about 10 hours) and then cryoprotected by immersion in 30% sucrose in PBS 1X overnight at 4 °C. Tissues were frozen in OCT compound, sectioned at 10 µm in a cryostat, collected on slides SuperFrost Plus (Fischer), air dried for about 30 min, and stored at – 80 °C until use.

4.4 Preparation of single-stranded RNA probes

Single stranded RNA probes were synthesized by the *in vitro* transcription of sequences cloned into *p-GEM* vector containing specific T3 and T7 RNA polymerase promoter sites. By choosing the appropriate direction, either antisense or sense RNA –strands were synthesized.

They were linearized, treated with phenol/chloroform and finally precipitated. Linearized plasmids were resuspended in distilled water at a concentration of 1 µg/µl.

4.5 Preparation of Dig-labelled probe

According to the manufacturers' instructions, I mixed the following reagents on ice: linearized DNA: 1µg; transcription buffer 5X: 4µl (Promega); DTT 0,1M: 2µl (Promega); Dig-labeling-mix 10x (Roche): 2µl; RNase-OUT Recombinant Ribonuclease Inhibitor 40 U/µl: 1µl; SP6 and T7 RNA polymerases (Promega) 20 U/µl: 1µl; and H₂O up to 20µl. The reaction was then incubated at 37 °C for 1h 30' and subsequently treated with RQ1 RNase-free DNase (PROMEGA) for 20' at 37°C. 1µl of the transcription was run on a 1,5% not-denaturing agarose gel against known amounts of ribosomal RNA marker. Probes were stored at -80°C in the dark.

4.6 In situ hybridization protocol

Hybridization. In order to improve signal and reduce the background, sections were subjected to several pre-treatment steps before the probe addition. The following protocol is adapted for the cryostat-cut sections.

Slides were left to dry at least for 30 minutes. After this step slides were immersed in 4% paraformaldehyde/1x PBS for 10 minutes and then washed with PBS twice, for 5 minutes.

Slides were immersed in HCl 0.2 M for 5 minutes, washed with PBS three times for 5 minutes and incubated in 0.5 µg/ml of proteinase K (Roche) in 50 mM Tris-HCl pH=8, 5 mM EDTA at 30°C for 10 minutes. The proteinase K reaction was stopped by washing slides twice with Glycine 4 mg/ml/PBS for 5 minutes. Slides were washed with PBS for 5 minute, twice.

Slides were quickly washed in distilled water and finally placed in a box containing 0.1 M Triethanolamine-HCl pH=8 set up with a rotating stir bar for 5 minutes. 0.4 ml of acetic anhydride was then added twice for 5 minutes. Slides were washed in sterile water twice for 2 minutes and subsequently used for probe-hybridization.

Washing of sections. The hybridization mix (*Denhardt's* salts 1x, DTT 50 mM, Polyadenilic acid 500 µg/ml, Ribonucleic acid transfer 53,5 µg/ml, Dextran sulfate 10%, Formamide 50%) including probe was heated at 80°C for 10 minutes and applied to the slides.

Clean coverslips increased spread the hybridization mix over the sections. Slides were placed horizontally in a sealed plastic box, together with paper soaked in 50% formamide, 5x SSC and incubated overnight at 60°C. The following day, slides were washed in a solution of 5x SSC- β -mercaptoethanol at room temperature (RT) for 30 minutes. Cover-slips were removed. Slides were incubated in stringent buffer (50% formamide-1x SSC- β -mercaptoethanol) at 60°C for 30 minutes. They were then washed with NTE buffer (0.5M NaCl; 10 mM Tris-HCl pH=8; 5 mM EDTA pH=8) two times for 15 minutes each, at 37°C. Slides were then incubated with 2x-SSC for 15 minutes, then with 0.2x-SSC for additional 15 minutes. This two last steps were done at room temperature. From this point slides were incubated twice in B1 solution (0.1 M Tris-HCl pH=7.4; NaCl 0.15) for 5 minutes and then blocked in B1 solution containing 10% of Heat inactivated fetal bovine serum (FBS-Gibco) for 1 hour at room temperature. Slides were next incubated in B1 containing 0.5% FBS and the α -Dig-AP (Roche) at the concentration of 1:2000, overnight at 4°C. The following day, sections were washed three times in B1 solution before incubation in B2 buffer (0.1 M Tris-HCl pH=9.5; 0.1 M NaCl; 50 mM MgCl₂) containing 3.5 μ l of NBT and 3.5 μ l of BCIP (Roche) for each ml. The development of these sections was followed using the microscope.

4.7 Probes used for the in situ hybridization

Not radioactive in situ hybridization was performed as previously described, with minor modifications (Muzio and Mallamaci., 2005). Two riboprobes were used: *Emx2OS*, corresponding to mouse chromosome 19: nt 59,500,768-59,501,561 and *Reln*, corresponding to the 3.3 kb "EcoRI-EcoRI" fragment from the BS6 clone (a gift by A. Bulfone). Hybridized embryo sections were imaged and analyzed using a fluorescent Nikon (Tokyo, Japan) Eclipse 80i microscope and a DS-2MBWC digital microscope camera. All images were processed by Adobe Photoshop CS3 software.

4.8 Cell cultures

Primary cells. Cortical primordia and rhombo-spinal tracts were dissected from E12.5 mouse embryos and mechanically dissociated to single cells, by gentle pipetting. Dissociated neural precursor cells were cultured at 700 cells/ μ l in DMEM/F12/Glutamax medium (Invitrogen™), integrated with N2 supplement (Invitrogen™), 1 mg/ml BSA, 0.6% w/v glucose, 2 μ g/ml heparin, 10 pg/ml Fgf2, 20 pg/ml Egf, 1X Pen/Strept (Gibco), 10 pg/ml fungizone. Cultures were usually blocked and underwent RNA extraction 72 hours after dissection. When a longer culturing time was required, primary neurospheres were dissociated to single cells by trypsin-DNaseI and re-plated at the same initial density. When required, doxycyclin was added to the culture medium at 2 μ g/ μ l.

HeLa cells and NIH/3T3 cells. Cells were cultured in DMEM-Glutamax-I™ (Gibco) plus 10%FBS, according to standard protocols. When appropriate, α -dicer (5' GGCTT TTCAA TCATC CAGTG TTTCT 3') and control (5' TCTTT GTGAC CTA CTACT AACTT TTCGG 3') morpholinos were delivered to cells at 10 μ M, by 6 μ M EndoPorter™ carrier (GeneTools), according to manufacturer's instructions. When required, doxycyclin was added to the culture medium at 2 μ g/ μ l.

4.9 Quantitative RT-PCR

RNA preparation. RNA was extracted from CNS explants and cell cultures by Trizol™ (Invitrogen), according to manufacturer instructions.

cDNA preparation. At least 1 μ g of RNA from each sample was retrotranscribed by SuperScriptIII™ (Invitrogen) in the presence of random hexamers, according to manufacturer instructions, with minor modifications. In the case of pre-mRNA levels evaluation, at least 4 μ g of RNA preparation from each sample, previously treated by DNaseI™ (Promega), were used.

Quantitative PCR. 1/25 of each cDNA sample was analyzed by the SybrGreen™ qPCR platform (Biorad). Each PCR reaction was run at least in triplicate and results averaged. Averages were further normalized against *Tbp*, except data in Fig. 5B (left and middle graphs), conversely normalized against *GAPDH*. Specifically in the case of pre-mRNA levels evaluation (reported in Fig. 5B, right graph), to reconcile sensitivity and specificity, 1/2 of each cDNA sample was linearly pre-amplified and 1/100 of the resulting primary reaction product was used as substrate of the subsequent quantitative PCR reaction, in turn driven by nested, internal primers. Finally, supplementary amplifications on not-retrotranscribed samples were run, as negative controls.

Oligonucleotides. Genomic localization of oligonucleotides used in this study are shown in Fig. 1A. Amplicons and corresponding oligos are as follows: *Emx2*-mRNA (E2S/N2F: 5' GGAAA GGAAG CAGCT GGCTC ACAGT CTCAG TCTTA C 3'; E2S/N2R: 5' GTGGT GTGTC CCTTT TTTCT TCTGT TGAGA ATCTG AGCCT TC 3'); *Emx2OS*-ncRNA (Emx2OS/P1: 5' CCCGC GCCCG GGTCA CTGAG ATGGC TTCG 3'; Emx2OS/P3: 5' GATGA GCAGG TGAGT GGTAG ATGGT TGTA GCTGT AC 3'); *Emx2*-pre-mRNA-primary PCR (I1: 5' GTCTC TGAAG CTCGT TTGGG TTA CT G 3'; I4: 5' AGTGA GTGTA GAGCA GAGTT GAAGT CC 3'); *Emx2*-pre-mRNA-secondary PCR (I2: 5' GCGAG GTCTT TGAAT CCTGT TTC 3'; I3: 5' GCAGA GTTGA AGTCC AGTGA ACC 3'); *Tbp*-mRNA (Tbp-b/Fw: 5' ATTCT CAAAC TCTGA CCACT GCACC GTTG 3'; Tbp-b/Rev: 5' TTAGG TCAAG TTTAC AGCCA AGATT CACGG TAG 3'); *Gapdh*-mRNA (Gapd/FW: 5' CAACA GCAAC TCCA CTCTT CCACC TTCG 3'; Gapd/REV: 5' GGTGG TCCAG GGTTT CTTAC TCCTT GGAGG 3'); *Tbp*-pre-mRNA-primary PCR (TBP-FW/EXT: 5' CTCAG TTTGA TGGCT CAGTT TCC 3'; TBP-REV/EXT: 5' GTATA ACCAG TTATT TATCC AGATC TC 3'); *Tbp*-pre-mRNA-secondary PCR (TBP-FW/INT: 5' CAAAA GATGA AAACC CAGAA AACAG CC 3'; TBP-REV/INT: 5' GTTTA CTGAA CGCTT GATTA TATAG 3').

qPCR programs. Emx2-mRNA/*Emx2OS*-ncRNA/ *Tbp*-mRNA/*Gapdh*-mRNA:

- Incubate at 95°C for 00:03:00
- Incubate at 95°C for 00:00:10
- Incubate at 65°C for 00:00:35
- Plate Read
- Incubate at 80°C for 00:00:01
- Plate Read
- Go to line 2 for 39 more times
- Melting curve from 60°C to 95°C, read every 0.5°C, hold 00:00:01
- END

Emx2 & Tbp -pre-mRNA-primary PCR

- Incubate at 95°C for 00:03:00
- Incubate at 55°C for 00:00:10
- Incubate at 72°C for 00:00:40
- Plate Read
- Incubate at 80°C for 00:00:01
- Plate Read
- Incubate at 95°C for 00:01:00
- Go to line 2 for 14 more times
- Melting curve from 45°C to 95°C, read every 1°C, hold 00:00:01
- END

Emx2 & Tbp -pre-mRNA-secondary PCR

- Incubate at 95°C for 00:03:00
- Incubate at 55°C for 00:00:10
- Incubate at 72°C for 00:00:40
- Plate Read
- Incubate at 80°C for 00:00:01
- Plate Read
- Incubate at 95°C for 00:01:00
- Go to line 2 for 39 more times
- Melting curve from 45°C to 95°C, read every 1°C, hold 00:00:01
- END

4.10 Plasmids construction

Structures of plasmids and lentivectors used in this study are summarized in Fig. 1B,C. In particular, the miR-RE module harbored by plasmids in Fig. 1B, namely a cDNA fragment corresponding to nt767-1308 of Genbank AY117414.1, was amplified from E12 cortex cDNA.

The pri-miR fragments included in plasmids and lentivectors of the same panel were prepared as follows. Each of the two sequences 5' TGCTG CATAT TTGCA CTTCT CCGAA GGTTT TGGCC ACTGA CTGAC CTTCG GAGGT GCAAA TATGC AGG 3' and 5' TGCTG CGAAC TTAGA CTCAG ATTCC CGTTT TGGCC ACTGA CTGAC GGGAA TCTGT CTAAG TTCGC AGG 3' was cloned into pcDNA™6.2-GW/EmGFP-miR (Invitrogen), in-between mmu-miR-155 flanking regions, according to manufacturer's instructions, and the resulting SalI-XhoI chimeric pri-miR cDNA fragments, encoding for miR-aEmx2OS-542 and miR-aEmx2OS-774, respectively, were obtained. Finally, the SalI-XhoI cDNA fragment from "pcDNA™6.2-GW/EmGFP-miR_neg_control_plasmid" was used as control pri-miR.

4.11 3rd generation Lentiviral vectors: production titration and usage

Lentiviruses were prepared and titrated as previously described (De Palma M and Naldini L, 2002; Follenzi A and Naldini L, 2002; Sastry et al., 2006), with minor modifications. Cell infections were performed without polybrene, at multiplicities of infection (m.o.i.'s) reported in Results. The protocols used for lentiviral production and titration are reported below.

Protocol for transient lipofection of 3rd generation lentiviral vectors. 16/24 hours before transfection, 7.0*10⁶ Hek293T cells were plated in 10 cm (Nunc) plates, supplied with 7 ml of Iscove's Modified Dulbecco's Medium, (IMDM-glutaMAX™ GIBCO), 10% FCS (Sigma). Low passages cells number was used (P12-P13).

3 Accessory plasmids

accessory plasmids	quantities
ENV-plasmid	3 µg/plate
Packaging plasmid (pMDLg/p RRE	5 µg/plate
Rev plasmid (Prsv-rev) 2.5 µg for plate	2,5µg/plate

plus 16-18 µg of self inactivating Gene Transfer plasmid (containing the expression cassette of the transgene) were diluted in 1.5 ml of medium (no serum & antibiotics added)/plate. Another mix, containing 60 µl of Lipofectamine 2000 (Invitrogen) plus 1.5 ml of medium (no serum &

antibiotics added)/plate was prepared. The two preparations were then incubated for 5 minutes, and subsequently mixed and incubated for 20 minutes, at RT. This solution was now added to plates. After 5 hours, medium was removed and cells supplied with a fresh one. Cells were left for 14-16 hours at 37°C; and then incubated with 5 ml of fresh medium for the lentiviral collection to begin. Cells' supernatants were collected at 24 hours and the pooled supernatants were filtered with a 0.45µm filter (Corning), in order to remove the cellular debris. Supernatants were stored at 4°C overnight. The removed medium was replaced with 5 ml of fresh medium/plate. This step was repeated at 48 hours. Then, supernatants of 24 and 48 hours were pooled and transferred in centrifuge polyallomer bottles (Beckman 357003). All the bottles were equilibrated (not more than 0,0050 g unbalanced) and loaded in a centrifuge at 50000 RCF, 2 hours and 30 minutes at 4 °C (20500 RPM in a JA 25.50 rotor). After the centrifuge, supernatants were removed by inverting the bottles. Residual medium was removed with a 1000 µl pipette. 200 µl of PBS were added to the first bottle and the pellet resuspended. This first lentiviral suspension was used to resuspend also the second pellet. The pooled mix was put in aliquots and immediately frozen in dry ice. Aliquots were stored at -80°C.

Titration. Depending on the type of lentiviral vector used, titration was made in HeLa or Hek293T-rtTA responsive cells. Fluorescence titration consists in estimate the number of productive integrations of a lentiviral vector containing a fluorescent tracing detectable by microscope. Lentiviral vector expression is under control of an active promoter. Such a system results to be extremely dependent on both cell type and the type of promoter of the expression cassette. The titer, TU/µl (Transducing Units/Volume Unit), is obtained estimating the number of transduced cells/total cells, in the appropriate serial dilution (positivity in the range of 1-15%).

Briefly, steps are the follows: at day 0, 1×10^6 cells/well are plated in a 6 well multi-well (Nunc). The number of wells, is proportional to the serial dilution considered, *plus* a supplementary well used for the cell count. At day 1, before the infection, cells belonging to one well are counted using a Bürker cell, as an average of cells in each well. Then we proceed to the infection. The old medium is removed and additional 500 µl of new medium plus Polybrene (Hexadimethrine bromide; Sigma) are given at a final concentration of 9 µg/ml, to maximize the transduction. Then, the lentiviral vector, diluted in 500 µl of medium is added to each well. At day 3, cells are dissociated from each single well and transferred in 6 cm wells (Nunc). The plate considered for the titration should contain about 10% of fluorescence cells.

Cells are then photographed in white and fluorescence, and counted with the Adobe Photoshop CS3 software. The titer is calculated as follows:

$TU/\mu l = (N^{\circ} \text{ positive}/N^{\circ} \text{ total}) * DF * N^{\circ} \text{ at day 1}$

$N^{\circ} \text{ positive}$ = number of green fluorescence cells at day 3

$N^{\circ} \text{ total}$ = number of total cells at day 3

$N^{\circ} \text{ at day 1}$ = number of cells at the time of infection

DF= dilution factor

4.12 Statistical analysis

All experiments were performed at least in biological triplicate. *Tbp-* (or *GAPDH-*) normalized qRT-PCR data relative to each treatment were further averaged and the corresponding s.e.m.'s were determined. Resulting averages were finally normalized against the control treatment, as reported in Legends to Figures. Statistical significance of differences among results was evaluated by one- or two-ways ANOVA.

5 Tables

Table 1

NATs mechanisms of regulation of gene expression

Mechanism	Example	Reference
Transcriptional interference	The yeast <i>GAL10</i> and <i>GAL7</i> genes, organized naturally in tandem, were rearranged in a convergent orientation. Transcription initiation was carried out normally but, as soon as the two transcripts began to overlap, elongation stalled and mRNA levels were severely reduced.	Prescott & Proudfoot, 2002
RNA masking	Expression of <i>RevErb</i> , overlapping <i>erbA</i> (encoding α -thyroid hormone receptor) strongly correlates with an increase in the ratio of splice variants <i>erbAα1/erbAα2</i> . <i>RevErb</i> overlaps only with <i>erbAα2</i> and is thought to block its splicing by masking splicing regulatory <i>cis</i> -elements. Artificial antisense RNAs complementary to the <i>Erbα2</i> -specific exon were shown to efficiently and specifically block <i>ErbAα2</i> splicing <i>in vitro</i> .	Hastings et al, 1997; Munroe & Lazar, 1991
dsRNA-dependent mechanisms	Salt tolerance in <i>Arabidopsis</i> is regulated by two siRNAs produced from a pair of tail-to-tail overlapping protein-encoding genes: <i>P5CDH</i> (a stress-related gene) and <i>SRO5</i> (of unknown function). When both transcripts are present, an RNA duplex is formed and two types of siRNA are produced: 24 nucleotides (nt) and 21 nt. The 24-nt siRNA causes initial cleavage of the <i>P5CDH</i> transcript, which is followed by the generation of 21-nt siRNA and further cleavage of the <i>P5CDH</i> transcript. The expression of <i>SRO5</i> is induced by salt and this induction is required to initiate siRNA formation.	Borsani et al, 2005

<p>dsRNA-dependent mechanisms</p>	<p>Response to iron deficiency in Cyanobacteria is mediated through the formation of an RNA duplex. Cyanobacteria responds to iron deficiency by expressing IsiA (iron stress-induced protein A), which forms a giant ring structure around photosystem I. IsiA is regulated by its <i>cis</i>-encoded antisense IsrR (iron stress-repressed RNA). Artificial overexpression of IsrR under iron stress causes a strongly diminished number of IsiA–photosystem supercomplexes, whereas IsrR depletion results in premature expression of IsiA. The mRNAs IsrR and isiA form a perfect duplex and undergo coupled degradation.</p>	<p>Duhring et al, 2006</p>
<p>dsRNA-dependent mechanisms</p>	<p>Silencing of <i>Drosophila melanogaster</i> Stellate repeats in testis is essential for male fertility and involves dsRNA. Stellate silencing is mediated by the homologous Su (Ste) tandem repeats. Both strands of the repressor repeats are transcribed producing a sense–antisense duplex. This duplex is further cleaved into short 25–27-nucleotide fragments, which confer specific silencing of the Stellate repeats.</p>	<p>Aravin et al, 2001</p>
<p>Effect on methylation</p>	<p>The head-to-head overlapping gene pair <i>Sphk1/Khps1</i> have been shown to undergo antisense-induced methylation.</p>	<p>Imamura et al, 2004</p>

6 References

- Alcántara, S., Ruiz, M., D'Arcangelo, G., Ezan, F., de Lecea, L., Curran, T., Sotelo, C., Soriano, E., 1998. Regional and cellular patterns of reelin mRNA expression in the forebrain of the developing and adult mouse. *J Neurosci.* 18(19), 7779-7799.
- Alfano, G., Vitiello, C., Caccioppoli, C., Caramico, T., Carola, A., Szego, M.J., McInnes, R.R., Auricchio, A., and Banfi, S., 2005. Natural antisense transcripts associated with genes involved in eye development. *Human Molecular Genetics* 14(7), 913-923.
- Amaral, P.P., Mattick, J.S., 2008. Noncoding RNA in development. *Mamm. Genome* 19, 454-492.
- Ambros, V., 2004. The functions of animal microRNAs. *Nature* 428, 431(7006):350-5.
- Anderson, G.J., Darshan, D., 2008. Small-molecule dissection of BMP signaling. *Nature Chemical Biology* 4, 15-16.
- Aoto, K., Nishimura, T., Eto, K., et al. 2002. Mouse GLI3 regulates Fgf8 expression and apoptosis in the developing neural tube, face, and limb bud. *Dev Biol.* 251(2), 320-332.
- Armentano, M., Chou, S.J., Tomassy, G.S., Leingärtner, A., O'Leary, D.D., Studer, M., 2007. COUP-TFI regulates the balance of cortical patterning between frontal/motor and sensory areas. *Nat Neurosci.* 10(10), 1277-86.
- Ashe, H.L., Monks, J., Wijgerde, M., Fraser, P., Proudfoot, N.J., 1997. Intergenic transcription and transinduction of the human β -globin locus. *Genes & Dev.* 11, 2494-2509.
- Babajko, S., Petit, S., Fernandes, I., Méary, F., LeBihan, J., Pibouin, L., Berdal, A., 2009. Msx1 expression regulation by its own antisense RNA: consequence on tooth development and bone regeneration. *Cells Tissues Organs* 189(1-4), 115-21.
- Badger, J.H., Olsen, G.J., 1999. CRITICA: Coding region identification tool invoking comparative analysis. *Mol Biol Evol.* 16, 512-524.
- Barlow, A.J., Francis-West, P.H., 1997. Ectopic application of recombinant BMP-2 and BMP-4 can change patterning of developing chick facial primordia. *Development* 124, 391-398.
- Barlow, D.P., and Bartolomei, M.S., 2007. Genomic imprinting in mammals. *Epigenetics* 357-375.
- Barrell, B.G., Air, G.M., Hutchison, C.A., 1976. Overlapping genes in bacteriophage ϕ X174. *Nature* 264, 34-41.
- Bayer, S.A., Altman, J., 1991. Development of the endopiriform nucleus and the claustrum in the rat brain. *Neuroscience* 45(2), 391-412.
- Beiter, T., Reich, E., Williams, R.W., Simon, P., 2009. Antisense transcription: a critical look in both directions. *Cell Mol Life Sci.* 66(1), 94-112.

Belloni, E., Muenke, M., Roessler, E., et al. 1996. Identification of Sonic hedgehog as a candidate gene responsible for holoprosencephaly. *Nat Genet.* 14(3), 353-356.

Beltran, M., Puig, I., Peça, C., GarcPeça, R., Bonilla, F., and de Herreros, A.G., 2008. A natural antisense transcript regulates Zeb2/Sip1 gene expression during Snail1-induced epithelial-mesenchymal transition. *Genes Dev.* 22, 756-769.

Berdal, A., Lezot, F., Pibouin, L., Hotton, D., Ghoul-Mazgar, S., Teillaud, C., Robert, B., MacDougall, M., Blin, C., 2002. Msx1 homeogene antisense mRNA in mouse dental and bone cells. *Connect Tissue Res.* 43(2-3), 148-52.

Bernstein, E., Allis, C.D., 2005. RNA meets chromatin. *Genes Dev.* 19, 1635-1655.

Bertone, P., Stolc, V., Royce, T.E., Rozowsky, J.S., Urban, A.E., Zhu, X., Rinn, J.L., Tongprasit, W., Samanta, M., Weissman, S., Gerstein, M., Snyder, M., 2004. Global identification of human transcribed sequences with genome tiling arrays. *Science* 2242-2246.

Bielle, F., Griveau, A., Narboux-Nême, N., Vigneau, S., Sigrist, M., Arber, S., Wassef, M., Pierani, A., 2005. Multiple origins of Cajal-Retzius cells at the borders of the developing pallium. *Nat Neurosci.* 8(8), 1002-12.

Bishop, K.M., Goudreau, G., O'Leary, D.D., 2000. Regulation of area identity in the mammalian neocortex by Emx2 and Pax6. *Science* 288(5464), 344-349.

Bishop, K.M., Rubenstein, J.L., O'Leary, D.D., 2002. Distinct actions of Emx1, Emx2, and Pax6 in regulating the specification of areas in the developing neocortex. *J Neurosci.* (17), 7627-38.

Blackshaw, S., Harpavat, S., Trimarchi, J., Cai, L., Huang, H., Kuo, W.P., et al. 2004. Genomic analysis of mouse retinal development. *PLoS Biol.* 2, E247.

Blin-Wakkach, C., Lezot, F., Ghoul-Mazgar, S., Hotton, D., Monteiro, S., Teillaud, C., Pibouin, L., Orestes-Cardoso, S., Papagerakis, P., Macdougall, M., Robert, B., Berdal, A., 2001. Endogenous Msx1 antisense transcript: in vivo and in vitro evidences, structure, and potential involvement in skeleton development in mammals. *Proc Natl Acad Sci U S A* 98(13),7336-7341.

Bolland, D.J., Wood, A.L., Johnston, C.M., Bunting, S.F., Morgan, G., Chakalova, L., Fraser, P.J., Corcoran, A.E., 2004. Antisense intergenic transcription in V(D)J recombination. *Nat. Immunol.* 5, 630-637.

Borsani, G., Tonlorenzi, R., Simmler, M.C., Dandolo, L., Arnaud, D., et al., 1991. Characterization of a murine gene expressed from the inactive X chromosome. *Nature* 351: 325-329.

Bouvier, M., Sharma, C.M., Mika, F., Nierhaus, K.H., Vogel J 2008. Small RNA binding to 5' mRNA coding region inhibits translational initiation. *Mol Cell.* 32(6), 827-837.

Braun, M.M., Etheridge, A., Bernard, A., Robertson, C.P., Roelink, H., 2003. Wnt signaling is required at distinct stages of development for the induction of the posterior forebrain. *Development.* 130(23), 5579-87.

Brockdorff, N., Ashworth, A., Kay, G.F., McCabe, V.M., Norris, D.P., et al., 1992. The product of the mouse *Xist* gene is a 15 kb inactive X-specific transcript containing no conserved ORF and located in the nucleus. *Cell* 71, 515-526.

Brunet, L.J., McMahon, J.A., McMahon, A.P., Harland, R.M., 1998. *Noggin*, cartilage morphogenesis, and joint formation in the mammalian skeleton. *Science* 280, 1455-1457.

Bulchand, S., Grove, E.A., Porter, F.D., Tole, S., 2001. LIM-homeodomain gene *Lhx2* regulates the formation of the cortical hem. *Mech Dev.* 100(2), 165-75.

Carninci, P., Kasukawa, T., Katayama, S., Gough, J., Frith, M.C., et al. 2005. The transcriptional landscape of the mammalian genome. *Science* 309, 1559-1563.

Carninci, P., Sandelin, A., Lenhard, B., Katayama, S., Shimokawa, K., Ponjavic, J., Semple, C. A., Taylor, M.S., Engström, P.G., Frith, M.C., Forrest, A.R., Alkema, W.B., Tan, S.L., Plessy, C., Kodzius, R., Ravasi, T., Kasukawa, T., Fukuda, S., Kanamori-Katayama, M., Kitazume, Y., Kawaji, H., Kai, C., Nakamura, M., Konno, H., Nakano, K., Mottagui-Tabar, S., Arner, P., Chesi, A., Gustincich, S., Persichetti, F., Suzuki, H., Grimmond, S.M., Wells, C.A., Orlando, V., Wahlestedt, C., Liu, E.T., Harbers, M., Kawai, J., Bajic, V.B., Hume, D.A., Hayashizaki, Y., 2006. Genome-wide analysis of mammalian promoter architecture and evolution. *Nat. Genet.* 38, 626-635.

Cawley, S., Bekiranov, S., Ng, H.H., Kapranov, P., Sekinger, E.A., Kampa, D., Piccolboni, A., Sementchenko, V., Cheng, J., Williams, A.J., Wheeler, R., Wong, B., Drenkow, J., Yamanaka, M., Patel, S., Brubaker, S., Tammana, H., Helt, G., Struhl, K., Gingeras, T.R., 2004. Unbiased mapping of transcription factor binding sites along human chromosomes 21 and 22 points to widespread regulation of noncoding RNAs. *Cell* 116(4), 499-509.

Cecchi, C., Boncinelli, E., 2000. *Emx* homeogenes and mouse brain development. *Trends Neurosci.* 23(8), 347-52.

Chang, H.Y., Chi, J.T., Dudoit, S., Bondre, C., van de Rijn, M., Botstein, D., Brown, P.O., 2002. Diversity, topographic differentiation, and positional memory in human fibroblasts. *Proc Natl Acad Sci U S A* 99, 12877-12882.

Chen, J., Sun, M., Kent, W.J., Huang, X., Xie, H., Wang, W., Zhou, G., Shi, R.Z. and Rowley, J.D., 2004. Over 20 % of human transcripts might form sense-antisense pairs. *Nucleic Acids Res.* 32, 4812-4820.

Chen, J., Sun, M., Rowley, J.D., Hurst, L.D., 2005. The small introns of antisense genes are better explained by selection for rapid transcription than by "genomic design". *Genetics* 171, 2151-2155.

Chen, Z., Place, R.F., Jia, Z.J., Pookot, D., Dahiya, R., Li, L.C., 2008. Antitumor effect of dsRNA-induced p21(WAF1/CIP1) gene activation in human bladder cancer cells. *Mol Cancer Ther.* 7(3), 698-703.

Cheng, J., Kapranov, P., Drenkow, J., Dike, S., Brubaker, S., Patel, S., Long, J., Stern, D., Tammana, H., Helt, G., Sementchenko, V., Piccolboni, A., Bekiranov, S., Bailey, D.K., Ganesh,

M., Ghosh, S., Bell, I., Gerhard, D.S., Gingeras, T.R., 2005. Transcriptional maps of 10 human chromosomes at 5-nucleotide resolution. *Science* 308, 1149-1154.

Clément-Lacroix, P., Ai, M., Morvan, F., Roman-Roman, S., Vayssière, B., Belleville, C., Estrera, K., Warman, M.L., Baron, R., and Georges Rawadi, G., 2005. Lrp5-independent activation of Wnt signaling by lithium chloride increases bone formation and bone mass in mice. *Proc Natl Acad Sci U S A* 102(48), 17406-17411.

Coleman, J., Green, P.J., Inouye, M., 1984. The use of RNAs complementary to specific mRNAs to regulate the expression of individual bacterial genes. *Cell* 37(2), 429-36.

Corbin, J.G., Rutlin, M., Gaiano, N., et al. 2003. Combinatorial function of the homeodomain proteins Nkx2.1 and Gsh2 in ventral telencephalic patterning. *Development* 130(20), 4895-4906.

Core, L.J., Waterfall, J.J., Lis, J.T., 2008. Nascent RNA Sequencing Reveals Widespread Pausing and Divergent Initiation at Human Promoters. *Science* 322, 1845-1848.

Coudert, A.E, Pibouin, L., Vi-Fane, B., Thomas, B.L., Macdougall, M., Choudhury, A., Robert, B., Sharpe, P.T., Berdal, A., Lezot, F., 2005. Expression and regulation of the Msx1 natural antisense transcript during development. *Nucleic Acids Res* 33(16), 5208-5218.

D'Arcangelo, G., Miao, G.G., Chen, S.C., Soares, H.D., Morgan, J.I., Curran, T., 1995. A protein related to extracellular matrix proteins deleted in the mouse mutant reeler. *Nature* 374(6524), 719-23.

Darfeuille, F., Unoson, C., Vogel, J., Wagner, E.G., 2007. An antisense RNA inhibits translation By competing with standby ribosomes. *Mol Cell* 26(3), 381-92.

De Palma, M., Naldini, L., 2002. Transduction of a gene expression cassette using advanced generation lentiviral vectors. *Methods Enzymol.* 346, 514-529.

De Pietri Tonelli, D., Pulvers, J.N., Haffner, C., Murchison, E.P., Hannon, G.J., Huttner, W.B., 2008. miRNAs are essential for survival and differentiation of newborn neurons but not for expansion of neural progenitors during early neurogenesis in the mouse embryonic neocortex. *Development* 135, 3911-3921.

Dinger, M.E., Amaral, P.P., Mercer, T.R., Pang, K.C., Bruce, S.J., Gardiner, B.B., AskariAmiri, M.E., Ru, K., Soldà, G., Simons, C., Sunkin, S.M., Crowe, M.L., Grimmond, S.M., Perkins, A.C., Mattick, J.S., 2008. Long noncoding RNAs in mouse embryonic stem cell pluripotency and differentiation. *Genome Res.* 18(9), 1433-45.

Engström, P.G., Suzuki, H., Ninomiya, N., Akalin, A., Sessa, L., Lavorgna, G., Brozzi, A., Luzi, L., Tan, S.L., Yang, L., Kunarso, G., Ng, E.L., Batalov, S., Wahlestedt, C., Kai, C., Kawai, J., Carninci, P., Hayashizaki, Y., Wells, C., Bajic, V.B., Orlando, V., Reid, J.F., Lenhard, B., Lipovich, L., 2006. Complex Loci in human and mouse genomes. *PLoS Genet.* 2, e47.

Ericson, J., Muhr, J., Placzek, M., et al. 1995. Sonic hedgehog induces the differentiation of ventral forebrain neurons: A common signal for ventral patterning within the neural tube. *Cell* 81(5), 747-756.

Feng, J., Bi, C., Clark, B.S., Mady, R., Shah, P., Kohtz, J.D., 2006. The Evf-2 noncoding RNA is transcribed from the Dlx-5/6 ultraconserved region and functions as a Dlx-2 transcriptional coactivator. *Genes & Development* 20, 1470-1484.

Finocchiaro, G., Carro, M.S., Francois, S., Parise, P., Di Ninni, V., Muller, H., 2007. Localizing hotspots of antisense transcription. *Nucleic Acids Res.* 35, 1488-1500.

Follenzi, A., Naldini, L., 2002. Generation of HIV-1 derived lentiviral vectors. *Methods Enzymol.* 346, 454-465.

Frith, M.C., Bailey, T.L., Kasukawa, T., Mignone, F., Kummerfeld, S.K., et al., 2006. Discrimination of non-protein-coding transcripts from protein-coding mRNA. *RNA Biol.* 3(1), 40-8.

Furuta, Y., Piston, D.W., Hogan, B.L., 1997. Bone morphogenetic proteins (BMPs) as regulators of dorsal forebrain development. *Development* 124, 2203-2212.

Galli, R., Fiocco, R., De Filippis, L., Muzio, L., Gritti, A., Mercurio, S., Broccoli, V., Pellegrini, M., Mallamaci, A., Vescovi, A.L., 2002. Emx2 regulates the proliferation of stem cells of the adult mammalian central nervous system. *Development* 129(7), 1633-1644.

Gangemi, R.M., Daga, A., Marubbi, D., Rosatto, N., Capra, M.C., Corte, G., 2001. Emx2 in adult neural precursor cells. *Mech Dev.* 109(2), 323-329.

Gangemi, R.M., Daga, A., Muzio, L., Marubbi, D., Coccozza, S., Perera, M., Verardo, S., Bordo, D., Griffero, F., Capra, M.C., Mallamaci, A., Corte, G., 2006. Effects of Emx2 inactivation on the gene expression profile of neural precursors. *Eur J Neurosci.* 23(2), 325-34.

Gangemi, R.M., Perera, M., Corte, G., 2004. Regulatory genes controlling cell fate choice in embryonic and adult neural stem cells. *J Neurochem.* 89(4), 1056.

Ge, X., Wu, Q., Jung, Y.C., Chen, J., Wang, S.M., 2006. A large quantity of novel human antisense transcripts detected by LongSAGE. *Bioinformatics* 22, 2475-2479.

Geng, X., Lavado, A., Lagutin, O.V., Liu, W., Oliver, G., 2007. Expression of Six3 Opposite Strand (Six3OS) during mouse embryonic development. *Gene Expr Patterns* 7(3), 252-257.

Gierman, H.J., Indemans, M.H., Koster, J., Goetze, S., Seppen, J., Geerts, D., van Driel, R., Versteeg, R., 2007. Domain-wide regulation of gene expression in the human genome. *Genome Res.* 17, 1286-1295.

Golden, J.A., Bracilovic, A., McFadden, K.A., Beesley, J.S., Rubenstein, J.L.R., Grinspan, J.B., 1999. Ectopic bone morphogenetic proteins 5 and 4 in the chicken forebrain lead to cyclopia and holoprosencephaly. *Proc. Natl. Acad. Sci. USA* 96, 2439-2444.

Götz, M., Stoykova, A., Gruss, P., 1998. Pax6 controls radial glia differentiation in the cerebral cortex. *Neuron* 21(5), 1031-44.

Gribnau, J., Diderich, K., Pruzina, S., Calzolari, R., Fraser, P., 2000. Intergenic transcription and developmental remodeling of chromatin subdomains in the human β -globin locus. *Mol. Cell* 5, 377-386.

Grindley, J.C., Davidson, D.R., Hill, R.E., 1995. The role of Pax-6 in eye and nasal development. *Development* 121(5), 1433-42.

Gulisano, M., Broccoli, V., Pardini, C., Boncinelli, E., 1996. Emx1 and Emx2 show different patterns of expression during proliferation and differentiation of the developing cerebral cortex in the mouse. *Eur J Neurosci.* 8(5), 1037-50.

Gunhaga, L., Marklund, M., Sjödal, M., Hsieh, J.C., Jessell, T.M., Edlund, T., 2003. Specification of dorsal telencephalic character by sequential Wnt and FGF signaling. *Nat Neurosci.* 6(7), 701-7.

Hamasaki, T., Leingärtner, A., Ringstedt, T., O'Leary, D.D., 2004. EMX2 regulates sizes and positioning of the primary sensory and motor areas in neocortex by direct specification of cortical progenitors. *Neuron* 43(3), 359-72.

Hammerschmidt, M., Serbedzija, G.N., McMahon, A.P., 1996. Genetic analysis of dorsoventral pattern formation in the zebrafish: requirement of a BMP-like ventralizing activity and its dorsal repressor. *Genes Dev.* 10, 2452-2461.

Hanashima, C., Shen, L., Li, S.C., Lai, E., 2002. Brain factor-1 controls the proliferation and differentiation of neocortical progenitor cells through independent mechanisms. *J Neurosci.* 22(15), 6526-36.

Hanashima, C., Li, S.C., Shen, L., Lai, E., Fishell, G., 2004. Foxg1 suppresses early cortical cell fate. *Science.* Jan 2;303(5654):56-9.

Hastings, M.L., Ingle, H.A., Lazar, M.A., Munroe, S.H., 2000. Post-transcriptional regulation of thyroid hormone receptor expression by cis-acting sequences and a naturally occurring antisense RNA. *J. Biol. Chem.* 275, 11507-11513.

Hatzigeorgiou, A.G., Fiziev, P., Reczko, M., 2001. DIANA-EST: a statistical analysis. *Bioinformatics* 17(10), 913-9.

Haussecker, D., Proudfoot, N.J., 2005. Dicer-dependent turnover of intergenic transcripts from the human beta-globin gene cluster. *Mol Cell Biol.* 25(21), 9724-33.

He, Y., Vogelstein, B., Velculescu, V.E., Papadopoulos, N., Kinzler, K.W., 2008. The Antisense Transcriptomes of Human Cells. *Science* 322, 1855-1857.

Heins, N., Cremisi, F., Malatesta, P., Gangemi, R.M., Corte, G., Price, J., Goudreau, G., Gruss, P., Götz, M., 2001. Emx2 promotes symmetric cell divisions and a multipotential fate in precursors from the cerebral cortex. *Mol Cell Neurosci.* 18(5), 485-502.

Hill, R.E., Favor, J., Hogan, B.L., Ton, C.C., Saunders, G.F., Hanson, I.M., Prosser, J., Jordan, T., Hastie, N.D., van Heyningen, V.. 1991. Mouse small eye results from mutations in a paired-like homeobox-containing gene. *Nature* 354(6354), 522-5.

Holley, S.A., Jackson, P.D., Sasai, Y., Lu, B., DeRobertis, E.M., Hoffmann, F.M., Ferguson, E.L., 1995. A conserved system for dorsal-ventral patterning in insects and vertebrates involving sog and chordin. *Nature* 376, 249-253.

Holley, S.A., Neul, J.L., Attisano, L., Wrana, J.L., Sasai, Y., O'Connor, M.B., DeRobertis, E.M., Ferguson, E.L., 1996. The *Xenopus* dorsalizing factor noggin ventralizes *Drosophila* embryos by preventing DPP from activating its receptor. *Cell* 86, 607-617.

Hurst, L.D., P_1, C., Lercher, M.J., 2004. The evolutionary dynamics of eukaryotic gene order. *Nat. Rev. Genet.* 5, 299-310.

Incardona, J.P., William Gaffield, W., Raj, P., Kapur, R.P., Henk Roelink, H., 1998. The teratogenic Veratrumalkaloid cyclopamine inhibits Sonic hedgehog signal transduction. *Development* 125, 3553-3562.

Jin, P., Alisch, R.S., Warren, S.T., 2004. RNA and microRNAs in fragile X mental retardation. *Nat Cell Biol.* 6, 1048-1053.

Kalmykova, A.I., Nurminsky, D.I., Ryzhov, D.V., Shevelyov, Y.Y., 2005. Regulated chromatin domain comprising cluster of co-expressed genes in *Drosophila melanogaster*. *Nucleic Acids Res.* 33, 1435-1444.

Kampa, D., Cheng, J., Kapranov, P., Yamanaka, M., Brubaker, S., Cawley, S., Drenkow, J., Piccolboni, A., Bekiranov, S., Helt, G., Tammana, H., Gingeras, T.R., 2004. Novel RNAs identified from an in-depth analysis of the transcriptome of human chromosomes 21 and 22. *Genome Res.* 14, 331-342.

Kapranov, P., Drenkow, J., Cheng, J., Long, J., Helt, G., et al. 2005. Examples of the complex architecture of the human transcriptome revealed by RACE and highdensity tiling arrays. *Genome Res* 15, 987-997.

Kapranov, P., Willingham, A.T., Gingeras, T.R., 2007. Genome-wide transcription and the implications for genomic organization. *Nat Rev Genet.* 8, 413-423.

Katayama, S., Tomaru, Y., Kasukawa, T., Waki, K., Nakanishi, M., Nakamura, M., Nishida, H., Yap, C.C., Suzuki, M., Kawai, J., Suzuki, H., Carninci, P., Hayashizaki, Y., Wells, C., Frith, M., Ravasi, T., Pang, K.C., Hallinan, J., Mattick, J., Hume, D.A., Lipovich, L., Batalov, S., Engström, P.G., Mizuno, Y., Faghihi, M.A., Sandelin, A., Chalk, A.M., Mottagui-Tabar, S., Kawasaki, H., Taira, K., 2004. MicroRNA-196 inhibits HOXB8 expression in myeloid differentiation of HL60 cells. *Nucleic Acids* (48), 211-2.

Kiecker, C., Lumsden, A., 2005. Compartments and their boundaries in vertebrate brain development. *Nat Rev Neurosci.* 6(7), 553-64.

Kiyosawa, H., Mise, N., Iwase, S., Hayashizaki, Y., Abe, K., 2005. Disclosing hidden transcripts: Mouse natural senseantisense transcripts tend to be poly(A) negative and nuclear localized. *Genome Res.* 15, 463-474.

Kiyosawa, H., Yamanaka, I., Osato, N., Kondo, S., Hayashizaki, Y., 2003. Antisense transcripts with FANTOM2 clone set and their implications for gene regulation. RIKEN GER Group; GSL Members. *Genome Res.* 13(6B), 1324-34.

Kmita, M., Duboule, D., 2003. Organizing axes in time and space; 25 years of colinear tinkering. *Science*; 301, 331-333.

Knee, R., Murphy, P.R., 1997. Regulation of gene expression by natural antisense RNA transcripts. *Neurochem Int.* 31, 379-392.

Korneev, S.A., Park, J.H., O'Shea, M., 1999. Neuronal expression of neural nitric oxide synthase (nNOS) protein is suppressed by an antisense RNA transcribed from an NOS pseudogene. *J Neurosci.* 19, 7711-7720.

Kramer, C., Loros, J.J., Dunlap, J.C., Crosthwaite, S.K., 2003. Role for antisense RNA in regulating circadian clock function in *Neurospora crassa*. *Nature* 421, 948-952.

Kroll, T.T., O'Leary, D.D., 2005. Ventralized dorsal telencephalic progenitors in Pax6 mutant mice generate GABA interneurons of a lateral ganglionic eminence fate. *Proc Natl Acad Sci U S A* 102(20), 7374-9.

Kumar, M., Carmichael, G.G., 1998. Antisense RNA: function and fate of duplex RNA in cells of higher eukaryotes. *Microbiol Mol Biol Rev.* 62, 1415-1434.

Lagutin, O.V., Zhu, C.C., Kobayashi, D., Topczewski, J., Shimamura, K., Puellas, L., et al. 2003. Six3 repression of Wnt signaling in the anterior neuroectoderm is essential for vertebrate forebrain development. *Genes Dev.* 17,368-379.

Lapidot, M., and Pilpel, Y., 2006. Genome-wide natural antisense transcription: Coupling its regulation to its different regulatory mechanisms. *EMBO* 7, 1216-1222.

Lehner, B., Williams, G., Campbell, R.D., Sanderson, C.M., 2002. Antisense transcripts in the human genome. *Trends Genet.* 18, 63-65.

Lemons, D., McGinnis, W., 2006. Genomic evolution of Hox gene clusters. *Science* 313, 1918-1922.

Leupin, O., Attanasio, C., Marguerat, S., Tapernoux, M., Antonarakis, S.E., Conrad, B., 2005. Transcriptional activation by bidirectional RNA polymerase II elongation over a silent promoter. *EMBO* 6, 956-960.

Levanon, E.Y., Eisenberg, E., Yelin, R., Nemzer, S., Hallegger, M., Shemesh, R., Fligelman, Z.Y., Shoshan, A., Pollock, S.R., Szybel, D., Olshansky, M., Rechavi, G., Jantsch, M.F., 2004. Systematic identification of abundant A-to-I editing sites in the human transcriptome. *Nat Biotechnol.* 22(8), 1001-5.

Lewis, A., Reik, W., 2006. How imprinting centres work. *Cytogenet. Genome Res.* 113, 81-89.

Li, L.C., Okino, S.T., Zhao, H., Pookot, D., Place, R.F., Urakami, S., Enokida, H., Dahiya, R., 2006. Small dsRNAs induce transcriptional activation in human cells. *PNAS* 103(46): 17337-17342.

Li, Y.Y., Qin, L., Guo, Z.M., Liu, L., Xu, H., Hao, P., Su, J., Shi, Y., He, W.Z., Li, Y.X., 2006. In silico discovery of human natural antisense transcripts. *BMC Bioinformatics* 7, 18.

Liang, Z., Lenhard, B., Wahlestedt, C., 2005. Antisense transcription in the mammalian transcriptome. *Science* 309, 1564–1566.

Lin, J.M., Collins, P.J., Trinklein, N.D., Fu, Y., Xi, H., Myers, R.M., Weng, Z., 2007. Transcription factor binding and modified histones in human bidirectional promoters. *Genome Res.* 17, 818-827.

Liu, E.T., Kuznetsov, V.A., Miller, L.D., 2006. In the pursuit of complexity: systems medicine in cancer biology. *Cancer Cell.* 9(4), 245-7.

López-Bendito, G., Chan, C.H., Mallamaci, A., Parnavelas, J., Molnár, Z., 2002. Role of *Emx2* in the development of the reciprocal connectivity between cortex and thalamus. *J Comp Neurol.* 451(2), 153-69.

Machon, O., Backman, M., Machonova, O., Kozmik, Z., Vacik, T., Andersen, L., Krauss, S., 2007. A dynamic gradient of Wnt signaling controls initiation of neurogenesis in the mammalian cortex and cellular specification in the hippocampus. *Dev Biol.* 311(1), 223-37.

Mainguy, G., Koster, J., Woltering, J., Jansen, H., Durston, A., 2007. Extensive polycistronism and antisense transcription in the Mammalian *Hox* clusters. *PLoS ONE* 2(4), e356.

Majdalani, N., Vanderpool, C.K., Gottesman, S., 2005. Bacterial small RNA regulators. *Crit Rev Biochem Mol Biol.* 40(2), 93-113.

Mallamaci, A., Iannone, R., Briata, P., Pintonello, L., Mercurio, S., Boncinelli, E., Corte, G., 1998. *EMX2* protein in the developing mouse brain and olfactory area. *Mech Dev.* 77(2), 165-172.

Mallamaci, A., Mercurio, S., Muzio, L., Cecchi, C., Pardini, C.L., Gruss, P., Boncinelli, E., 2000a. The lack of *Emx2* causes impairment of Reelin signaling and defects of neuronal migration in the developing cerebral cortex. *J Neurosci.* 20(3), 1109-1118.

Mallamaci, A., Muzio, L., Chan, C.H., Parnavelas, J., Boncinelli, E., 2000b. Area identity shifts in the early cerebral cortex of *Emx2*^{-/-} mutant mice. *Nat Neurosci* 3(7):679-686. Mallamaci, A., Stoykova, A., 2006. Gene networks controlling early cerebral cortex arealization. *Eur J Neurosci.* 23(4), 847-56.

Mao, Q., Li, Y., Zheng, X., Yang, K., Shen, H., Qin, J., Bai, Y., Kong, D., Jia, X., Xie, L., 2008. Up-regulation of E-cadherin by small activating RNA inhibits cell invasion and migration in 5637 human bladder cancer cells. *Biochem Biophys Res Commun.* 375(4), 566-570.

Marín, O., Rubenstein, J.L., 2001. A long, remarkable journey: tangential migration in the telencephalon. *Nat. Rev. Neurosci.* 2(11), 780-790.

Marklund, M., Sjödal, M., Beehler, B.C., Jessell, T.M., Edlund, T., Gunhaga, L., 2004. Retinoic acid signalling specifies intermediate character in the developing telencephalon. *Development* 131(17), 4323-32.

Martynoga, B., Morrison, H., Price, D.J., Mason, J.O., 2005. Foxg1 is required for specification of ventral telencephalon and region-specific regulation of dorsal telencephalic precursor proliferation and apoptosis. *Dev Biol.* 283(1), 113-27.

McMahon, J.A., Takada, S., Zimmerman, L.B., Fan, C.M., Harland, R.M., McMahon, A.P., 1998. Noggin-mediated antagonism of BMP signaling is required for growth and patterning of the neural tube and somite. *Genes Dev.* 12, 1438-1452.

Mehler, M.F., 2002. Mechanisms regulating lineage diversity during mammalian cerebral cortical neurogenesis and gliogenesis. *Results Probl Cell Differ.*;39:27-52.

Mehler, M.F., 2002. Regional forebrain patterning and neural subtype specification: implications for cerebral cortical functional connectivity and the pathogenesis of neurodegenerative diseases. *Results Probl Cell Differ.* 39, 157-78.

Miyamoto, N., Yoshida, M., Kuratani, S., Matsuo, I., Aizawa, S., 1997. Defects of urogenital development in mice lacking Emx2. *Development* 124(9), 1653-1664.

Molnár, Z., Métin, C., Stoykova, A., Tarabykin, V., Price, D.J., Francis, F., Meyer, G., Dehay, C., Kennedy, H., 2006. Comparative aspects of cerebral cortical development. *Eur J Neurosci.* 23(4), 921-34.

Monuki, E.S., Porter, F.D., Walsh, C.A., 2001. Patterning of the dorsal telencephalon and cerebral cortex by a roof plate-Lhx2 pathway. *Neuron* 32(4), 591-604.

Morita, T., Nitta, H., Kiyama, Y., Mori, H., Mishina, M., 1995. Differential expression of two zebrafish emx homeoprotein mRNAs in the developing brain. *Neurosci.* 198(2), 131-4.

Morita, T., Aiba, H., 2006. RNA silencing mediated by small RNAs in *Escherichia coli*. *Tanpakushitsu Kakusan Koso.* 51, 2478-83.

Munroe, S.H., Zhu, J., 2006. Overlapping transcripts, double-stranded RNA and antisense regulation: A genomic perspective. *Cell. Mol. Life Sci.* 63, 2102-2118.

Muzio, L., Di Benedetto, B., Stoykova, A., Boncinelli, E., Gruss, P., Mallamaci, A., 2002a. Emx2 and Pax6 control regionalization of the pre-neuronogenic cortical primordium. *Cereb Cortex* 12(2), 129-139.

Muzio, L., Di Benedetto, B., Stoykova, A., Boncinelli, E., Gruss, P., Mallamaci, A., 2002b. Conversion of cerebral cortex into basal ganglia in Emx2(-/-) Pax6(Sey/Sey) double-mutant mice. *Nat Neurosci.* 5(8), 737-745.

Muzio, L., and Mallamaci, A., 2003. Emx1, emx2 and pax6 in specification, regionalization and arealization of the cerebral cortex. *Cereb Cortex* 13(6), 641-7.

Muzio, L., Mallamaci, A., 2005. Foxg1 confines Cajal-Retzius neuronogenesis and hippocampal morphogenesis to the dorso-medial pallium. *J Neurosci.* 25, 435-441.

Muzio, L., Soria, J.M., Pannese, M., Piccolo, S., Mallamaci, A., 2005. A mutually stimulating loop involving emx2 and canonical wnt signalling specifically promotes expansion of occipital cortex and hippocampus. *Cereb Cortex* 15(12), 2021-2028.

Noonan, F.C., Goodfellow, P.J., Staloch, L.J., Mutch, D.G., Simonc, T.C., 2003. Antisense transcripts at the EMX2 locus in human and mouse. *Genomics* 81, 58-66.

Ogawa, Y., Sun, B.K., Lee, J.T., 2008. Intersection of the RNA Interference and X-Inactivation Pathways. *Science* 320, 1336-1341.

Ohkubo, Y., Chiang, C., Rubenstein, J.L., 2002. Coordinate regulation and synergistic actions of BMP4, SHH and FGF8 in the rostral prosencephalon regulate morphogenesis of the telencephalic and optic vesicles. *Neuroscience* 111(1), 1-17.

Okamura, K., Balla, S., Martin, R., Liu, N., Lai, E.C., 2008. Two distinct mechanisms generate endogenous siR-NAs from bidirectional transcription in *Drosophila melanogaster*. *Nat. Struct. Mol. Biol.* 15, 581-590.

Okazaki, Y., Furuno, M., Kasukawa, T., Adachi, J., Bono, H., et al. 2002. Analysis of the mouse transcriptome based on functional annotation of 60,770 full-length cDNAs. *Nature* 420, 563-573.

O'Leary, D.D., Schlaggar, B.L., Tuttle, R., 1994. Specification of neocortical areas and thalamocortical connections. *Annu Rev Neurosci.* 17, 419-39.

Oliver, G., Mailhos, A., Wehr, R., Copeland, N.G., Jenkins, N.A., Gruss, P., 1995. Six3, a murine homologue of the sine oculis gene, demarcates the most anterior border of the developing neural plate and is expressed during eye development. *Development* 121, 4045-4055.

Pabst, O., Herbrand, H., Takuma, N., et al. 2000. NKX2 gene expression in neuroectoderm but not in mesendodermally derived structures depends on sonic hedgehog in mouse embryos. *Dev Genes Evol.* 210(1), 47-50.

Pandey, R.R., Mondal, T., Mohammad, F., Enroth, S., Redrup, L., Komorowski, J., Nagano, T., Mancini-Dinardo, D., Kanduri, C., 2008. Kcnq1ot1 antisense noncoding RNA mediates lineage-specific transcriptional silencing through chromatin-level regulation. *Mol Cell* 32(2), 232-246.

Pannese, M., Lupo, G., Kablar, B., Boncinelli, E., Barsacchi, G., Vignali, R., 1998. The *Xenopus* Emx genes identify presumptive dorsal telencephalon and are induced by head organizer signals. *Mech Dev.* 73(1), 73-83.

Park, H.C., Shin, J., & Appel, B., 2004. Spatial and temporal regulation of ventral spinal cord precursor specification by Hedgehog signaling. *Development* 131, 5959-5969.

Patarnello, T., Bargelloni, L., Boncinelli, E., Spada, F., Pannese, M., Broccoli, V., 1997. Evolution of Emx genes and brain development in vertebrates. *Proc Biol Sci.* 264(1389), 1763-6.

Pauler, F.M., Barlow, D.P., 2006. Imprinting mechanisms – it only takes two. *Genes Dev.* 20, 1203–1206. Pellegrini, M., Mansouri, A., Simeone, A., Boncinelli, E., Gruss, P., 1996. Dentate gyrus formation requires *Emx2*. *Development* 122(12), 3893-3898.

Petit, S., Meary, F., Pibouin, L., Jeanny, J.C., Fernandes, I., Poliard, A., Hotton, D., Berdal, A., Babajko, S., 2009. Autoregulatory loop of *Msx1* expression involving its antisense transcripts. *J Cell Physiol.* 220(2), 303-10.

Place, R.F., Li, L.C., Pookot, D., Noonan, E.J., Dahiya, R., 2008. MicroRNA-373 induces expression of genes with complementary promoter sequences. *PNAS* 105(5), 1608 -1613.

Pollard, K.S., Salama, S.R., Lambert, N., Lambot, M.A., Coppens, S., Pedersen, J.S., Katzman, S., King, B., Onodera, C., Siepel, A., Kern, A.D., Dehay, C., Igel, H., Manuel Ares, J., Vanderhaeghen, P., Haussler, D., 2006. An RNA gene expressed during cortical development evolved rapidly in humans. *Nature* 443, 167-172.

Poyatos, J.F., Hurst, L.D., 2006. Is optimal gene order impossible?. *Trends Genet.* 22, 420-423.

Prasanth, K.V., Spector, D.L., 2007. Eukaryotic regulatory RNAs: An answer to the “genome complexity” conundrum. *Genes Dev.* 21, 11-42.

Preker, P., Nielsen, J., Kammler, S., Lykke-Andersen, S., Christensen, M.S., Mapendano, C.K., Schierup, M.H., Jensen, T.H., 2008. RNA Exosome Depletion Reveals Transcription Upstream of Active Human Promoter. *Science* 322, 1851-1854.

Purmann, A., Toedling, J., Schueler, M., Carninci, P., Lehrach, H., Hayashizaki, Y., Huber, W. and Sperling, S., 2007. Genomic organization of transcriptomes in mammals: Coregulation and cofunctionality. *Genomics* 89, 580-587.

Rallu, M., Corbin, J.G., Fishell, G., 2002. Parsing the prosencephalon. *Nat Rev Neurosci.* 3(12), 943-51.

Rallu, M., Machold, R., Gaiano, N., Corbin, J.G., McMahon, A.P., Fishell, G., 2002. Dorsoventral patterning is established in the telencephalon of mutants lacking both *Gli3* and Hedgehog signaling. *Development* 129(21), 4963-4974.

Richards, M., Tan, S. P., Chan, W. K. and Bongso, A., 2006. Reverse serial analysis of gene expression (SAGE) characterization of orphan SAGE tags from human embryonic stem cells identifies the presence of novel transcripts and antisense transcription of key pluripotency genes. *Stem Cells* 24, 1162-1173.

RIKEN Genome Exploration Research Group and Genome Science Group (Genome Network Project Core Group) and the FANTOM Consortium 2005. Antisense Transcription in the Mammalian Transcriptome. *Science* 309, 1564-1566.

Ringrose, L., Paro, R., 2007. Polycomb/Trithorax response elements and epigenetic memory of cell identity. *Development* 134, 223-232.

Rinn, J.L., Bondre, C., Gladstone, H.B., Brown, P.O., Chang, H.Y., 2006. Anatomic demarcation by positional variation in fibroblast gene expression programs. *PLoS Genet.* 2(7), e119.

Rinn, J.L., Kertesz, M., Wang, J.K., Squazzo, S.L., Xu, X., Bruggmann, S.A., Goodnough, L.H., Helms, J.A., Farnham, P.J., Segal, E., Chang, H.Y., 2007. Functional demarcation of active and silent chromatin domains in human HOX loci by noncoding RNAs. *Cell* 129(7), 1311-1323.

Roessler, E., Belloni, E., Gaudenz, K., Jay, P., Berta, P., Scherer, S.W., Tsui, L.C., Muenke, M., 1996. Mutations in the human Sonic Hedgehog gene cause holoprosencephaly. *Nat Genet.* 14(3), 357-60.

Romby, P., Vandenesch, F., Wagner, E.G., 2006. The role of RNAs in the regulation of virulence-gene expression. *Curr Opin Microbiol.* 9(2), 229-36.

Ross, J., 1996. Control of messenger RNA stability in higher eukaryotes. *Trends Genet.* 12(5), 171-175.

S_mon, M., and Duret, L., 2006. Evolutionary origin and maintenance of coexpressed gene clusters in mammals. *Mol. Biol. Evol.* 23, 1715-1723.

Sasai, Y., de Robertis, E.M., 1997. Ectodermal patterning in vertebrate embryos. *Dev. Biol.* 182, 5-20.

Sastry, L., Johnson, T., Hobson, M.J., Smucker, B., Cornetta, K., 2006. Titering lentiviral vectors: comparison of DNA, RNA and marker expression methods. *Gene Ther.* 9(17), 1155-62.

Seila, A.C., Calabrese, J.M., Levine, S.S., Yeo, G.W., Rahl, P.B., Flynn, R.A., Young, R.A., Sharp, P.A., 2008. Divergent Transcription from Active Promoters. *Science* 322, 1849-1851.

Seimiya, M., Gehring, W.J., 2000. The Drosophila homeobox gene *optix* is capable of inducing ectopic eyes by an *eyeless*-independent mechanism. *Development* 127, 1879-1886.

Sémon, M., Duret, L., 2006. Evolutionary origin and maintenance of coexpressed gene clusters in mammals. *Mol Biol Evol.* 23(9), 1715-23.

Sessa, L., Breiling, A., Lavorgna, G., Silvestri, L., Casari, G., Orlando, V., 2007. Noncoding RNA synthesis and loss of Polycomb group repression accompanies the colinear activation of the human HOXA cluster. *RNA* 13, 223-239.

Shendure, J., Church, G.M., 2002. Computational discovery of sense-antisense transcription in the human and mouse genomes. *Genome Biol.* 3(9), 0044.1-0044.14.

Shinozaki, K., Miyagi, T., Yoshida, M., Miyata, T., Ogawa, M., Aizawa, S., Suda, Y., 2002. Absence of Cajal-Retzius cells and subplate neurons associated with defects of tangential cell migration from ganglionic eminence in *Emx1/2* double mutant cerebral cortex. *Development* 129(14), 3479-3492.

Shinozaki, K., Yoshida, M., Nakamura, M., Aizawa, S., Suda, Y., 2004. Emx1 and Emx2 cooperate in initial phase of archipallium development. *Mech Dev.* 121(5), 475-89.

Simeone, A., Gulisano, M., Acampora, D., Stornaiuolo, A., Rambaldi, M., Boncinelli, E., 1992a. Two vertebrate homeobox genes related to the *Drosophila* empty spiracles gene are expressed in the embryonic cerebral cortex. *EMBO* 11(7), 2541-2550.

Simeone, A., Acampora, D., Gulisano, M., Stornaiuolo, A., Boncinelli, E., 1992b. Nested expression domains of four homeobox genes in developing rostral brain. *Nature* 358(6388), 687-690.

Sleutels, F., Ronald Zwart, R., Barlow, D.P., 2001. The non-coding Air RNA is required for silencing autosomal imprinted genes. *Nature* 415, 810-813.

Spahn, L., and Barlow, D.P., 2003. An ICE pattern crystallizes. *Nat. Genet.* 35, 11-12.

Sproul, D., Gilbert, N., and Bickmore, W.A., 2005. The role of chromatin structure in regulating the expression of clustered genes. *Nat. Rev. Genet.* 6, 775-781.

Storz, G., Opdyke, J.A., Zhang, A., 2004. Controlling mRNA stability and translation with small, noncoding RNAs. *Curr Opin Microbiol.* 7(2), 140-4.

Stoykova, A., Götz, M., Gruss, P., Price, J., 1997. Pax6-dependent regulation of adhesive patterning, R-cadherin expression and boundary formation in developing forebrain. *Development* 124(19), 3765-77.

Stoykova, A., Treichel, D., Hallonet, M., Gruss, P., 2000. Pax6 modulates the dorsoventral patterning of the mammalian telencephalon. *J Neurosci.* 20(21), 8042-50.

Summerton, J., 2007. Morpholino, siRNA, and S-DNA Compared: Impact of Structure and Mechanism of Action on Off-Target Effects and Sequence Specificity. *Med Chem.* 7(7), 651-660.

Takebayashi, H., *et al.* 2002. The basic helix-loop-helix factor olig2 is essential for the development of motoneuron and oligodendrocyte lineages. *Curr. Biol.* 12, 1157-1163.

Takiguchi-Hayashi, K., Sekiguchi, M., Ashigaki, S., Takamatsu, M., Hasegawa, H., Suzuki-Migishima, R., Yokoyama, M., Nakanishi, S., Tanabe, Y., 2004. Generation of reelin-positive marginal zone cells from the caudomedial wall of telencephalic vesicles. *J Neurosci.* 24(9), 2286-95.

Tam, O.H., Aravin, A.A., Stein, P., Girard, A., Murchison, E.P., Cheloufi, S., Hodges, E., Anger, M., Sachidanandam, R., Schultz, R.M., Hannon, G.J., 2008. Pseudogene-derived small interfering RNAs regulate gene expression in mouse oocytes. *Nature* 453, 534-538.

Theil, T., Alvarez-Bolado, G., Walter, A., Ruther, U., 1999. Gli3 is required for Emx gene expression during dorsal telencephalon development. *Development* 126, 3561-3571.

Theil, T., Aydin, S., Koch, S., Grotewold, L., Rütger, U., 2002. Wnt and Bmp signalling cooperatively regulate graded *Emx2* expression in the dorsal telencephalon. *Development* 129(13), 3045-54.

Tole, S., Goudreau, G., Assimacopoulos, S. Grove, E.A., 2000. *Emx2* is required for growth of the hippocampus but not for hippocampal field specification. *J Neurosci.* 20(7), 2618-25.

Tomizawa, J., Itoh, T., Selzer, G., Som, T., 1981. Inhibition of ColE1 RNA primer formation by a plasmid-specified small RNA. *Proc Natl Acad Sci USA* 78, 1421-1425.

Trinklein, N.D., Aldred, S.F., Hartman, S.J., Schroeder, D.I., O'tillar, R.P., and Myers, R.M., 2004. An abundance of bidirectional promoters in the human genome. *Genome Res.* 14, 62-66.

Veeramachaneni, V., Makołowski, W., Galdzicki, M., Sood, R., and Makołowska, I., 2004. Mammalian overlapping genes: The comparative perspective. *Genome Res.* 14, 280-286.

Vyas, A., Saha, B., Lai, E., Tole, S., 2003. Paleocortex is specified in mice in which dorsal telencephalic patterning is severely disrupted. *J Comp Neurol.* 466(4), 545-53.

Wagner, E.G., Flärth, K., 2002. Antisense RNAs everywhere?. *Trends Genet.* 18(5), 223-6.

Wagner, E.G., Simons, R.W., 1994. Antisense RNA control in bacteria, phages, and plasmids. *Annu Rev Microbiol.* 48, 713-742.

Walther, C., Gruss, P., 1991. *Pax-6*, a murine paired box gene, is expressed in the developing CNS. *Development* 113(4), 1435-49.

Watanabe, T., Totoki, Y., Toyoda, A., Kaneda, M., Kuramochi-Miyagawa, S., Obata, Y., Chiba, H., Kohara, Y., Kono, T., Nakano, T., Surani, M.A., Sakaki, Y., Sasaki, H., 2008. Endogenous siRNAs from naturally formed dsRNAs regulate transcripts in mouse oocytes. *Nature* 453, 539-543.

Werner, A., Carlile, M., Swan, D., 2009. What do natural antisense transcripts regulate?. *RNABiol.* 6(1), 43-8.

Werner, A., Schmutzler, G., Carlile, M., Miles, C.G., and Peters, H., 2007. Expression profiling of antisense transcripts on DNA arrays. *Physiol. Genomics* 28, 294-300.

Williams, T., Fried, M., 1986. A mouse locus at which transcription from both DNA strands produces mRNAs complementary at their 3' ends. *Nature* 322, 275-279.

Wutz, A., and Gribnau, J., 2007. X inactivation Xplained. *Curr. Opin. Genet. Dev.* 17, 387-393.

Xuan, S., Baptista, C.A., Balas, G., Tao, W., Soares, V.C., Lai, E., 1995. Winged helix transcription factor *BF-1* is essential for the development of the cerebral hemispheres. *Neuron* 14(6), 1141-52.

Yelin, R., Dahary, D., Sorek, R., Levanon, E.Y., Goldstein, O., Shoshan, A., Diber, A., Biton, S., Tamir, Y., Khosravi, R., Nemzer, S., Pinner, E., Walach, S., Bernstein, J., Savitsky, K., Rotman, G., 2003. Widespread occurrence of antisense transcription in the human genome. *Nat. Biotechnol.* 21, 379-386.

Yoshida, M., Suda, Y., Matsuo, I., Miyamoto, N., Takeda, N., Kuratani, S., Aizawa, S., 1997. *Emx1* and *Emx2* functions in development of dorsal telencephalon. *Development* 124(1), 101-111.

Zaki, P.A., Quinn, J.C., Price, D.J., 2003. Mouse models of telencephalic development. *Curr. Opin. Genet. Dev.* 13(4), 423-437.

Zhang, Y., Liu, X. S., Liu, Q.R., and Wei, L., 2006. Genomewide in silico identification and analysis of cis natural antisense transcripts (cis-NATs) in ten species. *Nucleic Acids Res.* 34, 3465-3475.

Acknowledgements

In the achievement of my PhD-Thesis, I really want to thank some of the people that supported me during these years of studying.

In primis, my supervisor, Prof. Antonio Mallamaci, that was every day on my side with his patience and knowledge.

My family, for having always trust and support me with patience and true love.

All my friends and colleagues that during these years in SISSA I had the opportunity to enjoy and appreciate during pauses from our jobs and that with their preparation have represented a valuable standing point.

Elisa, Marilena, Rossana, for being so present... My staying in Trieste would be worst without your friendship. I will miss you!

Simona, who is always present, although the distances.

Finally, my dear grandfather, whosre memory I never had nor will forget.